UNIVERSITY OF RIJEKA
FACULTY OF CIVIL ENGINEERING

Edita Papa Dukić

CONFIGURATION–DEPENDENT INTERPOLATION IN NON–LINEAR HIGHER–ORDER 2D BEAM FINITE ELEMENTS

DOCTORAL THESIS

Rijeka, 2013

UNIVERSITY OF RIJEKA
FACULTY OF CIVIL ENGINEERING

Edita Papa Dukić

CONFIGURATION–DEPENDENT INTERPOLATION IN NON–LINEAR HIGHER–ORDER 2D BEAM FINITE ELEMENTS

DOCTORAL THESIS

Supervisor: prof. dr. sc. Gordan Jelenić

Rijeka, 2013.

Mentor: prof. dr. sc. Gordan Jelenić

Doktorski rad obranjen je dana _____

u/na _____, pred povjerenstvom u sastavu:

1. prof. dr. sc. Nenad Bićanić, Sveučilište u Rijeci, Građevinski fakultet, predsjednik povjerenstva

2. prof. dr. sc. Ivica Kožar, Sveučilište u Rijeci, Građevinski fakultet, član

3. izv. prof. dr. sc. Dejan Zupan, Univerza v Ljubljani, Fakulteta za gradbeništvo in geodezijo, vanjski član

Acknowledgement

Veliko hvala...

mojoj obitelji i Hrvoju
za svu ljubav i podršku...

Mom mentoru, prof. Gordanu Jeleniću, hvala za sve sate strpljivog mentorstva.

Rezultati prikazani u ovom radu su dobiveni u sklopu projekta br. 114–0000000–3025: "Improved accuracy in non–linear beam elements with finite 3D rotations" kojeg je financijski poduprlo Ministarstvo znanosti, obrazovanja i sporta Republike Hrvatske.

Abstract

In this thesis two topics of the beam theory are considered. The first of them is concerned with the linear Timoshenko beam theory and within it a new interpolation called the linked interpolation has been proposed. This interpolation is derived from the exact solutions of the Timoshenko beam differential equations and therefore results in the finite element giving the exact solutions in linear analysis. The second topic is concerned with the non–linear geometrically exact beam theory of Reissner and Simo. Within this theory another interpolation is proposed; the non–linear configuration–dependent interpolation. In this work a particular form of the configuration–dependent interpolation is derived which coincides with the linked interpolation in case when displacements and rotations become small, or in other words, in linear analysis. Both of these proposed interpolations are given in a general form for an arbitrary number of nodes per element. In order to conduct the numerical analysis, a new non–linear 2D beam finite–element computer code has been created. The proposed interpolation is free of shear–locking thus having the potential to be used in various problems in material non–linearity where higher–order quadrature may be needed.

Key words: Finite element method, 2D beam theory, linear analysis, linked interpolation, configuration–dependent interpolation, non–linear analysis.

Sažetak

U ovoj disertaciji obrađena su dva poglavlja gredne teorije. Jedno poglavlje se tiče linearne Timošenkove gredne teorije u okviru koje je predložena nova interpolacija koja polazi od točnih rješenja diferencijalnih jednadžbi problema te samim time rezultira konačnim elementima s točnim rješenjima u linearnoj analizi. Vezana interpolacija je u radu predstavljena na dva načina. Prva formulacija predstavlja interpolaciju ovisnu o materijalnim karakteristikama nosača (nazvana *problem–dependent* interpolacija) koja slijedi iz diferencijalnih jednadžbi uz uvođenje svih rubnih uvjeta. Druga formulacija predstavlja interpolaciju neovisnu o materijalnim karakteristikama, stoga je nazvana *problem–independent* interpolacija. Za obje formulacije je pokazano da daju točnu matricu krutosti koja je poznata i dana u literaturi.

Drugo poglavlje obuhvaća nelinearnu grednu teoriju u okviru koje je obrađena Reissnerova gredna teorija velikih pomaka i velikih rotacija te je predložena nova interpolacija koja je nazvana interpolacija ovisna o konfiguraciji. U ovome radu poseban oblik interpolacije ovisne o konfiguraciji je izveden, kojem je granični slučaj u linearnoj teoriji upravo vezana interpolacija. Predložene interpolacije su dane u generaliziranom obliku za proizvoljan broj čvorova grednog konačnog elementa. Za potrebe analiza koje su se provele u numeričkom dijelu ovog rada sastavljen je algoritam za nelinearni proračun konstrukcija sastavljenih od ravninskih konačnih grednih elemenata u programskom paketu Wolfram Mathematica te je on u potpunosti autorsko djelo doktoranta. Predložena interpolacija je otporna na *shear–locking* efekt te ima potencijala za korištenje u različitim problemima povezanim s materijalnom nelinearnošću gdje je potrebna integracija višeg reda.

Ključne riječi: Metoda konačnih elemenata, ravninska gredna teorija, linearna analiza, vezana interpolacija, interpolacija ovisna o konfiguraciji, nelinearna analiza.

Contents

1 Introduction

This thesis is divided into five major chapters. After a brief overview of the field given in the first chapter, the second chapter deals with the linear Timoshenko beam theory within which the new interpolation, called the *linked interpolation* is proposed. Beam is considered to be a 3D body with two of its dimensions considerably smaller than the third – the longitudinal dimension along which the beam has a certain length.

Generally, linear beam theory can be divided into Euler–Bernoulli and Timoshenko beam theory depending on the thickness of the beam. The Euler–Bernoulli beam theory is rather simple, it omits shear deformations of the beam cross–section, thus making the displacement and the rotation field dependent quantities. Also, this theory assumes that cross–section remains planar and orthogonal to the deformed line of the beam. On the other hand, the Timoshenko beam theory includes shear deformations of the beam cross–section and in this way makes the rotational and displacement field independent of one another. When talking about the Timoshenko beam problem, it should be stated that this is one of the classic problems in elasticity that has attracted a widespread attention owing to its obvious usefulness in practical engineering design as well as simplicity in finite–element implementation including generalisation in non–linear analysis. In contrast to many other problems in computational mechanics and structural engineering, the Timoshenko beam problem is relatively simple, its behavior well understood and its closed-form solution widely reported [29].

When this solution is to be used in large–scale structural problems it becomes of interest to express it in terms of a set of basic unknown parameters that are appropriate for application of a particular numerical method. These unknown parameters are usually taken to be the displacement and rotation vectors at chosen nodal points, and and in this particular case we talk about interpolating the problem solution for displacement and rotation fields exactly. Important thing to mention here is that usually interpolations are not exact, since they represent only numerical approximation of the unknown field.

Such exact interpolation that provides exact solution in linear analysis has been widely reported [25, 30, 31, 39, 40] and often praised for automatically eliminating shear–locking [39, 41]. Closer inspection reveals that this interpolation can take a number of forms, from highly coupled one in which the displacement and the rotation field depend on the nodal displacements and rotations as well as the material, geometric and loading data [27, 30, 31, 40] to a completely uncoupled interpolation of the

displacement and the rotation fields [20]. Tessler and Dong in [39] have studied this plurality of interpolation choices that lead to the same answer and have introduced a family of *virgin elements* with presumed independent interpolation of the rotation and the displacement field. Next, Tessler and Dong [39] deal with a family of *constrained elements* in which a number of internal degrees of freedom is eliminated by reducing the shear strain in the element to a certain theoretically justified lower order, leading to *the interdependent interpolation.*

In the first chapter we introduce the linked interpolation that can be presented as the *problem–dependent* interpolation or the *problem–independent* interpolation. The first term is used because of the dependence of the interpolation on the material, geometric and loading characteristics and the second term if all the material and geometric characteristic as well as the loading parameters are absent from the interpolation functions. In a numerical part of the second chapter a problem–independent interpolation has been considered depending on the relation of the number of the nodes with translational degrees of freedom towards the number of the rotational degrees of freedom. It has been shown that, in the case when the nodes for the rotational degrees of freedom match those of the displacement degrees of freedom, a particularly elegant form (both mathematically and computationally) is obtained. This result is here presented in a general form of which some of the known linked interpolations reported in the literature [41] have been shown to be the special cases.

When faced with such a number of interpolation choices with all of them leading to the exact solution, it is quite natural to take the one with the smallest number of unknown parameters and implement it into a numerical procedure. However, in certain problems, we may wish to have interpolation that is free from the problem parameters, e.g. when handling materially non–linear problems. In geometrically non–linear problems, extra degrees of freedom are also very useful in describing departure from the shape of the deformation in linear case.

The third chapter of the thesis deals with the non–linear beam theory of Reissner [32] and Simo [33] that has provided the basis for many of the finite element formulations for 3D beams [9, 17, 21, 36, 43] and many others. The geometrically exact theory provides the relationship between the configuration and the adopted strain measures that are fully consistent with the virtual work principle and the differential equations of motion regardless of the magnitude of the displacement, rotation or strains involved [32].

If a standard Lagrangian interpolation is applied to the total or incremental rotation vector or the infinitesimal change of the rotation matrix, a certain problem of non–objectivity of the strain measures arises. In their work [18] Jelenić and Crisfield propose a strain–invariant and path–independent, geometrically exact isoparametric 3D beam element of arbitrary order to overcome this problem. The essence of this formulation is the interpolation of the current local rotations. Even though the proposed method is different from the conventional approaches [9, 17, 21, 34, 37], authors further introduce generalised shape functions that enables the method to take a similar form to the ones of the conventional approaches mentioned.

A different approach is taken by Borri and Bottasso in [4]. This approach aims at resolving a more general type of non–objectivity of the numerical results with respect to the chosen reference line. Authors have named the interpolation introduced therein a *helicoidal interpolation* that enables interdependence between the rotation and the displacement field in a way that the rotations of the considered beam cross–section generate corresponding displacements of the reference line. The formulation proposed is quite different from the classical beam formulations based on polynomial interpolations of the independent field. The authors resolve the constant strain problem analytically to derive appropriate shape functions. The proposed methodology results in the same interpolation functions for the rotation and the displacement field which are also identical to the generalised interpolation for rotations in the work of Jelenić and Crisfield [18]. This helicoidal formulation, however, is applicable to two–noded elements only and the given methodology is strictly limited to that case.

The third chapter of this thesis synthesises this two [4, 18] independent formulations for 3D geometrically exact non–linear beams of which each has a certain anomaly. The approach proposed here extends the results of the second formulation [4] to multi–noded elements by applying the methodology of the first formulation [18] resulting in a configuration–dependent interpolation proposed here and given for the position vector for 3D beam elements of arbitrary order. As the name states, this interpolation uses the current deformed configuration to interpolate the current position of the reference line of the beam.

We will show that for linear problems the proposed configuration–dependent interpolation may easily take a form which reduces to the linked interpolation and that, for the two–noded non–linear elements, it is equivalent to the helicoidal interpolation of Borri and Bottasso. In this way we obtain a very elegant form that binds the linear and the non–linear analysis with the family of the same interpolation functions.

Finite element method, used in this work, is a method that allows us to describe and analyse mechanical problems numerically [42]. It is based on dividing continuum into segments that are called finite elements, each element has two or more nodal points with at least two of them at the boundaries of the element. Displacements and rotations of the nodal points present basic unknown parameters of the problem considered in which the finite elements are of the beam type. Displacements and rotations between the nodes are approximated by interpolation functions. Together with the kinematic and constitutive equations as well as the applied loading, the problem is presented in a variational form leading to the system of discrete equations from which the basic unknown parameters of the system can be obtained.

The finite element method has an approximate character that stems from the interpolation functions introduced, hence the accuracy of the calculation highly depends on the chosen interpolation functions. Standard procedure [34] uses the same order Lagrangian polynomials to describe the unknown displacement and rotation field leading to the numerical anomaly known as the *shear locking* [3]. The shear strain is defined by the theory as a difference between the derivative of the lateral displacement with respect to the length co–ordinate and the rotation of the cross section. With equal–order Lagrangian interpolation, it is impossible to consider the state of pure bending and obtain the solution with no shear strains. The cure for this anomaly is the widely used reduced integration [42] leading to underintegration of some elements of the stiffness matrix. The linked interpolation and the configuration–dependent interpolation proposed here do not produce such numerical anomalies.

The forth chapter consists of some numerical tests to assess the performance of these elements against the elements with Lagrangian or linked interpolation.

Each of these chapters of the thesis will have the short introduction before the problem is exposed. Joint conclusion of the linear and non–linear analysis will be given at the end of the thesis in the forth chapter.

2 Static linear analysis of 3D thick beam elements and linked interpolation of arbitrary order

2.1 Overview of the finite element procedures in linear analysis

The standard application of the finite–element method to Timoshenko beam theory assumes independent approximation for the displacement and the rotation field using a polynomial interpolation of the same order [41, 3], e.g

$$\mathbf{u}(x_1) = \sum_{i=1}^{N} I_i(x_1)\mathbf{u}_i, \quad \boldsymbol{\theta}(x_1) = \sum_{i=1}^{N} I_i(x_1)\boldsymbol{\theta}_i, \tag{1}$$

where $0 \leq x_1 \leq L$ is the length coordinate of the beam centroidal axis, $\mathbf{u}(x_1)$ is the displacement field, $\boldsymbol{\theta}(x_1)$ is the rotation field, $(\mathbf{u}_i,\ \boldsymbol{\theta}_i)$ are the unknown nodal displacements and rotations and $I_i(x_1)$ are the Lagrangian polynomials of order $N-1$ for an $N-$ noded element.

The Timoshenko beam theory assumes that in the deformed state, the cross–sections are not necessary orthogonal to the centroidal axis of the beam. To simplify representation, in Figure 2.1 this is shown for a 2D case.

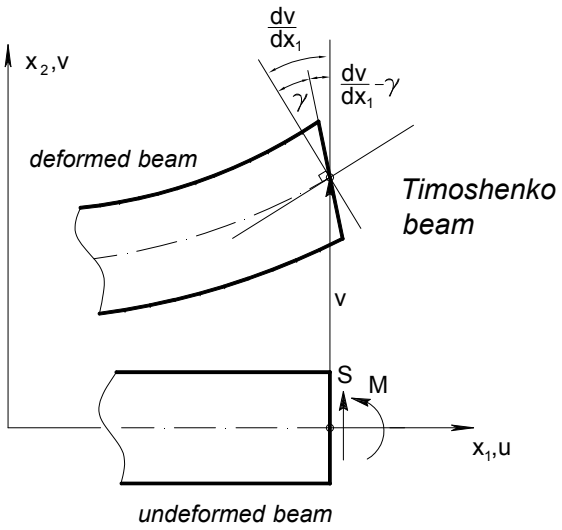

Figure 2.1: Timoshenko beam.

As it can be seen, an additional rotation γ exists as a result of the shear forces which cause slipping of the cross–section. This can be described by the following equation

$$\theta(x_1) = \frac{dv}{dx_1} - \gamma, \tag{2}$$

where v is the vertical displacement of the point on the axis, $\theta(x_1)$ is the rotation of the cross–section and γ is the shear angle.

The standard interpolation given by (1) imposes a non–physical constraint between the displacement and the rotation field which becomes exceedingly prominent in the problems of thin beams leading to completely wrong results. This problem is known as the shear locking and is usually eliminated by using the so–called uniformly reduced integration [3]. This means that functions are integrated using less sampling points than needed leading to under–integration of some elements of stiffness matrix. Presented in this way, the reduced integration seems like just a mathematical trick that is used to compute the stiffness matrix and the internal force vector in an inaccurate way. Justification for this trick becomes apparent when the problem is formulated using the Hellinger–Reissner functional with appropriate interpolation for the displacement, rotation and strain fields [3]. This technique applies to the correction of the stiffness matrix only and not to the non-physical interpolation of the displacement and the rotation fields.

An alternative approach is utilised in [30, 40], where the appropriate polynomial distribution for the displacement and the rotation field are sought from the condition that the finite–element solution should coincide with the exact solution. The theory–induced dependence of the lateral displacement field on the cross–sectional rotations is now inherited by the finite–element interpolation, the resulting interpolation is said to be *field consistent* [40] and is explicitly given in [30] and [40]. The resulting stiffness matrices therefore coincide with the results of the engineering thick beam theory presented in [29] but, in addition, these references also give the *exact field distribution*, which in turn provides unique results for the strain measures and the stress resultants irrespective of whether they are obtained from the equilibrium equations or the constitutive equations.

For the Timoshenko beam theory considered here, such a field–consistent interpolation is necessarily dependent on the cross–sectional material and geometric properties and in [41] an alternative interpolation is presented which is independent of the problem parameters at the expense of introducing an additional internal degree of freedom. Such a plurality of interpolation choices leading to the same answer is studied further in [39], where a family of so–called *virgin elements* is introduced, in which independent interpolation for the rotation and the lateral displacement field is presumed at the outset with the interpolation for the rotation field. In [31] such an interpolation is called *the consistent interpolation*. A family of constrained elements is proposed

next in [39], in which a number of internal degrees of freedom are eliminated by reducing the shear strain in the element to a certain theoretically justified lower order, thus leading to what the authors call *the interdependent interpolation* of the rotation and the lateral displacement fields. Further elimination of the internal degrees of freedom will eventually lead to the problem–dependent interpolation of [30, 40] as shown in [25] and [31]. In contrast to [39], it is this interpolation that the authors call *the interdependent interpolation*.

In this chapter it will be shown that, for arbitrary static polynomial loading, this approach can be generalised to arbitrary order of interpolation giving a family of exact interpolation functions for the Timoshenko beam which follow a very structured pattern. The result is made possible by the fact that the homogeneous parts of the governing differential equations have polynomial solutions and would naturally cease to be exact for the problem where this is not true, e.g. for dynamically loaded beams and beams on elastic foundation as well as for the plate structures. Dependence of the lateral displacements on the rotational degrees of freedom similar to that existing in the static beam solutions has been often assumed in order to improve the performance of the finite element analysis of plate structures. The resulting elements are given in [2, 16, 38, 41] and the references therein and from here we borrow the term "linked interpolation".

We derive our linked interpolation by consistently providing a sufficient number of nodal points for the displacement and the rotation degrees of freedom, where this number depends on the order of the polynomial describing the applied loading. In this way the virgin interpolation of [39] or the consistent interpolation of [31] may be obtained. Expressing some of the internal degrees of freedom in terms of the remaining degrees of freedom leads to various types of the constrained interpolation of [39] and we particularly emphasise the one with the equal number of nodes for the rotation and the displacement degrees of freedom. If all the internal degrees of freedom are expressed in terms of the boundary degrees of freedom we are left with the solution of Rakowski [30] and Yunhua [40] as well as the interdependent interpolation of Reddy [31] enriched by the contributions due to the applied distributed loading.

Additionally, in contrast to all the references mentioned, here we apply this methodology to a full 3D Timoshenko beam problem.

2.2 Differential equations of a 3D Timoshenko beam problem

2.2.1 Kinematic equations

The Timoshenko beam theory assumes a beam to be a 3D body with two of its dimensions considerably smaller than the third one, which is called the longitudinal dimension of the beam and its length will be denoted by L. Intersection of the beam with a plane orthogonal to its longitudinal dimension is defined as a beam cross–section, which the theory defines as rigid. In contrast, the line of centroids, defined as the line that connects the centroids C (Figure 2.2) of the cross–section, is deformable. Timoshenko beam of a uniform cross–section made of a linearly elastic material is considered here.

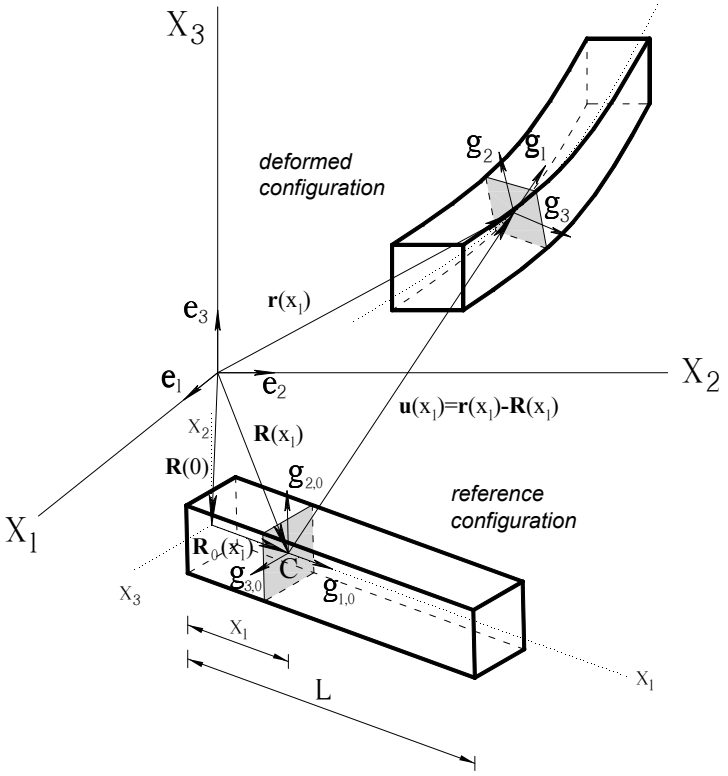

Figure 2.2: Kinematics of the problem.

The beam axis in reference configuration is taken to be a straight line which coincides with the x_1 axis of the Cartesian frame with the orthonormal unit base vectors $\mathbf{g}_{01}$, $\mathbf{g}_{02}$, $\mathbf{g}_{03}$. The orthonormal triad $\mathbf{e}_1$, $\mathbf{e}_2$, $\mathbf{e}_3$ defines spatial frame. These two frames are connected with the initial rotational matrix $\mathbf{\Lambda}_0$ which depends only on the angle of inclination of the beam in the undeformed state φ_0. Equation that defines connection between these two frames is given by

$$\mathbf{g}_{0i} = \mathbf{\Lambda}_0 \, \mathbf{e}_i, \, i = 1, 2, 3. \tag{3}$$

Similar connection can be defined for the orientation of the cross section in the deformed configuration as

$$\mathbf{g}_i = \mathbf{\Lambda} \, \mathbf{e}_i, \; i = 1, 2, 3 \; , \tag{4}$$

where $\mathbf{g}_i$ is the orthonormal triad that defines the cross section in the deformed configuration, with $\mathbf{\Lambda}$ as a rotational matrix that depends on the rotations of the cross-section in the deformed state and satisfies the standard conditions of unimodularity $det\mathbf{\Lambda} = 1$ and orthogonality $\mathbf{\Lambda}\mathbf{\Lambda}^T = \mathbf{I}$, with $\mathbf{I}$ as a 3×3 unit matrix. The first member of this triad $\mathbf{g}_1$ is perpendicular to the plane of the cross section while the other two members $\mathbf{g}_2, \mathbf{g}_3$ are spanning the plane of the cross section.

The position vector $\mathbf{X}(x_1, x_2, x_3)$ of an arbitrary point of the deformed beam is defined by three parameters (x_1, x_2, x_3) where the first one is the coordinate of the length along the axis of the beam and the other two are the coordinates of the cross–section along its principal axes. This can be written as

$$\mathbf{X}(x_1, x_2, x_3) = \mathbf{r}(x_1) + \mathbf{\Lambda}(x_1) \begin{Bmatrix} 0 \\ x_2 \\ x_3 \end{Bmatrix} \; , \tag{5}$$

where $\mathbf{r}(x_1)$ is the position vector of the point on the deformed axis of the beam, $\mathbf{\Lambda}$ is the rotational matrix of the cross section and $[0 \;\; x_2 \;\; x_3]^T$ is the vector within the cross section for a given x_1 in the reference state. In this way the kinematics of the beam is completely defined by a position vector on the axis of the beam and the orientation of the cross section $(\mathbf{r}(x_1), \mathbf{\Lambda}(x_1))$. Further, the position vector $\mathbf{r}(x_1)$ can be expressed in terms of the displacement vector $\mathbf{u}(x_1)$ and the position vector of the point on the axis of the beam in the undeformed state $\mathbf{R}(x_1)$ as $\mathbf{r}(x_1) = \mathbf{R}(x_1) + \mathbf{u}(x_1)$ with $\mathbf{\Lambda}(x_1)$ given by Rodrigues formula [33] as

$$\mathbf{\Lambda}(x_1) = exp \; \hat{\boldsymbol{\theta}} = \mathbf{I} + \frac{\sin\theta}{\theta}\hat{\boldsymbol{\theta}} + \frac{1 - \cos\theta}{\theta^2}(\hat{\boldsymbol{\theta}})^2 \; , \tag{6}$$

where $\hat{\boldsymbol{\theta}}$ is a skew–symmetric matrix of a rotation vector $\boldsymbol{\theta} = [\theta_1 \;\; \theta_2 \;\; \theta_3]^T$ of a magnitude $\theta = \sqrt{\theta_1^2 + \theta_2^2 + \theta_3^2}$ and the components along the coordinate axis $x_1, \; x_2, \; x_3$ denoted as $\theta_1, \; \theta_2, \; \theta_3$.

The hat ($\hat{}$) above a 3D vector here and throughout the text denotes a cross-product operator such that for any two vectors $\mathbf{v}, \; \mathbf{w}$ we have $\hat{\mathbf{v}}\mathbf{w} = \mathbf{v} \times \mathbf{w} = -\mathbf{w} \times \mathbf{v} = -\hat{\mathbf{w}}\mathbf{v}$, i.e.

$$\hat{\mathbf{v}} = \begin{bmatrix} 0 & -v_3 & v_2 \\ v_3 & 0 & -v_1 \\ -v_2 & v_1 & 0 \end{bmatrix} ,$$

with $v_1,\ v_2,\ v_3$ as the Cartesian components of $\mathbf{v}$ in a chosen basis.
The Timoshenko beam theory is based upon the hypothesis that while the initially planar cross-sections of the beam remain planar after the deformation (the Bernoulli hypothesis), the angle which they close with the centroidal axis is not necessarily retained during the deformation. This theory is widely applied to linear analysis of engineering beam problems and it follows from the non-linear Simo–Reissner theory if all the non–linearities with respect to the position and rotations of the cross-section are consistently eliminated. Assuming the rotation vector to be infinitesimally small, $\sin\theta \to \theta,\ \cos\theta \to 1$ and all the higher-order terms in $\boldsymbol{\theta}$ vanish, so that (6) reduces to

$$\boldsymbol{\Lambda}(x_1) = \begin{bmatrix} 1 & -\theta_3 & \theta_2 \\ \theta_3 & 1 & -\theta_1 \\ -\theta_2 & \theta_1 & 1 \end{bmatrix} . \tag{7}$$

2.2.2 Strain measures

Strain measures are given as [34]

$$\boldsymbol{\Gamma} = \boldsymbol{\Lambda}^T \frac{d\mathbf{r}}{dx_1} - \mathbf{G}_1 , \tag{8}$$

$$\hat{\boldsymbol{\kappa}} = \boldsymbol{\Lambda}^T \frac{d\boldsymbol{\Lambda}}{dx_1} , \tag{9}$$

where $\boldsymbol{\Gamma}$ is a vector of translational strain measures made up of one axial (ϵ) and two shear strains (γ_2, γ_3). The skew–symmetric matrix of rotational strain measures is represented with a symbol $\hat{\boldsymbol{\kappa}}$ and it consists of one torsional (κ_1) and two bending strains (κ_2, κ_3). The material vector is given as $\mathbf{G}_1 = \begin{Bmatrix} 1 \\ 0 \\ 0 \end{Bmatrix}$.
Neglecting non–linear terms and taking (7), expression (8) can be written in terms of displacements and rotations as

$$\boldsymbol{\Gamma} = \begin{Bmatrix} \epsilon \\ \gamma_2 \\ \gamma_3 \end{Bmatrix} = \begin{bmatrix} 1 & -\theta_3 & \theta_2 \\ \theta_3 & 1 & -\theta_1 \\ -\theta_2 & \theta_1 & 1 \end{bmatrix}^T \begin{Bmatrix} \frac{dr_1}{dx_1} \\ \frac{dr_2}{dx_1} \\ \frac{dr_3}{dx_1} \end{Bmatrix} - \begin{Bmatrix} 1 \\ 0 \\ 0 \end{Bmatrix} = \begin{Bmatrix} \frac{du}{dx_1} \\ \frac{dv}{dx_1} - \theta_3 \\ \frac{dw}{dx_1} + \theta_2 \end{Bmatrix} = \frac{d\mathbf{u}}{dx_1} + \mathbf{G}_1 \times \boldsymbol{\theta}, \tag{10}$$

since

$$\frac{d\mathbf{r}}{dx_1} = \frac{d\mathbf{R}}{dx_1} + \frac{d\mathbf{u}}{dx_1} = \lim_{\Delta x_1 \to 0} \frac{\mathbf{R}(x_1 + \Delta x_1) - \mathbf{R}(x_1)}{\Delta x_1} + \frac{d\mathbf{u}}{dx_1} = \begin{Bmatrix} 1 + \frac{du}{dx_1} \\ \frac{dv}{dx_1} \\ \frac{dw}{dx_1} \end{Bmatrix} = \mathbf{G}_1 + \frac{d\mathbf{u}}{dx_1}.$$

The matrix of rotational strain measures (9) can be written in terms of the rotation components

$$\begin{bmatrix} 0 & -\kappa_3 & \kappa_2 \\ \kappa_3 & 0 & -\kappa_1 \\ -\kappa_2 & \kappa_1 & 0 \end{bmatrix} = \begin{bmatrix} 1 & \theta_3 & -\theta_2 \\ -\theta_3 & 1 & \theta_1 \\ \theta_2 & -\theta_1 & 1 \end{bmatrix} \begin{bmatrix} 0 & -\frac{d\theta_3}{dx_1} & \frac{d\theta_2}{dx_1} \\ \frac{d\theta_3}{dx_1} & 0 & -\frac{d\theta_1}{dx_1} \\ -\frac{d\theta_2}{dx_1} & \frac{d\theta_1}{dx_1} & 0 \end{bmatrix} = \begin{bmatrix} 0 & -\frac{d\theta_3}{dx_1} & \frac{d\theta_2}{dx_1} \\ \frac{d\theta_3}{dx_1} & 0 & -\frac{d\theta_1}{dx_1} \\ -\frac{d\theta_2}{dx_1} & \frac{d\theta_1}{dx_1} & 0 \end{bmatrix},$$

after eliminating the higher–order terms. The vector of the rotational strain measures is thus

$$\boldsymbol{\kappa} = \begin{Bmatrix} \kappa_1 \\ \kappa_2 \\ \kappa_3 \end{Bmatrix} = \begin{Bmatrix} \frac{d\theta_1}{dx_1} \\ \frac{d\theta_2}{dx_1} \\ \frac{d\theta_3}{dx_1} \end{Bmatrix} = \frac{d\boldsymbol{\theta}}{dx_1}. \tag{11}$$

2.2.3 Constitutive equations

The constitutive law for a linear elastic material is given by

$$\mathbf{N} = \mathbf{C}_N \boldsymbol{\Gamma}\,, \quad \mathbf{M} = \mathbf{C}_M \boldsymbol{\kappa}\,, \tag{12}$$

where $\mathbf{C}_N = diag(EA, GA_2, GA_3)$ and $\mathbf{C}_M = diag(GI_t, EI_2, EI_3)$ are constant constitutive matrices of a linear elastic material. $\mathbf{N}$ and $\mathbf{M}$ are the stress and stress–couple resultant vectors. Here, E and G denote the Young's and shear modulus of the material, A is the cross–sectional area, A_2 and A_3 are the shear areas of the cross section, I_t is the torsional constant and I_2 and I_3 are the second moments of area of the cross–section.
Using (10) and (25), the stress resultant vector can be written as

$$\mathbf{N} = \begin{Bmatrix} EA\frac{du}{dx_1} \\ GA_2(\frac{dv}{dx_1} - \theta_3) \\ GA_3(\frac{dw}{dx_1} + \theta_2) \end{Bmatrix}, \tag{13}$$

and the stress–couple resultant vector can be written as

$$\mathbf{M} = \begin{Bmatrix} GI_t \frac{d\theta_1}{dx_1} \\ EI_2 \frac{d\theta_2}{dx_1} \\ EI_3 \frac{d\theta_3}{dx_1} \end{Bmatrix}. \tag{14}$$

2.2.4 Equilibrium equations

Differential equilibrium equations follow from the equilibrium of an infinitesimally small part of the beam of length dx_1 as shown in Figure 2.3. Here, $\mathbf{n}$ and $\mathbf{m}$ denote vectors of the applied distributed forces and torques.

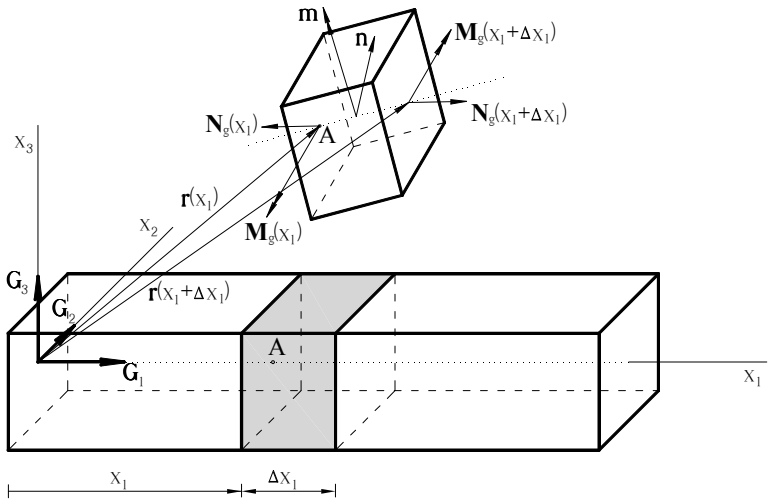

Figure 2.3: Equilibrium of an infinitesimal part of the beam in deformed state.

With $\mathbf{N}_g = \mathbf{\Lambda N}$ and $\mathbf{M}_g = \mathbf{\Lambda M}$ from Figure 2.3 force equilibrium follows as

$$-\mathbf{N}_g(x_1) + \mathbf{N}_g(x_1 + \Delta x_1) + \mathbf{n}\Delta x_1 = \mathbf{0},$$

and the torque equilibrium with respect to point A is

$$-\mathbf{M}_g(x_1) + \mathbf{M}_g(x_1 + \Delta x_1) + \mathbf{m}\Delta x_1 + \Big(\mathbf{r}(x_1 + \Delta x_1) - \mathbf{r}(x_1)\Big) \times \mathbf{N}_g(x_1 + \Delta x_1)$$

$$+\frac{1}{2}\Big(\mathbf{r}(x_1 + \Delta x_1) - \mathbf{r}(x_1)\Big) \times \mathbf{n}\Delta x_1 = \mathbf{0}$$

If both of these equations are divided by Δx_1, their limiting case (when $\Delta x_1 \to 0$) is

$$\frac{d\mathbf{N}_g}{dx_1} + \mathbf{n} = \mathbf{0} \tag{15}$$

$$\frac{d\mathbf{M}_g}{dx_1} + \frac{d\mathbf{r}}{dx_1} \times \mathbf{N}_g + \mathbf{m} = \mathbf{0}. \tag{16}$$

Inserting linear expressions (7), (13) and (14) into (15) and (16) and eliminating the non–linear terms that arise when multiplying $\mathbf{\Lambda}$ and $\mathbf{N}$ as well as $\mathbf{\Lambda}$ and $\mathbf{M}$, a system of two linear differential equations is obtained which is given as

$$\frac{d^3\boldsymbol{\theta}}{dx_1^3} = \mathbf{C}_M^{-1}\left(\mathbf{G}_1 \times \mathbf{n} - \frac{d\mathbf{m}}{dx_1}\right) \tag{17}$$

and

$$\frac{d^2\mathbf{r}}{dx^2} = -\mathbf{C}_N^{-1}\mathbf{n} - \mathbf{G}_1 \times \frac{d\boldsymbol{\theta}}{dx_1}. \tag{18}$$

These two equations define the Timoshenko beam problem for a straight beam of a uniform cross–section made of a linearly elastic material.
Solution of these differential equations (with the particular boundary conditions) are the vector functions $\mathbf{r}(x_1)$ and $\boldsymbol{\theta}(x_1)$ that describe the position of the deformed centroidal axis and the rotation distribution of the cross–section along the length of the beam.

Let us introduce the natural coordinate system and the following linear transformation

$$x_1 = \frac{L}{2}(1+\xi) \;\Leftrightarrow \xi = 2\frac{x_1}{L} - 1 \;\Rightarrow dx_1 = \frac{dx_1}{d\xi}d\xi = \frac{L}{2}d\xi.$$

With dimensionless loading functions

$$\boldsymbol{\mu} = \frac{L^3}{8}\mathbf{C}_M^{-1}\left(\mathbf{G}_1 \times \mathbf{n} - \frac{d\mathbf{m}}{dx_1}\right) \tag{19}$$

and

$$\boldsymbol{\nu} = \frac{L}{2}\mathbf{C}_N^{-1}\mathbf{n}\,, \tag{20}$$

equations (17) and (18) can be re–written as

$$\boldsymbol{\theta}''' = \boldsymbol{\mu}\,, \tag{21}$$

$$\mathbf{r}'' = -\frac{L}{2}(\boldsymbol{\nu} + \mathbf{G}_1 \times \boldsymbol{\theta}')\,. \tag{22}$$

Here, the prime (') denotes differentiation with respect to the natural coordinate ξ. Assuming the load is independent on the position or the rotation vector, solution of equations (21) and (22) is

$$\boldsymbol{\theta} = \iiint \boldsymbol{\mu}\, d\xi d\xi d\xi + \frac{1}{2}\mathbf{C}_1\xi^2 + \mathbf{C}_2\xi + \mathbf{C}_3 \tag{23}$$

$$\mathbf{r} = -\frac{L}{2}\left[\iint \boldsymbol{\nu} d\xi d\xi + \mathbf{C}_4\xi + \mathbf{C}_5 + \mathbf{G}_1 \times \left(\iiint\int \boldsymbol{\mu} d\xi d\xi d\xi d\xi + \frac{1}{6}\mathbf{C}_1\xi^3 + \frac{1}{2}\mathbf{C}_2\xi^2\right)\right], \tag{24}$$

where $\mathbf{C}_1, ..., \mathbf{C}_5$ represent vector integration constants which are to be determined from the boundary conditions.
Strain measures given in (10) and (25) can now be written using the solutions of the differential equations given above, allowing us to write them in terms of the integration constants $\mathbf{C}_1, ...\mathbf{C}_4$ as

$$\boldsymbol{\kappa} = \frac{2}{L}\left(\iint \boldsymbol{\mu} d\xi d\xi + \mathbf{C}_1\xi + \mathbf{C}_2\right), \tag{25}$$

$$\boldsymbol{\Gamma} = -\int \boldsymbol{\nu} d\xi - \mathbf{C}_4 + \mathbf{G}_1 \times \mathbf{C}_3 - \mathbf{G}_1. \tag{26}$$

The equations (25)–(26) represent relation between the strain measures $\boldsymbol{\Gamma}$ and $\boldsymbol{\kappa}$ and dimensionless loading functions $\boldsymbol{\mu}$ and $\boldsymbol{\nu}$. The translational strain measures $\boldsymbol{\Gamma}$ are described by a polynomial one order higher than the loading function $\boldsymbol{\nu}$, i.e. for a polynomial force loading $\mathbf{n}$ of order N, the translational strain measures are always a polynomial of order $N + 1$. On the other hand, the rotational strain measures are described by a polynomial two degrees higher than the polynomial that is describing the loading function $\boldsymbol{\mu}$.

2.3 Problem–dependent exact finite–element representation of the solution

Integration constants in (23) and (24) can be computed from a sufficient number of kinematic or static boundary conditions. They can be expressed in terms of the known boundary values for $\boldsymbol{\theta}$ and $\mathbf{r}$ thus leading to a finite element capable of providing the analytic solution [27].

2.3.1 Kinematic boundary conditions

We will evaluate equations (23) and (24) at the boundaries ($\xi = -1$ and $\xi = 1$) to obtain the kinematic boundary conditions. By doing so, we can write

$$\frac{1}{2}\mathbf{C}_1 - \mathbf{C}_2 + \mathbf{C}_3 = \boldsymbol{\theta}_0 \tag{27}$$

$$\frac{1}{2}\mathbf{C}_1 + \mathbf{C}_2 + \mathbf{C}_3 = \boldsymbol{\theta}_L - \bar{\boldsymbol{\mu}} \tag{28}$$

$$-\mathbf{C}_4 + \mathbf{C}_5 + \mathbf{G}_1 \times \left(-\frac{1}{6}\mathbf{C}_1 + \frac{1}{2}\mathbf{C}_2\right) = -\frac{2}{L}\mathbf{r}_0 \tag{29}$$

$$\mathbf{C}_4 + \mathbf{C}_5 + \mathbf{G}_1 \times \left(\frac{1}{6}\mathbf{C}_1 + \frac{1}{2}\mathbf{C}_2\right) = -\frac{2}{L}\mathbf{r}_L - \bar{\boldsymbol{\nu}}, \tag{30}$$

where

$$\bar{\boldsymbol{\mu}} = \int_{-1}^{1}\iint \boldsymbol{\mu} d\xi d\xi d\xi, \qquad \bar{\boldsymbol{\nu}} = \int_{-1}^{1}\int \left(\boldsymbol{\nu} + \mathbf{G}_1 \times \iint \boldsymbol{\mu} d\xi d\xi\right) d\xi d\xi. \tag{31}$$

Integration constants $\mathbf{C}_2$ and $\mathbf{C}_5$ can be computed respectively if expression (27) is subtracted from expression (28) and if the expressions (29) and (30) are summed together. This leaves us with

$$\mathbf{C}_2 = \frac{1}{2}\left(\boldsymbol{\theta}_L - \boldsymbol{\theta}_0\right) - \frac{1}{2}\bar{\boldsymbol{\mu}} \tag{32}$$

$$\mathbf{C}_5 = -\frac{1}{L}\left(\mathbf{r}_0 + \mathbf{r}_L\right) - \frac{1}{4}\mathbf{G}_1 \times \left(\boldsymbol{\theta}_L - \boldsymbol{\theta}_0\right) - \frac{1}{2}\bar{\boldsymbol{\nu}} + \frac{1}{4}\mathbf{G}_1 \times \bar{\boldsymbol{\mu}}. \tag{33}$$

The remaining integration constants can be written in terms of the other constants, therefore summing up equations (27) and (28) and subtracting expression (29) from (30) enables us to write constants $\mathbf{C}_3$ and $\mathbf{C}_4$ in terms of $\mathbf{C}_1$ as

$$\mathbf{C}_3 = \frac{1}{2}\left(\boldsymbol{\theta}_L + \boldsymbol{\theta}_0\right) - \frac{1}{2}\bar{\boldsymbol{\mu}} - \frac{1}{2}\mathbf{C}_1 \tag{34}$$

and

$$\mathbf{C}_4 = -\frac{1}{L}\left(\mathbf{r}_L - \mathbf{r}_0\right) - \frac{1}{2}\bar{\boldsymbol{\nu}} - \frac{1}{6}\mathbf{G}_1 \times \mathbf{C}_1. \tag{35}$$

One more condition is thus needed to evaluate constants $\mathbf{C}_1$, $\mathbf{C}_3$ and $\mathbf{C}_4$ and they will be calculated using the equilibrium of the beam.

2.3.2 Static boundary conditions

Let our beam of length L be subjected to point forces and torques $\mathbf{F}_0$ and $\mathbf{T}_0$ at $x_1 = 0$ and $\mathbf{F}_L$, $\mathbf{T}_L$ at $x_1 = L$ and also to distributed force and moment loadings $\mathbf{n}$ and $\mathbf{m}$ as shown in Figure 2.4.

The equilibrium equations of the whole beam in the reference configuration read

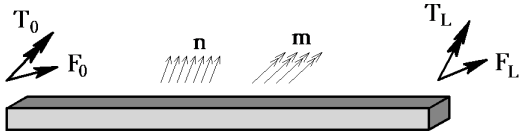

Figure 2.4: Load acting on the reference line of the beam, here taken to be the centroidal axis.

$$\mathbf{F}_0 + \mathbf{F}_L + \int_0^L \mathbf{n} dx_1 = \mathbf{0} \tag{36}$$

and

$$\mathbf{T}_0 + \mathbf{T}_L + L\mathbf{G}_1 \times \mathbf{F}_L + \int_0^L (\mathbf{m} + x_1 \mathbf{G}_1 \times \mathbf{n}) dx_1 = \mathbf{0}. \tag{37}$$

Noting the static boundary conditions $\mathbf{F}_0 = -\mathbf{N}_0$, $\mathbf{T}_0 = -\mathbf{M}_0$, $\mathbf{F}_L = \mathbf{N}_L$ and $\mathbf{T}_L = \mathbf{M}_L$, constitutive equations (12), and evaluating the strain measures at the boundaries, the above equations turn into

$$-\mathbf{C}_N \int_{-1}^{1} \boldsymbol{\nu} d\xi + \int_0^L \mathbf{n} dx_1 = \mathbf{0}, \tag{38}$$

$$\frac{2}{L}\mathbf{C}_M \left(\int_{-1}^{1} \int \boldsymbol{\mu} d\xi d\xi + 2\mathbf{C}_1 \right) + L\mathbf{G}_1 \times \mathbf{C}_N \left(- \int_{-1}^{1} \boldsymbol{\nu} d\xi - \mathbf{C}_4 + \mathbf{G}_1 \times \mathbf{C}_3 - \mathbf{G}_1 \right) + \int_0^L (\mathbf{m} + x_1 \mathbf{G}_1 \times \mathbf{n}) \, dx_1 = \mathbf{0}. \tag{39}$$

The first of these equations is identical as equation (20), hence does not represent additional equation required to evaluate the integration constants. With already introduced substitution $x_1 = \frac{L}{2}(1 + \xi)$, we are able to simplify the sum of the first and the second term in (39)

$$\frac{2}{L}\mathbf{C}_M \int_{-1}^{1} \int \boldsymbol{\mu} d\xi d\xi + \int_0^L (\mathbf{m} + x_1 \mathbf{G}_1 \times \mathbf{n}) \, dx_1 = \frac{L}{2} \int_{-1}^{1} \left(\mathbf{G}_1 \times \mathbf{C}_N \int \boldsymbol{\nu} d\xi - \mathbf{m} \right) d\xi +$$

$$\frac{L}{2} \int_{-1}^{1} [\mathbf{m} + (1 + \xi)\mathbf{G}_1 \times \mathbf{C}_N \boldsymbol{\nu}] \, d\xi = \frac{L}{2} \mathbf{G}_1 \times \mathbf{C}_N \int_{-1}^{1} \left[(1 + \xi)\boldsymbol{\nu} + \int \boldsymbol{\nu} d\xi \right] d\xi,$$

which when considered the moment equilibrium equation (39) and noting that $\mathbf{G}_1 \times$

$\mathbf{C}_N\mathbf{G}_1 = \mathbf{0}$ gives

$$\frac{4}{L}\mathbf{C}_M\mathbf{C}_1 + L\mathbf{G}_1 \times \mathbf{C}_N(\mathbf{G}_1 \times \mathbf{C}_3 - \mathbf{C}_4) = \frac{L}{2}\mathbf{G}_1 \times \mathbf{C}_N\bar{\boldsymbol{\eta}}, \tag{40}$$

where,

$$\bar{\boldsymbol{\eta}} = \int_{-1}^{N}\left[(1-\xi)\boldsymbol{\nu} - \int \boldsymbol{\nu} d\xi\right] d\xi. \tag{41}$$

With five equations (27), (28), (29), (30), (40) defining the boundary conditions, all five integration constants can be determined. Constants $\mathbf{C}_2$ and $\mathbf{C}_5$ have been determined earlier and are given by (32) and (33) respectively. Remaining three constants $\mathbf{C}_1$, $\mathbf{C}_3$ and $\mathbf{C}_4$ are obtained from (34), (35), (40) and are given as follows:

$$\mathbf{C}_1 = -\mathbf{A}\left[\frac{1}{L}(\mathbf{r}_L - \mathbf{r}_0) + \frac{1}{2}\hat{\mathbf{G}}_1(\boldsymbol{\theta}_0 + \boldsymbol{\theta}_L) - \frac{1}{2}\bar{\boldsymbol{\eta}} - \frac{1}{2}\hat{\mathbf{G}}_1\bar{\boldsymbol{\mu}} + \frac{1}{2}\bar{\boldsymbol{\nu}}\right], \tag{42}$$

$$\mathbf{C}_3 = \frac{1}{2L}\mathbf{A}(\mathbf{r}_L - \mathbf{r}_0) + \frac{1}{2}\left(\mathbf{I} + \frac{1}{2}\mathbf{A}\hat{\mathbf{G}}_1\right)(\boldsymbol{\theta}_0 + \boldsymbol{\theta}_L) - \frac{1}{4\mathbf{A}}\bar{\boldsymbol{\eta}} - \frac{1}{2}\left(\mathbf{I} + \frac{1}{2}\mathbf{A}\hat{\mathbf{G}}_1\right)\bar{\boldsymbol{\mu}} + \frac{1}{4}\mathbf{A}\bar{\boldsymbol{\nu}} \tag{43}$$

and

$$\mathbf{C}_4 = -\left(\mathbf{I} - \frac{1}{6}\hat{\mathbf{G}}_1\mathbf{A}\right)\left[\frac{1}{L}(\mathbf{r}_L - \mathbf{r}_0) + \frac{1}{2}\bar{\boldsymbol{\nu}}\right] + \frac{1}{12}\hat{\mathbf{G}}_1\mathbf{A}\left[\hat{\mathbf{G}}_1(\boldsymbol{\theta}_0 + \boldsymbol{\theta}_L - \bar{\boldsymbol{\mu}}) - \bar{\boldsymbol{\eta}}\right], \tag{44}$$

with

$$\mathbf{A} = \frac{L^2}{4}\left(\mathbf{C}_M - \frac{L^2}{12}\hat{\mathbf{G}}_1\mathbf{C}_N\hat{\mathbf{G}}_1\right)^{-1}\hat{\mathbf{G}}_1\mathbf{C}_N = 3\begin{bmatrix} 0 & 0 & 0 \\ 0 & 0 & -\dfrac{1}{1+\phi_3} \\ 0 & \dfrac{1}{1+\phi_2} & 0 \end{bmatrix}, \tag{45}$$

where

$$\phi_2 = \frac{12EI_3}{L^2GA_2} \tag{46}$$

$$\phi_3 = \frac{12EI_2}{L^2GA_3}. \tag{47}$$

2.3.3 Exact solution in terms of the boundary kinematics and the problem data

Having determined all the integration constants $\mathbf{C}_1, ..., \mathbf{C}_5$, exact solutions of the differential equations (23) and (24) can now be expressed in terms of the boundary kine-

matics and the problem data. The exact solution for the rotation field thus becomes

$$\boldsymbol{\theta} = [\mathbf{R}_{r0} \;\; \mathbf{R}_{\theta 0} \;\; \mathbf{R}_{rL} \;\; \mathbf{R}_{\theta L}] \begin{Bmatrix} \mathbf{r}_0 \\ \boldsymbol{\theta}_0 \\ \mathbf{r}_L \\ \boldsymbol{\theta}_L \end{Bmatrix} + [\mathbf{0} \;\; \mathbf{R}_{rL} \;\; \mathbf{R}_{\theta L}] \begin{Bmatrix} \frac{L}{2}\bar{\boldsymbol{\eta}} \\ \frac{L}{2}(\bar{\boldsymbol{\nu}} - \bar{\boldsymbol{\eta}}) \\ -\bar{\boldsymbol{\mu}} \end{Bmatrix} + \iiint \boldsymbol{\mu} d\xi d\xi d\xi, \quad (48)$$

where

$$\mathbf{R}_{r0} = -\frac{1-\xi^2}{2L}\mathbf{A} \quad (49)$$

$$\mathbf{R}_{\theta 0} = \frac{1}{2}\left[\left(\mathbf{I} + \frac{1}{2}\mathbf{A}\hat{\mathbf{G}}_1\right) - \mathbf{I}\xi - \frac{1}{2}\mathbf{A}\hat{\mathbf{G}}_1\xi^2\right] \quad (50)$$

$$\mathbf{R}_{rL} = \frac{1-\xi^2}{2L}\mathbf{A} \quad (51)$$

$$\mathbf{R}_{\theta L} = \frac{1}{2}\left[\left(\mathbf{I} + \frac{1}{2}\mathbf{A}\hat{\mathbf{G}}_1\right) + \mathbf{I}\xi - \frac{1}{2}\mathbf{A}\hat{\mathbf{G}}_1\xi^2\right]. \quad (52)$$

The exact solution for the displacement field expressed in terms of the boundary kinematics and the problem data becomes

$$\mathbf{r} = [\mathbf{P}_{r0} \;\; \mathbf{P}_{\theta 0} \;\; \mathbf{P}_{rL} \;\; \mathbf{P}_{\theta L}] \begin{Bmatrix} \mathbf{r}_0 \\ \boldsymbol{\theta}_0 \\ \mathbf{r}_L \\ \boldsymbol{\theta}_L \end{Bmatrix} + \left[\frac{1+\xi}{2}\mathbf{I} \;\; \mathbf{P}_{rL} \;\; \mathbf{P}_{\theta L}\right] \begin{Bmatrix} \frac{L}{2}\bar{\boldsymbol{\eta}} \\ \frac{L}{2}(\bar{\boldsymbol{\nu}} - \bar{\boldsymbol{\eta}}) \\ -\bar{\boldsymbol{\mu}} \end{Bmatrix} - \frac{L}{2}\iint \left(\boldsymbol{\nu} + \hat{\mathbf{G}}_1 \iint \boldsymbol{\mu} d\xi d\xi\right) d\xi d\xi, \quad (53)$$

with

$$\mathbf{P}_{r0} = \frac{1-\xi}{2}\mathbf{I} + \xi\frac{1-\xi^2}{12}\hat{\mathbf{G}}_1\mathbf{A} \quad (54)$$

$$\mathbf{P}_{\theta 0} = \frac{L}{8}\left[-\hat{\mathbf{G}}_1 - \frac{\xi}{3}\hat{\mathbf{G}}_1\mathbf{A}\hat{\mathbf{G}}_1 + \xi^2\hat{\mathbf{G}}_1 + \frac{\xi^3}{3}\hat{\mathbf{G}}_1\mathbf{A}\hat{\mathbf{G}}_1\right] \quad (55)$$

$$\mathbf{P}_{rL} = \frac{1+\xi}{2}\mathbf{I} - \xi\frac{1-\xi^2}{12}\hat{\mathbf{G}}_1\mathbf{A} \quad (56)$$

$$\mathbf{P}_{\theta L} = \frac{L}{8}\left[\hat{\mathbf{G}}_1 - \frac{\xi}{3}\hat{\mathbf{G}}_1\mathbf{A}\hat{\mathbf{G}}_1 - \xi^2\hat{\mathbf{G}}_1 + \frac{\xi^3}{3}\hat{\mathbf{G}}_1\mathbf{A}\hat{\mathbf{G}}_1\right]. \tag{57}$$

It should be noted that, for a 2D case, the functions in (49)-(52)and (54)–(57) coincide with the results given by Rakowski [30] in Table 1.

Yunhua introduced *field–consistent interpolation* in [40] and Reddy introduced *interdependent interpolation* in [31]. The denominations *consistent* and *interdependent* originate from the consistence of interpolation between the kinematic fields and the interdependence between the fields. These interpolations are independent of the beam material and cross–sectional properties, which is exactly the opposite from the solutions proposed in (48) and (53) of this work. And for this reason, we call the interpolations introduced here the *problem–dependent interpolation*.

2.3.4 Finite element implementation of the problem-dependent interpolation

Equations (48) and (53) can be used to derive the beam equilibrium in the finite–element sense, using e.g. the principle of stationarity of the total potential energy $V = V_{def} - U$, where V_{def} is the strain energy and U is the potential of the applied loading. The strain energy is defined as

$$V_{def} = \frac{1}{2}\int_0^L \left\langle \boldsymbol{\Gamma}^T \;\; \boldsymbol{\kappa}^T \right\rangle \begin{bmatrix} \mathbf{C}_N & \mathbf{0} \\ \mathbf{0} & \mathbf{C}_M \end{bmatrix} \begin{Bmatrix} \boldsymbol{\Gamma} \\ \boldsymbol{\kappa} \end{Bmatrix} dx_1, \tag{58}$$

and the potential of the applied loading is

$$U = \int_0^L \left\langle \mathbf{u}^T \;\; \boldsymbol{\theta}^T \right\rangle \begin{Bmatrix} \mathbf{n} \\ \mathbf{m} \end{Bmatrix} dx_1 + \left\langle \mathbf{u}_0^T \;\; \boldsymbol{\theta}_0^T \right\rangle \begin{Bmatrix} \mathbf{F}_0 \\ \mathbf{T}_0 \end{Bmatrix} + \left\langle \mathbf{u}_L^T \;\; \boldsymbol{\theta}_L^T \right\rangle \begin{Bmatrix} \mathbf{F}_L \\ \mathbf{T}_L \end{Bmatrix}. \tag{59}$$

For the conservative loading and the considered beam problem the principle of minimum total potential energy reads

$$\begin{aligned} \delta V = \delta V_{def} - \delta U = \int_0^L \left\langle \delta\boldsymbol{\Gamma}^T \;\; \delta\boldsymbol{\kappa}^T \right\rangle \begin{bmatrix} \mathbf{C}_N & \mathbf{0} \\ \mathbf{0} & \mathbf{C}_M \end{bmatrix} \begin{Bmatrix} \boldsymbol{\Gamma} \\ \boldsymbol{\kappa} \end{Bmatrix} dx_1 - \int_0^L \left\langle \delta\mathbf{u}^T \;\; \delta\boldsymbol{\theta}^T \right\rangle \begin{Bmatrix} \mathbf{n} \\ \mathbf{m} \end{Bmatrix} dx_1 \\ - \left\langle \delta\mathbf{u}_0^T \;\; \delta\boldsymbol{\theta}_0^T \right\rangle \begin{Bmatrix} \mathbf{F}_0 \\ \mathbf{T}_0 \end{Bmatrix} - \left\langle \delta\mathbf{u}_L^T \;\; \delta\boldsymbol{\theta}_L^T \right\rangle \begin{Bmatrix} \mathbf{F}_L \\ \mathbf{T}_L \end{Bmatrix}, \end{aligned} \tag{60}$$

where $\delta\boldsymbol{\Gamma}$, $\delta\boldsymbol{\kappa}$, $\delta\mathbf{u}$, $\delta\boldsymbol{\theta}$ are the variations of the translational and rotational strain measures, displacements and rotation. Substituting strain measures from (10, 25) gives

$$\delta V_{def} = \int_{-1}^{1} \left\langle \delta \mathbf{u}'^T \;\; \delta\boldsymbol{\theta}^T \;\; \delta\boldsymbol{\theta}'^T \right\rangle \begin{bmatrix} \frac{2}{L}\mathbf{C}_N & \mathbf{C}_N\hat{\mathbf{G}}_1 & \mathbf{0} \\ -\hat{\mathbf{G}}_1\mathbf{C}_N & -\frac{L}{2}\hat{\mathbf{G}}_1\mathbf{C}_N\hat{\mathbf{G}}_1 & \mathbf{0} \\ \mathbf{0} & \mathbf{0} & \frac{2}{L}\mathbf{C}_M \end{bmatrix} \begin{Bmatrix} \mathbf{u}' \\ \boldsymbol{\theta} \\ \boldsymbol{\theta}' \end{Bmatrix} d\xi \tag{61}$$

and

$$\delta U = \left\langle \delta\mathbf{u}_0^T \;\; \delta\boldsymbol{\theta}_0^T \;\; \delta\mathbf{u}_L^T \;\; \delta\boldsymbol{\theta}_L^T \right\rangle \underbrace{\left(\frac{L}{2}\int_{-1}^{1} \begin{bmatrix} \mathbf{P}_{r0}^T & \mathbf{R}_{r0}^T \\ \mathbf{P}_{\theta 0}^T & \mathbf{R}_{\theta 0}^T \\ \mathbf{P}_{rL}^T & \mathbf{R}_{rL}^T \\ \mathbf{P}_{\theta L}^T & \mathbf{R}_{\theta L}^T \end{bmatrix} \begin{Bmatrix} \mathbf{n} \\ \mathbf{m} \end{Bmatrix} d\xi + \begin{Bmatrix} \mathbf{F}_0 \\ \mathbf{T}_0 \\ \mathbf{F}_L \\ \mathbf{T}_L \end{Bmatrix} \right)}_{\mathbf{R}} . \tag{62}$$

Substituting (48) and (53) into the minimum of the total potential energy results in a standard finite–element equilibrium

$$\delta\mathbf{p}^T(\mathbf{K}\mathbf{p} - \mathbf{R}) = 0 \quad \Longrightarrow \quad \mathbf{K}\mathbf{p} - \mathbf{R} = \mathbf{0}, \tag{63}$$

where $\mathbf{p}^T = \left\langle \mathbf{u}_0^T \;\; \boldsymbol{\theta}_0^T \;\; \mathbf{u}_L^T \;\; \boldsymbol{\theta}_L^T \right\rangle$, $\mathbf{K}$ is the element stiffness matrix and $\mathbf{R}$ is the vector of the equivalent nodal loading given in (62). The stiffness matrix and the equivalent loading vector obtained in this way are identical to the ones obtained from the engineering beam theory given in [29]. That this is so in the case of the stiffness matrix, it is obvious from (61) after terms with $\mathbf{u}'$ and $\boldsymbol{\theta}'$ are integrated by parts

$$\begin{aligned} \delta V_{def} = \delta\mathbf{p}^T\mathbf{K}\mathbf{p} = & \left(\left\langle \delta\mathbf{u}'^T \;\; \delta\boldsymbol{\theta}^T \;\; \delta\boldsymbol{\theta}'^T \right\rangle \begin{bmatrix} \frac{2}{L}\mathbf{C}_N & \mathbf{0} \\ -\hat{\mathbf{G}}_1\mathbf{C}_N & \mathbf{0} \\ \mathbf{0} & \frac{2}{L}\mathbf{C}_M \end{bmatrix} \begin{Bmatrix} \mathbf{u} \\ \boldsymbol{\theta} \end{Bmatrix} \right) \Bigg|_{-1}^{1} \\ & - \frac{2}{L}\int_{-1}^{1} \left\{ \left[\mathbf{C}_N(\delta\mathbf{r}' + \frac{L}{2}\hat{\mathbf{G}}_1\delta\boldsymbol{\theta})' \right] \mathbf{u} + \left[\mathbf{C}_M\delta\boldsymbol{\theta}''' + \hat{\mathbf{G}}_1\mathbf{C}_N\frac{L}{2}(\delta\mathbf{r}' + \frac{L}{2}\hat{\mathbf{G}}_1\delta\boldsymbol{\theta}) \right] \boldsymbol{\theta} \right\} d\xi \, , \end{aligned} \tag{64}$$

where the second term vanishes since the expression in the brackets represent the variations of the differential equations. This is the sufficient condition for a finite–element formulation to result in the exact nodal solution, as it is shown in the Appendix H of [42]. The stiffness matrix for the problem-dependent interpolation follows from (64) as

$$\mathbf{K} = \frac{2}{L}\left(\begin{bmatrix} (\mathbf{P}'_{r0} + \frac{L}{2}\hat{\mathbf{G}}_1\mathbf{R}_{r0})^T & \mathbf{R}'^T_{r0} \\ (\mathbf{P}'_{\theta 0} + \frac{L}{2}\hat{\mathbf{G}}_1\mathbf{R}_{\theta 0})^T & \mathbf{R}'^T_{\theta 0} \\ (\mathbf{P}'_{rL} + \frac{L}{2}\hat{\mathbf{G}}_1\mathbf{R}_{rL})^T & \mathbf{R}'^T_{rL} \\ (\mathbf{P}'_{\theta L} + \frac{L}{2}\hat{\mathbf{G}}_1\mathbf{R}_{\theta L})^T & \mathbf{R}'^T_{\theta L} \end{bmatrix} \begin{bmatrix} \mathbf{C}_N & \mathbf{0} \\ \mathbf{0} & \mathbf{C}_M \end{bmatrix} \begin{bmatrix} \mathbf{P}_{r0} & \mathbf{P}_{\theta 0} & \mathbf{P}_{rL} & \mathbf{P}_{\theta L} \\ \mathbf{R}_{r0} & \mathbf{R}_{\theta 0} & \mathbf{R}_{rL} & \mathbf{R}_{\theta L} \end{bmatrix} \right) \Bigg|_{-1}^{1} \tag{65}$$

Substituting (49)–(52) and (54)–(57) in the first matrix of the above expression and multiplying it with the constitutive matrix gives

$$\mathbf{K} = \frac{2}{L}\left(\begin{bmatrix} -\frac{1}{2}(\mathbf{I} + \frac{1}{3}\hat{\mathbf{G}}_1\mathbf{A})\mathbf{C}_N & \frac{\xi}{L}\mathbf{A}^T\mathbf{C}_M \\ -\frac{L}{4}\hat{\mathbf{G}}_1(\mathbf{I} + \frac{1}{3}\hat{\mathbf{G}}_1\mathbf{A})\mathbf{C}_N & -\frac{1}{2}(\mathbf{I} + \xi\mathbf{A}\hat{\mathbf{G}}_1)\mathbf{C}_M \\ \frac{1}{2}(\mathbf{I} + \frac{1}{3}\hat{\mathbf{G}}_1\mathbf{A})\mathbf{C}_N & -\frac{\xi}{L}\mathbf{A}^T\mathbf{C}_M \\ -\frac{L}{4}\hat{\mathbf{G}}_1(\mathbf{I} + \frac{1}{3}\hat{\mathbf{G}}_1\mathbf{A})\mathbf{C}_N & \frac{1}{2}(\mathbf{I} - \xi\mathbf{A}\hat{\mathbf{G}}_1)\mathbf{C}_M \end{bmatrix} \begin{bmatrix} \mathbf{P}_{r0} & \mathbf{P}_{\theta 0} & \mathbf{P}_{rL} & \mathbf{P}_{\theta L} \\ \mathbf{R}_{r0} & \mathbf{R}_{\theta 0} & \mathbf{R}_{rL} & \mathbf{R}_{\theta L} \end{bmatrix} \right) \Bigg|_{-1}^{1} \tag{66}$$

With $\frac{L}{4}\hat{\mathbf{G}}_1(\mathbf{I} + \frac{1}{3}\hat{\mathbf{G}}_1\mathbf{A})\mathbf{C}_N = \frac{1}{L}\mathbf{C}_M\mathbf{A}$ and substituting (49)–(52) and (54)–(57) in the second matrix of the upper expression finally gives the stiffness matrix in a form

$$\mathbf{K} = \begin{bmatrix} \frac{1}{L}(\mathbf{I} + \frac{1}{3}\hat{\mathbf{G}}_1\mathbf{A})\mathbf{C}_N & & & \textit{Symm.} \\ \frac{2}{L^2}\mathbf{C}_M\mathbf{A} & \frac{1}{L}(\mathbf{I} - \mathbf{A}\hat{\mathbf{G}}_1)\mathbf{C}_M & & \\ -\frac{1}{L}(\mathbf{I} + \frac{1}{3}\hat{\mathbf{G}}_1\mathbf{A})\mathbf{C}_N & -\frac{2}{L^2}\mathbf{A}^T\mathbf{C}_M & \frac{1}{L}(\mathbf{I} + \frac{1}{3}\hat{\mathbf{G}}_1\mathbf{A})\mathbf{C}_N & \\ \frac{2}{L^2}\mathbf{C}_M\mathbf{A} & -\frac{1}{L}(\mathbf{I} + \mathbf{A}\hat{\mathbf{G}}_1)\mathbf{C}_M & -\frac{2}{L^2}\mathbf{C}_M\mathbf{A} & \frac{1}{L}(\mathbf{I} - \mathbf{A}\hat{\mathbf{G}}_1)\mathbf{C}_M \end{bmatrix}. \tag{67}$$

If the blocks of the stiffness matrix are written in terms of coefficients ϕ_2 and ϕ_3 from (46)–(47), it follows that

$$\frac{1}{L}(\mathbf{I} + \frac{1}{3}\hat{\mathbf{G}}_1\mathbf{A})\mathbf{C}_N = \begin{bmatrix} \frac{EA}{L} & 0 & 0 \\ 0 & \frac{12EI_3}{L^3(1+\phi_2)} & 0 \\ 0 & 0 & \frac{12EI_2}{L^3(1+\phi_3)} \end{bmatrix},$$

$$\frac{2}{L^2}\mathbf{C}_M\mathbf{A} = \begin{bmatrix} 0 & 0 & 0 \\ 0 & 0 & -\frac{6EI_2}{L^2(1+\phi_3)} \\ 0 & \frac{6EI_3}{L^2(1+\phi_2)} & 0 \end{bmatrix},$$

$$\frac{1}{L}(\mathbf{I}-\mathbf{A}\hat{\mathbf{G}}_1)\mathbf{C}_M=\begin{bmatrix}\dfrac{GI_t}{L} & 0 & 0\\ 0 & \dfrac{4+\phi_3}{1+\phi_3}\dfrac{EI_2}{L} & 0\\ 0 & 0 & \dfrac{4+\phi_2}{1+\phi_2}\dfrac{EI_3}{L}\end{bmatrix},$$

$$-\frac{1}{L}(\mathbf{I}+\mathbf{A}\hat{\mathbf{G}}_1)\mathbf{C}_M=\begin{bmatrix}-\dfrac{GI_t}{L} & 0 & 0\\ 0 & \dfrac{2-\phi_3}{1+\phi_3}\dfrac{EI_2}{L} & 0\\ 0 & 0 & \dfrac{2-\phi_2}{1+\phi_2}\dfrac{EI_3}{L}\end{bmatrix}.$$

These block matrices are the same as the result given by Przemieniecki in [29].

With $\mathbf{R}$ and $\mathbf{K}$ from (62) and (67) we write the element equilibrium $\mathbf{Kp}-\mathbf{R}=\mathbf{0}$ that enables us to obtain the nodal degrees of freedom $\mathbf{p}$ within the standard finite–element procedure. In this way the exact analytical distribution of the displacement and rotation fields follows from the problem–dependent interpolation defined by (53) and (48). Further, the exact analytical distribution of the strain measures and the stress and stress–couple resultants follow from (10) and (25).

2.4 Problem–independent exact finite–element representation of the solution

In the previous subsection a problem–dependent interpolation has been described. This interpolation depends on a minimum number of the unknown parameters, that include boundary positions and rotations, but also on the material and cross–sectional properties $\mathbf{C}_N$, $\mathbf{C}_M$ and the loading functions $\boldsymbol{\mu}(\xi)$ and $\boldsymbol{\nu}(\xi)$. For the mechanical problem considered here (linear problem, straight beam, constant cross section, static loading) there is very little motivation for re–shaping this result in an alternative form with additional nodal degrees of freedom, but such alternatives may become interesting in the situations where complete adherence to the analytical solution cannot be claimed. In materially non–linear problems, an additional internal kinematic constraint can be a better choice than the static boundary condition.

If the loading functions are given as polynomials of an arbitrary order:

$$\boldsymbol{\mu}=\sum_{i=0}^{m}\boldsymbol{\mu}_i\xi^i \quad \text{and} \quad \boldsymbol{\nu}=\sum_{i=0}^{n}\boldsymbol{\nu}_i\xi^i, \tag{68}$$

solutions of the differential equations (23) and (24) can be written in terms of finite number of parameters $\mathbf{C}_1,...\mathbf{C}_5,\boldsymbol{\mu}_0,...\boldsymbol{\mu}_m,\boldsymbol{\nu}_0,...\boldsymbol{\nu}_n$ in the following way

$$\boldsymbol{\theta} = \sum_{i=0}^{m} \frac{1}{i+3}\frac{1}{i+2}\frac{1}{i+1}\boldsymbol{\mu}_i \xi^{i+3} + \frac{1}{2}\mathbf{C}_1\xi^2 + \mathbf{C}_2\xi + \mathbf{C}_3, \tag{69}$$

$$\mathbf{r} = -\frac{L}{2}\Bigg[\sum_{i=0}^{n} \frac{1}{i+2}\frac{1}{i+1}\boldsymbol{\nu}_i \xi^{i+2} + \mathbf{C}_4\xi + \mathbf{C}_5 + \mathbf{G}_1 \times \left(\sum_{i=0}^{m} \frac{1}{i+4}\frac{1}{i+3}\frac{1}{i+2}\frac{1}{i+1}\boldsymbol{\mu}_i \xi^{i+4} + \frac{1}{6}\mathbf{C}_1\xi^3 + \frac{1}{2}\mathbf{C}_2\xi^2\right)\Bigg]. \tag{70}$$

These two expressions may be re–written in terms of the known nodal positions and rotation and in this way we may construct a so-called displacement–based finite element with exact polynomial interpolation. In the following subsections the exact solutions for the rotation and the position fields will be given in terms of the nodal rotations and nodal positions.

2.4.1 Exact solution for the rotation field

This solution for the rotational field will be given in terms of the nodal rotations. First, let us re–write expression (69) as

$$\boldsymbol{\theta}(\xi) = \sum_{q=0}^{m+3} \boldsymbol{\alpha}_q \xi^q, \tag{71}$$

where $\boldsymbol{\alpha}_0 = \mathbf{C}_3$, $\boldsymbol{\alpha}_1 = \mathbf{C}_2$, $\boldsymbol{\alpha}_2 = \frac{1}{2}\mathbf{C}_1$ and $\boldsymbol{\alpha}_q = \frac{1}{q}\frac{1}{q-1}\frac{1}{q-2}\boldsymbol{\mu}_{q-3}$ for $3 \leq q \leq m+3$. A finite element interpolation for the rotation field has to be of order $m+3$ or higher in order to provide the exact solution. For the chosen co–ordinates $\xi_1, ...\xi_M$, where the number of nodes M has to be $M \geq m+4$ ($M \geq 3$ if $\boldsymbol{\mu} = \mathbf{0}$), the nodal rotations are

$$\boldsymbol{\theta}_1 = \boldsymbol{\theta}(\xi_1), ...\boldsymbol{\theta}_M = \boldsymbol{\theta}(\xi_M).$$

Evaluating (71) at these points results in M conditions on the nodal rotations $\boldsymbol{\alpha}_0, ...\boldsymbol{\alpha}_{m+3}$.

To express this conditions in the terms of the nodal rotations $\boldsymbol{\theta}_1, ...\boldsymbol{\theta}_M$, let us re–write (71) as

$$\boldsymbol{\theta}(\xi) = \sum_{q=0}^{m+3} \boldsymbol{\alpha}_q \xi^q + \sum_{q=m+4}^{M-1} \overbrace{\boldsymbol{\alpha}_q}^{=0} \xi^q = \sum_{q=0}^{M-1} \boldsymbol{\alpha}_q \xi^q, \tag{72}$$

and evaluate it at the chosen nodal co–ordinates $\xi_1, ...\xi_M$ to obtain

$$\sum_{q=0}^{M-1} \xi_i^q \boldsymbol{\alpha}_q = \boldsymbol{\theta}_i, \quad i = 1, ..., M. \tag{73}$$

The above expression presents the system of linear equations where the coefficients constitute the so–called Vandermonde matrix. This matrix can be explicitly inverted as reported in e.g. [14, 13, 12]. The columns of this matrix are coefficients of Lagrangian polynomials expressed in the basis $(\xi^0, \xi^1, \xi^2, ..., \xi^{M-2}, \xi^{M-1})$. The proof is given in Appendix A. For a Lagrangian polynomial

$$I_p(\xi) = \sum_{q=0}^{M-1} d_{p,q} \xi^q, \tag{74}$$

where $p = 1, ...M$, the solution of (73) is $\boldsymbol{\alpha}_q = \sum_{p=1}^{M} d_{p,q} \boldsymbol{\theta}_p$ (for $q > m + 3$, $\boldsymbol{\alpha}_q = \mathbf{0}$), with coefficients $d_{p,q}$ also given in the Appendix A. When this is substituted into (72) we obtain

$$\boldsymbol{\theta}(\xi) = \sum_{q=0}^{M-1} \sum_{p=1}^{M} d_{p,q} \boldsymbol{\theta}_p \xi^q = \sum_{p=1}^{M} \sum_{q=0}^{M-1} d_{p,q} \xi^q \boldsymbol{\theta}_p = \sum_{p=1}^{M} I_p(\xi) \boldsymbol{\theta}_p. \tag{75}$$

This result shows that the standard Lagrangian interpolation for rotations of order $m + 3$ or higher provides exact solution for rotations of a thick beam problem. If the problem is limited to point loads only, or if $\mathbf{G}_1 \times \mathbf{n} - \dfrac{d\mathbf{m}}{dx_1} = \mathbf{0}$, a quadratic interpolation for rotations is sufficient for obtaining the exact solution.

2.4.2 Exact solution for the position field

The solution for the position field will be given in terms of the nodal positions and the nodal rotations. Let us first re–write expression (70) as

$$\mathbf{r}(\xi) = -\frac{L}{2} \left(\sum_{j=0}^{n+2} \boldsymbol{\beta}_j \xi^j + \mathbf{G}_1 \times \int_{-1}^{\xi} \boldsymbol{\theta} d\eta \right), \tag{76}$$

where $\boldsymbol{\beta}_0 = \mathbf{C}_5$, $\boldsymbol{\beta}_1 = \mathbf{C}_4$, and for $2 \leq j \leq n + 2$, $\boldsymbol{\beta}_j = \dfrac{1}{j} \dfrac{1}{j-1} \boldsymbol{\nu}_{j-2}$. To provide the exact solution, a finite–element interpolation for the part of the position field defined by parameters $\boldsymbol{\beta}_0, \boldsymbol{\beta}_1, ..., \boldsymbol{\beta}_{n+2}$ has to be of order $n + 2$ or higher for which $N \geq n + 3$ ($N \geq 2$ if $\boldsymbol{\nu} = \mathbf{0}$) nodes are needed. At a chosen set of nodal co-ordinates $\bar{\xi}_1, ..., \bar{\xi}_N$, that do not necessarily coincide with the ones used to interpolate rotations, these positions are

$$\mathbf{r}_1 = \mathbf{r}(\bar{\xi}_1), ..., \mathbf{r}_N = \mathbf{r}(\bar{\xi}_N). \tag{77}$$

If the sum in (76) is written in a way

$$\sum_{j=0}^{n+2} \boldsymbol{\beta}_j \xi^j = \sum_{j=0}^{n+2} \boldsymbol{\beta}_j \xi^j + \sum_{j=n+3}^{N-1} \overbrace{\boldsymbol{\beta}_j}^{=0} \xi^j = \sum_{j=0}^{N-1} \boldsymbol{\beta}_j \xi^j,$$

the summation limits in (76) may be changed and the expression re–written as

$$\mathbf{r}(\xi) = -\frac{L}{2} \left(\sum_{j=0}^{N-1} \boldsymbol{\beta}_j \xi^j + \mathbf{G}_1 \times \int_{-1}^{\xi} \boldsymbol{\theta} d\eta \right). \tag{78}$$

Evaluating it at the nodal points gives

$$\sum_{j=0}^{N-1} \bar{\xi}_i^j \boldsymbol{\beta}_j = -\left(\frac{2}{L} \mathbf{r}_i + \mathbf{G}_1 \times \int_{-1}^{\bar{\xi}_i} \boldsymbol{\theta}(\eta) d\eta \right), \quad i = 1, ..., N, \tag{79}$$

where $\boldsymbol{\beta}_0, ..., \boldsymbol{\beta}_{N-1}$ can be expressed in terms of the nodal positions and rotations (for $j > n+2$, $\boldsymbol{\beta}_j$ vanish). It can be seen from the upper equation that each of the unknown parameters consists of two parts: the one dependent on the nodal positions $\mathbf{r}_i$, $i = 1, ..., N$ and the other dependent on the nodal rotations $\boldsymbol{\theta}_p$, $p = 1, ..., M$. We will denote these parts as $\boldsymbol{\beta}_{j,r}$ and $\boldsymbol{\beta}_{j,\theta}$ respectively, so that for $j = 1, ..., N-1$

$$\boldsymbol{\beta}_j = \boldsymbol{\beta}_{j,r} + \boldsymbol{\beta}_{j,\theta}, \tag{80}$$

where $\boldsymbol{\beta}_{j,r}$ and $\boldsymbol{\beta}_{j,\theta}$ are obtained from the following two systems of linear equations:

$$\sum_{j=0}^{N-1} \bar{\xi}_i^j \boldsymbol{\beta}_{j,r} = -\frac{2}{L} \mathbf{r}_i \text{ and} \tag{81}$$

$$\sum_{j=0}^{N-1} \bar{\xi}_i^j \boldsymbol{\beta}_{j,\theta} = -\mathbf{G}_1 \times \int_{-1}^{\bar{\xi}_i} \boldsymbol{\theta}(\eta) d\eta, \tag{82}$$

for $i = 1, ..., N$. This means that the solution for the position field may be decomposed into a part related to nodal positions and the other part related to the nodal rotations, meaning it can be written as

$$\mathbf{r}(\xi) = \mathbf{r}_r(\xi) + \mathbf{r}_\theta(\xi), \tag{83}$$

with

$$\mathbf{r}_r(\xi) = -\frac{L}{2} \sum_{j=0}^{N-1} \boldsymbol{\beta}_{j,r} \xi^j \tag{84}$$

and

$$\mathbf{r}_\theta(\xi) = -\frac{L}{2}\left(\sum_{j=0}^{N-1}\boldsymbol{\beta}_{j,\theta}\xi^j + \mathbf{G}_1 \times \int_{-1}^{\xi}\boldsymbol{\theta}(\eta)d\eta\right). \tag{85}$$

From (84), (85) and (82) it follows that, at the nodes $(\bar{\xi}_1, ..., \bar{\xi}_N)$, $\mathbf{r}_r(\bar{\xi}_i)$ and $\mathbf{r}_\theta(\bar{\xi}_i)$ turn out to be

$$\mathbf{r}_r(\bar{\xi}_i) = \mathbf{r}_i \quad \text{and} \quad \mathbf{r}_\theta(\bar{\xi}_i) = \mathbf{0}. \tag{86}$$

This allows us to write $\mathbf{r}_r(\xi)$ in terms of Lagrangian polynomials

$$J_k(\xi) = \sum_{j=0}^{N-1}\bar{d}_{k,l}\xi^j \tag{87}$$

as

$$\mathbf{r}_r(\xi) = \sum_{k=1}^{N} J_k(\xi)\mathbf{r}_k. \tag{88}$$

Since it has been shown that $\mathbf{r}_\theta(\bar{\xi}_i) = \mathbf{0}$, we can say that $\mathbf{r}_\theta(\xi)$ is a polynomial with zeroes at the nodes $\bar{\xi}_1, ..., \bar{\xi}_N$, i.e. $\mathbf{r}_\theta(\xi)$ can be written as a product of a polynomial function with zeroes at the nodes $\Pi_{k=1}^{N+1}(\xi - \bar{\xi}_k)$ and a vector coefficient depending on the nodal rotations $\boldsymbol{\theta}_p = \boldsymbol{\theta}(\xi_p)$, $p = 1, ..., M$.

Part of the solution for the position field dependent on the nodal positions $\mathbf{r}_r(\xi)$ is obtained by solving the system of linear equations (81) for $\boldsymbol{\beta}_{j,r}$ and substituting the result into (84). The matrix of coefficients of this system is again the Vandermonde matrix and, as given in Appendix A, the solution of the Vandermonde system gives

$$\boldsymbol{\beta}_{j,r} = -\frac{2}{L}\sum_{k=1}^{N}\bar{d}_{k,j}\mathbf{r}_k, \tag{89}$$

with the parameters $\bar{d}_{k,j}$ as the coefficients of the Lagrangian polynomials for $j = 1, ..., N$. When (89) is substituted in (84) the following expression is obtained

$$\mathbf{r}_r(\xi) = -\frac{L}{2}\sum_{j=0}^{N-1}\left(-\frac{2}{L}\sum_{k=1}^{N}\bar{d}_{k,j}\mathbf{r}_k\right)\xi^j = \sum_{k=1}^{N}\sum_{j=0}^{N-1}\bar{d}_{k,j}\xi^j\mathbf{r}_k = \sum_{k=1}^{N}J_k(\xi)\mathbf{r}_k. \tag{90}$$

This results shows not only that $\mathbf{r}_r(\xi)$ may be given in terms of the Lagrangian polynomials $J_k(\xi)$ together with the nodal values $\mathbf{r}_k$, but in fact such a result is equivalent to (84).

Part of the solution for the position field dependent on the nodal rotations $\mathbf{r}_\theta(\xi)$ is obtained by solving the system of linear equations given by (82) for $\boldsymbol{\beta}_{j,\theta}$ and substituting

the result into (85). Again, we get the same Vandermonde matrix as for the previous case and the solution is

$$\boldsymbol{\beta}_{j,\theta} = -\sum_{k=1}^{N} \bar{d}_{k,j} \mathbf{G}_1 \times \int_{-1}^{\bar{\xi}_k} \boldsymbol{\theta} d\eta \ , \quad j = 1, ..., N. \tag{91}$$

Substituting parameters $\boldsymbol{\beta}_{j,\theta}$ into (85) gives

$$\begin{aligned} \mathbf{r}_\theta(\xi) &= \frac{L}{2} \left(\sum_{j=0}^{N-1} \sum_{k=1}^{N} \bar{d}_{k,j} \mathbf{G}_1 \times \int_{-1}^{\bar{\xi}_k} \boldsymbol{\theta} d\eta \xi^j - \mathbf{G}_1 \times \int_{-1}^{\xi} \boldsymbol{\theta} d\eta \right) \\ &= \frac{L}{2} \mathbf{G}_1 \times \left(\sum_{k=1}^{N} \sum_{j=0}^{N-1} \bar{d}_{k,j} \xi^j \int_{-1}^{\bar{\xi}_k} \boldsymbol{\theta} d\eta - \int_{-1}^{\xi} \boldsymbol{\theta} d\eta \right) = \frac{L}{2} \mathbf{G}_1 \times \left(\sum_{k=1}^{N} J_k \int_{-1}^{\bar{\xi}_k} \boldsymbol{\theta} d\eta - \int_{-1}^{\xi} \boldsymbol{\theta} d\eta \right). \end{aligned} \tag{92}$$

Since the completeness property of the Lagrangian polynomials states $\sum_{k=1}^{N} J_k(\xi) = 1$, the upper result can be written as

$$\mathbf{r}_\theta(\xi) = \frac{L}{2} \mathbf{G}_1 \times \sum_{k=1}^{N} J_k \left(\int_{-1}^{\bar{\xi}_k} \boldsymbol{\theta} d\eta - \int_{-1}^{\xi} \boldsymbol{\theta} d\eta \right) = \frac{L}{2} \mathbf{G}_1 \times \sum_{k=1}^{N} J_k \int_{\xi}^{\bar{\xi}_k} \boldsymbol{\theta} d\eta. \tag{93}$$

Substituting (74) and (75) this becomes

$$\begin{aligned} \mathbf{r}_\theta(\xi) = \frac{L}{2} \mathbf{G}_1 \times \sum_{p=1}^{M} \boldsymbol{\theta}_p \sum_{k=1}^{N} J_k \int_{\xi}^{\bar{\xi}_k} \sum_{q=0}^{M-1} d_{p,q} \xi^q d\eta &= \frac{L}{2} \mathbf{G}_1 \times \sum_{p=1}^{M} \boldsymbol{\theta}_p \sum_{k=1}^{N} J_k \sum_{q=0}^{M-1} \frac{\bar{\xi}_k^{q+1} - \xi^{q+1}}{q+1} d_q^p \\ &= \frac{L}{2} \mathbf{G}_1 \times \sum_{p=1}^{M} \boldsymbol{\theta}_p \sum_{q=0}^{M-1} \frac{\sum_{k=1}^{N} J_k \bar{\xi}_k^{q+1} - \sum_{k=1}^{N} J_k \xi^{q+1}}{q+1} d_{p,q}. \end{aligned} \tag{94}$$

Substituting (87) this further becomes

$$\mathbf{r}_\theta(\xi) = \frac{L}{2} \mathbf{G}_1 \times \sum_{p=1}^{M} \boldsymbol{\theta}_p \sum_{q=0}^{M-1} \frac{\sum_{j=0}^{N-1} \xi^j \sum_{k=1}^{N} \bar{d}_{k,j} \bar{\xi}_k^{q+1} - \xi^{q+1}}{q+1} d_{p,q}, \tag{95}$$

where, for $q+1 < N$, $\sum_{k=1}^{N} \bar{d}_{k,j} \bar{\xi}_k^{q+1} = \delta_{q+2,j+1}$, with $\delta_{s,r}$ as the Kronecker symbol that is equal to unity for $s = r$ and zero otherwise. The proof is given in Appendix A. Consequently, the sum over the fraction in the above expression becomes

$$\sum_{q=0}^{N-2}\frac{\sum_{j=0}^{N-1}\xi^j\delta_{q+2,j+1}-\xi^{q+1}}{q+1}d_{p,q}+\sum_{q=N-1}^{M-1}\frac{\sum_{j=0}^{N-1}\xi^j\sum_{k=1}^{N}\bar{d}_{k,j}\bar{\xi}_k^{q+1}-\xi^{q+1}}{q+1}d_{p,q},$$

where the first term vanishes leaving

$$\begin{aligned}\mathbf{r}_\theta(\xi)=\frac{L}{2}\mathbf{G}_1\times\sum_{p=1}^{M}\boldsymbol{\theta}_p\sum_{q=N-1}^{M-1}\frac{\sum_{k=1}^{N}(\sum_{j=0}^{N-1}\bar{d}_{k,j}\xi^j)\bar{\xi}_k^{q+1}-\xi^{q+1}}{q+1}d_{p,q}\\ =-\frac{L}{2}\mathbf{G}_1\times\sum_{p=1}^{M}\boldsymbol{\theta}_p\sum_{q=N-1}^{M-1}\frac{\sum_{k=1}^{N}J_k(\xi^{q+1}-\bar{\xi}_k^{q+1})}{q+1}d_{p,q},\end{aligned}\quad(96)$$

since $\sum_{j=0}^{N-1}\bar{d}_{k,j}\xi^j=J_k$ and $\sum_{k=1}^{N}J_k=1$. Further simplification of expression (96) can be done, since the sum $\sum_{k=1}^{N}J_k(\xi^{q+1}-\bar{\xi}_k^{q+1})$ may be simplified. To do so, let us first factorise the difference of equal powers $\xi^{q+1}-\bar{\xi}_k^{q+1}$ as

$$\xi^{q+1}-\bar{\xi}_k^{q+1}=(\xi-\bar{\xi}_k)(\xi^q+\xi^{q-1}\bar{\xi}_k+...+\bar{\xi}_k^q)=(\xi-\bar{\xi}_k)\sum_{r=1}^{q+1}\xi^{q+1-r}\bar{\xi}_k^{r-1}.$$

The Lagrangian polynomials (from Appendix A) can be written as

$$J_k(\xi)=\prod_{i=1,i\neq k}^{N}\frac{(\xi-\bar{\xi}_i)}{(\bar{\xi}_k-\bar{\xi}_i)}=\bar{d}_{k,N-1}\prod_{i=1,i\neq k}^{N}(\xi-\bar{\xi}_i)\quad(97)$$

and we obtain

$$\begin{aligned}\sum_{k=1}^{N}J_k(\xi^{q+1}-\bar{\xi}_k^{q+1})&=\sum_{k=1}^{N}\bar{d}_{k,N-1}\prod_{i=1,i\neq k}^{N}(\xi-\bar{\xi}_i)(\xi-\bar{\xi}_k)\sum_{r=1}^{q+1}\xi^{q+1-r}\bar{\xi}_k^{r-1}\\ &=\prod_{i=1}^{N}(\xi-\bar{\xi}_i)\sum_{r=1}^{q+1}\left(\sum_{k=1}^{N}\bar{d}_{k,N-1}\bar{\xi}_k^{r-1}\right)\xi^{q+1-r}=\xi^{q+1-N}\prod_{i=1}^{N}(\xi-\bar{\xi}_i)\end{aligned}\quad(98)$$

since, as shown in Appendix A, $\sum_{k=1}^{N}\bar{d}_{k,N-1}\bar{\xi}_k^{r-1}=\delta_{r,N}$. Finally, the solution for the position field dependent on the nodal rotations can be written as

$$\mathbf{r}_\theta(\xi)=-\frac{L}{2}\prod_{i=1}^{N}(\xi-\bar{\xi}_i)\mathbf{G}_1\times\sum_{p=1}^{M}\boldsymbol{\theta}_p\sum_{q=N-1}^{M-1}\frac{\xi^{q+1-N}}{q+1}d_{p,q}.\quad(99)$$

2.4.3 Relationship between the number of nodal points for positions and rotations

For an arbitrary number $M \geq m+4$ of nodal co–ordinates for rotations $\xi_1, ..., \xi_M$ and an arbitrary number $N \geq n+3$ of nodal co–ordinates for positions $\bar{\xi}_1, ..., \bar{\xi}_N$, the exact solution for the rotation vector is given in (75) and the exact solution for the position vector is obtained by substituting (90) and (99) into (83) giving

$$\boldsymbol{\theta}(\xi) = \sum_{p=1}^{M} I_p(\xi)\boldsymbol{\theta}_p \tag{100}$$

$$\mathbf{r}(\xi) = \sum_{k=1}^{N} J_k(\xi)\mathbf{r}_k - \frac{L}{2}\prod_{i=1}^{N}(\xi - \bar{\xi}_i)\mathbf{G}_1 \times \sum_{p=1}^{M}\boldsymbol{\theta}_p \sum_{j=0}^{M-N}\frac{d_{p,N-1+j}}{N+j}\xi^j, \tag{101}$$

where $d_{p,N-1+j}$ is a coefficient in p^{th} Lagrangian polynomial of order $N-1$ multiplying ξ^{N-1+j}. As explained earlier, m and n are the orders of the polynomial loading functions $\boldsymbol{\mu} = \frac{L^3}{8}\mathbf{C}_M^{-1}(\mathbf{G}_1 \times \mathbf{n} - \frac{d\mathbf{m}}{dx_1})$ and $\boldsymbol{\nu} = \frac{L}{2}\mathbf{C}_N^{-1}\mathbf{n}$, respectively.

With a minimum number of nodal points $M = m+4$ and $N = n+3$, the number of integration constants in solution (69) and (70) of the differential equations is exactly matched by the number of nodal rotations and positions. Interpolation (101) therefore implicitly includes the one–to–one correspondence between the two sets of parameters. A particularly interesting case is the one with $m = n$, i.e. the case where the distributed moment loading is of a degree at most one order higher than the degree of the distributed force loading, including the situation with no moment loading at all. The minimum number of nodes for the exact solution is then $M = n+4$ and $N = n+3$, i.e. $N = M-1$ and $\mathbf{r}(\xi)$ in (101) becomes

$$\begin{aligned}
\mathbf{r}(\xi) &= \sum_{k=1}^{M-1} J_k(\xi)\mathbf{r}_k - \frac{L}{2}\prod_{i=1}^{M-1}(\xi - \bar{\xi}_i)\mathbf{G}_1 \times \sum_{p=1}^{M}\boldsymbol{\theta}_p \sum_{j=0}^{1}\frac{d_{p,M-2+j}}{M-1+j}\xi^j \\
&= \sum_{k=1}^{M-1} J_k(\xi)\mathbf{r}_k - \frac{L}{2}\prod_{i=1}^{M-1}(\xi - \bar{\xi}_i)\mathbf{G}_1 \times \sum_{p=1}^{M}\boldsymbol{\theta}_p\left(\frac{d_{p,M-2}}{M-1} + \frac{d_{p,M-1}}{M}\xi\right) \\
&= \sum_{k=1}^{M-1} J_k(\xi)\mathbf{r}_k - \frac{L}{2}\prod_{i=1}^{M-1}(\xi - \bar{\xi}_i)\mathbf{G}_1 \times \sum_{p=1}^{M}\frac{\frac{\xi}{M} - \frac{\sum_{q=1,q\neq p}^{M}\xi_q}{M-1}}{\prod_{r=1,r\neq p}^{M}(\xi_p - \xi_r)}\boldsymbol{\theta}_p,
\end{aligned} \tag{102}$$

since $d_{p,M-2} = -d_{p,M-1}\sum_{q=1,q\neq p}^{M}\xi_q$ and $d_{p,M-1} = \dfrac{1}{\prod_{r=1,r\neq p}^{M}(\xi_p - \xi_r)}$ (see Appendix A).

This result can be understood as a generalisation of the result given in Chapter 10.5 of [41] for arbitrary order of interpolation. In this work the authors have considered Timoshenko beam subject to point loads for which they have presented an exact interpolation, which is free from geometric and material characteristics (problem–independent). For $M = 3$ and evenly spaced nodes, the solution for the position vector reads $\mathbf{r} = \frac{1-\xi}{2}\mathbf{r}_1 + \frac{1+\xi}{2}\mathbf{r}_2 + L(1-\xi^2)\mathbf{G}_1 \times \left[(\frac{\xi}{12} - \frac{1}{8})\boldsymbol{\theta}_1 - \frac{\xi}{6}\boldsymbol{\theta}_2 + (\frac{\xi}{12} + \frac{1}{8})\boldsymbol{\theta}_3\right]$, which is equivalent to the 2D form given in equation (10.75) of [41].

At times it may be convenient to use a larger set of mutually dependent nodal parameters, i.e. $M > m+4$ with $N = n+3$ or $N > n+3$ with $M = m+4$ or both. There exist two particularly interesting and computationally useful sets of such redundant degrees of freedom: the first with the number of the nodal points used for interpolating the position vector larger than the number of the nodal points used for interpolating the rotation vector by one ($N = M + 1$), and the second with the equal number of the same nodal points used for interpolating the position and the rotation vector ($M = N$ and $\bar{\xi}_i = \xi_i$ for $i = 1, ..., N$). These two cases will be analysed in more detail.

Number of nodal points for positions larger than the number of nodal points for rotations by one ($N = M + 1$).
In this case expression (101) turns into

$$\mathbf{r}(\xi) = \sum_{k=1}^{M+1} J_k(\xi)\mathbf{r}_k, \tag{103}$$

showing that for $M \geq m+4$ and $N \geq n+3$, $N = M+1$ is the minimum number of the position nodal points needed to separate the interpolation for positions from the rotational degrees of freedom. At the same time, therefore, it is also the minimum number of the position nodal points needed to express the exact solution using independent interpolations for the positions and the rotations (100) and (103). In [39] elements with this kind of interpolation are called the *virgin elements*.

Same nodal points for positions and rotations ($\bar{\xi}_i = \xi_i$ for $i = 1, ..., N$).
In this case $J_k(\xi) = I_k(\xi)$ and (101) simply turns into

$$\mathbf{r}(\xi) = \sum_{k=1}^{N} I_k(\xi)\mathbf{r}_k - \frac{L}{2}\prod_{i=1}^{N}(\xi - \xi_i)\mathbf{G}_1 \times \sum_{p=1}^{N} \boldsymbol{\theta}_p \frac{d_{p,N-1}}{N}. \tag{104}$$

From (74) note that $(N-1)st$ derivative of $I_p(\xi)$ is $I_p^{N-1}(\xi) = d_{p,N-1}(N-1)!$, the above result becomes

$$\mathbf{r}(\xi) = \sum_{k=1}^{N} I_k(\xi)\mathbf{r}_k - \frac{1}{N!}\frac{L}{2}\prod_{i=1}^{N}(\xi - \xi_i)\mathbf{G}_1 \times \boldsymbol{\theta}_p^{(N-1)} \tag{105}$$

showing that the standard Lagrangian interpolation using only the translational degrees of freedom suffices for the exact solution when $(N-1)st$ derivative of the interpolation for rotations vanishes. This, of course, is precisely the last situation analysed in which this derivative would vanish due to the fact that the rotation was interpolated using a polynomial of the order smaller than $N-1$. Equation (104) is worth analysing further. As, for $N = M$, $d_{p,N-1} = \dfrac{1}{\prod_{r=1,r\neq p}^{N}(\xi_p - \xi_r)}$ (Appendix A), this result turns into

$$\mathbf{r}(\xi) = \sum_{k=1}^{N} I_k(\xi)\mathbf{r}_k - \frac{1}{N}\frac{L}{2}\prod_{i=1}^{N}(\xi - \xi_i)\mathbf{G}_1 \times \sum_{p=1}^{N}\frac{\boldsymbol{\theta}_p}{\prod_{r=1,r\neq p}^{N}(\xi_p - \xi_r)} \tag{106}$$

and takes a particularly elegant form for the elements with equidistant spacing between the nodes. In this case, the nodal co–ordinates are given as $\xi_i = \dfrac{2i-(N+1)}{N-1}$ and $\left[\prod_{r=1,r\neq p}^{N}(\xi_p - \xi_r)\right]^{-1}$ becomes

$$\frac{1}{\prod_{r=1,r\neq p}^{N}(\xi_p - \xi_r)} = \frac{(\frac{N-1}{2})^{N-1}}{\prod_{r=1,r\neq p}^{N}(p-r)} = \frac{(\frac{N-1}{2})^{N-1}}{(p-1)(p-2)...1}\frac{1}{(-1)(-2)...(p-N)}$$

$$= \frac{(\frac{N-1}{2})^{N-1}}{(p-1)!}\frac{(-1)^{N-p}}{(N-p)!} = \left(\frac{N-1}{2}\right)^{N-1}\frac{(-1)^{p-N}\dfrac{(N-1)!}{(N-p)!}}{(N-1)!(p-1)!}$$

$$= \left(-\frac{N-1}{2}\right)^{N-1}\frac{(-1)^{p-1}}{(N-1)!}\binom{N-1}{p-1}.$$

As $\xi - \xi_i$ now turns out to be $2\left(\dfrac{1+\xi}{2} - \dfrac{i-1}{N-1}\right)$, expression (106) becomes

$$\mathbf{r} = \sum_{k=1}^{N} I_k\mathbf{r}_k - \frac{L}{N}\frac{(-(N-1))^{N-1}}{(N-1)!}\prod_{i=1}^{N}\left(\frac{1+\xi}{2} - \frac{i-1}{N-1}\right)\mathbf{G}_1 \times \sum_{p=1}^{N}(-1)^{p-1}\binom{N-1}{p-1}\boldsymbol{\theta}_p$$

$$= \sum_{k=1}^{N} I_k\mathbf{r}_k - \frac{L}{N}\prod_{j=2}^{N}\left(-\frac{N-1}{j-1}\right)\prod_{i=1}^{N}\left(\frac{1+\xi}{2} - \frac{i-1}{N-1}\right)\mathbf{G}_1 \times \sum_{p=1}^{N}(-1)^{p-1}\binom{N-1}{p-1}\boldsymbol{\theta}_p$$

$$= \sum_{k=1}^{N} I_k \mathbf{r}_k - \frac{L}{N}\frac{1+\xi}{2}\prod_{j=2}^{N}\left(1 - \frac{N-1}{i-1}\frac{1+\xi}{2}\right)\mathbf{G}_1 \times \sum_{p=1}^{N}(-1)^{p-1}\binom{N-1}{p-1}\boldsymbol{\theta}_p,$$

where the coefficients in the second sum are the binomial coefficients forming a Pascal triangle. Introducing a set of linear functions $N_i(\xi)$ that have a zero value at the node ξ_i and a unit value at the node $\xi_1 = -1$ (apart from $N_1(\xi)$ which has a unit value at the node $\xi_N = 1$), correspondingly defined as

$$N_1(\xi) = \frac{1+\xi}{2}, \text{ and } N_i(\xi) = 1 - \frac{N-1}{i-1}\frac{1+\xi}{2}, \text{ for } i = 2, ..., N. \tag{107}$$

These functions are shown in Figure 2.5. Interpolation from (106) now becomes

$$\mathbf{r}(\xi) = \sum_{k=1}^{N} I_k \mathbf{r}_k - \frac{L}{N}\prod_{i=1}^{N} N_i(\xi)\sum_{p=1}^{N}(-1)^{p-1}\binom{N-1}{p-1}\mathbf{G}_1 \times \boldsymbol{\theta}_p. \tag{108}$$

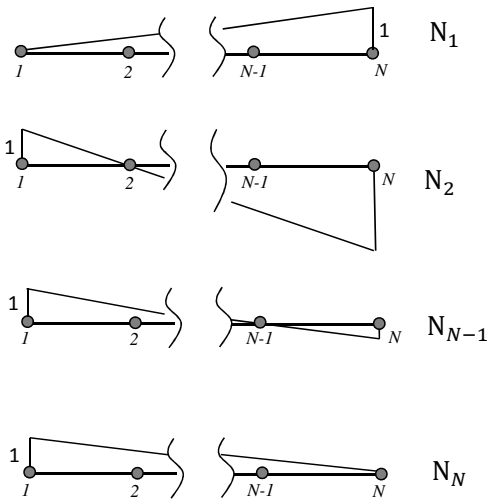

Figure 2.5: Linear functions $N_i(\xi)$ used in interpolation (108).

Some special cases of this result are well-known. For a two–noded element (106) gives $\mathbf{r}(\xi) = \frac{1-\xi}{2}\mathbf{r}_1 + \frac{1+\xi}{2}\mathbf{r}_2 + \frac{L}{8}(1-\xi^2)\mathbf{G}_1 \times (\boldsymbol{\theta}_1 - \boldsymbol{\theta}_2)$, that has been often used as a basis for development of constant strain beam elements (expression (10.84) in [41]) and also plate elements and their extensions (see [2] for an application to Mindlin plates). The three–node case of (106) reads $\mathbf{r}(\xi) = -\xi\frac{1-\xi}{2}\mathbf{r}_1 + (1-\xi^2)\mathbf{r}_2 + \xi\frac{1+\xi}{2}\mathbf{r}_3 - \frac{L}{12}\xi(1-\xi^2)\mathbf{G}_1 \times (\boldsymbol{\theta}_1 - 2\boldsymbol{\theta}_2 + \boldsymbol{\theta}_3)$ and has been also reported and used for development of higher–order Timoshenko beam elements [39] as well as triangular and rectangular Mindlin

plate elements [38, 16].
The schematic representation of the interpolation given in (108) is illustrated in Figure 2.6.

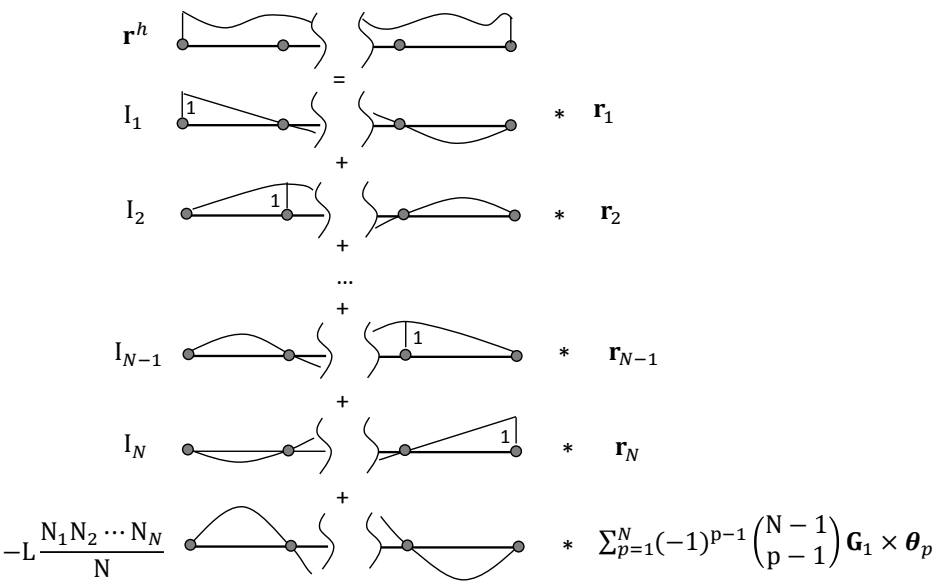

Figure 2.6: Graphical representation of interpolation (108).

Obviously, the exact solution is obtained by enhancing the standard Lagrangian interpolation of order $N-1$ with an extra polynomial of order N passing through all the nodal points scaled by a linear combination of the nodal rotations using the binomial coefficients proportional to the length of the beam and inversely proportional to the number of nodes.

Speaking of internal nodes with arbitrary spacing gives another illustrative view at equation (106). Since $I_k(\xi) = \prod_{i=1,i\neq k}^{N} \dfrac{(\xi-\xi_i)}{(\xi_k-\xi_i)}$, this equation simplifies considerably and becomes

$$\mathbf{r}(\xi) = \sum_{k=1}^{N} I_k(\xi)\mathbf{r}_k - \frac{1}{N}\frac{L}{2}\mathbf{G}_1 \times \sum_{p=1}^{N} I_p(\xi)(\xi-\xi_p)\boldsymbol{\theta}_p = \sum_{k=1}^{N} I_k(\xi)\left[\mathbf{r}_k - \frac{1}{N}\frac{L}{2}\mathbf{G}_1 \times (\xi-\xi_k)\boldsymbol{\theta}_k\right].$$

After introducing the material position vector $\mathbf{R}_0(\xi) = \dfrac{L}{2}(1+\xi)\mathbf{G}_1$ and having in mind that for a straight beam $\mathbf{R}_0 = \sum_{k=1}^{N} I_k \mathbf{R}_{0k}$, the upper expression can be re–written as

$$\mathbf{r}(\xi)=\sum_{k=1}^{N} I_k\left[\mathbf{r}_k-\frac{1}{N}(\mathbf{R}_0-\mathbf{R}_{0k})\times\boldsymbol{\theta}_k\right]=\sum_{k=1}^{N} I_k\mathbf{r}_k-\frac{1}{N}\left(\mathbf{R}_0\times\sum_{k=1}^{N} I_k\boldsymbol{\theta}_k-\sum_{k=1}^{N} I_k\mathbf{R}_{0k}\times\boldsymbol{\theta}_k\right)$$
$$=\sum_{k=1}^{N} I_k\mathbf{r}_k-\frac{1}{N}\left(\mathbf{R}_0\times\boldsymbol{\theta}-\sum_{k=1}^{N} I_k\mathbf{R}_{0k}\times\boldsymbol{\theta}_k\right)=\sum_{k=1}^{N} I_k\left[\mathbf{r}_k-\frac{1}{N}(\mathbf{R}_{0k}\times\boldsymbol{\theta}-\mathbf{R}_{0k}\times\boldsymbol{\theta}_k)\right]$$
$$=\sum_{k=1}^{N} I_k\left[\mathbf{r}_k+\frac{1}{N}(\boldsymbol{\theta}-\boldsymbol{\theta}_k)\times\mathbf{R}_{0k}\right]. \quad (109)$$

Since $\mathbf{u}(x_1)=\mathbf{r}(x_1)-\mathbf{R}(x_1)$ as it has been stated earlier, the same interpolation can also be applied to the displacement vector, i.e.

$$\mathbf{u}(\xi)=\sum_{k=1}^{N} I_k(\xi)\left[\mathbf{u}_k-\frac{1}{N}\frac{L}{2}\mathbf{G}_1\times(\xi-\xi_k)\boldsymbol{\theta}_k\right]=\sum_{k=1}^{N} I_k\left[\mathbf{u}_k+\frac{1}{N}(\boldsymbol{\theta}-\boldsymbol{\theta}_k)\times\mathbf{R}_{0k}\right], \quad (110)$$

because, from Figure 2.2 it can be stated

$$\mathbf{R}(x_1)=\mathbf{R}(0)+\mathbf{R}_0(x_1)=\mathbf{R}(0)+\sum_{k=1}^{N} I_k(x_1)\mathbf{R}_{0k}=\sum_{k=1}^{N} I_k(x_1)\mathbf{R}(0)+\sum_{k=1}^{N} I_k(x_1)\mathbf{R}_{0k}$$
$$=\sum_{k=1}^{N} I_k(x_1)[\mathbf{R}(0)+\mathbf{R}_{0k}]=\sum_{k=1}^{N} I_k(x_1)\mathbf{R}_k. \quad (111)$$

Very elegant alternative expression for the interpolation of the position vector follows from (109) by noting $\mathbf{r}_k=\mathbf{R}(0)+\mathbf{R}_{0k}+\mathbf{u}_k \Leftrightarrow \mathbf{R}_{0k}=\mathbf{r}_k-\mathbf{u}_k-\mathbf{R}(0)$:

$$\mathbf{r}(\xi)=\sum_{k=1}^{N} I_k\left\{\mathbf{r}_k+\frac{1}{N}\left[(\boldsymbol{\theta}-\boldsymbol{\theta}_k)\times\mathbf{r}_k-\overbrace{(\boldsymbol{\theta}-\boldsymbol{\theta}_k)\times\mathbf{u}_k}^{\text{sec.ord.term}}\right]\right\}-\frac{1}{N}\overbrace{\left(\boldsymbol{\theta}-\sum_{k=1}^{N} I_k\boldsymbol{\theta}_k\right)}^{=\mathbf{0}}\times\mathbf{R}(0). \quad (112)$$

Having in mind that in linear analysis all second order terms vanish, we further have [20]

$$\mathbf{r}(\xi)=\sum_{k=1}^{N} I_k\left(\mathbf{I}+\frac{1}{N}\widehat{\boldsymbol{\theta}-\boldsymbol{\theta}_k}\right)\mathbf{r}_k. \quad (113)$$

Let us introduce a generalised interpolation $\tilde{\mathbf{I}}_k$ and write

$$\mathbf{r} = \sum_{k=1}^{N} \tilde{\mathbf{I}}_k \mathbf{r}_k, \quad \text{with} \quad \tilde{\mathbf{I}}_k = I_k \left(\mathbf{I} + \frac{1}{N} \widehat{\boldsymbol{\theta} - \boldsymbol{\theta}_k} \right). \tag{114}$$

Expression (114) holds both for parameters ξ and x_1, depending on the parameters used for Lagrangian polynomial I_k and interpolated rotation vector $\boldsymbol{\theta}$. It appears that this result may be taken as a useful basis for the development of non–linear finite elements with a capability to provide the exact analytical result in a linear analysis.

2.4.4 Finite element implementation of the problem–independent interpolation

The exact problem–independent interpolation for the rotation and the position field is given by the expressions (100) and (101) that can be used for the derivation of the beam equilibrium in the finite-element sense in the same manner as done previously for the case of the problem–dependent interpolation, e.g. using the principle of minimum total potential energy $V = V_{def} - U$ with V_{def} as a strain energy and U as the work of the applied loading. Exact solution for the position field given by (101) can be re-written as

$$\mathbf{r}(\xi) = \sum_{i=1}^{N} J_i(\xi) \mathbf{r}_i + \sum_{p=1}^{M} K_p(\xi) \widehat{\mathbf{G}_1} \boldsymbol{\theta}_p, \tag{115}$$

where $K_p(\xi) = -\frac{L}{2} \prod_{j=1}^{N} (\xi - \bar{\xi}_i) \sum_{j=0}^{M-N} \frac{d_{p,N-1+j}}{N+j} \xi^j$. Variations of the strain energy and the work of the applied conservative loading are

$$\delta V_{def} = \sum_{i=1}^{N} \delta \mathbf{u}_i^T \sum_{j=1}^{N} \int_{-1}^{1} [J_i' \mathbf{I} \;\; \mathbf{0} \;\; \mathbf{0}] \begin{bmatrix} \frac{2}{L}\mathbf{C}_N & \mathbf{C}_N \widehat{\mathbf{G}_1} & \mathbf{0} \\ -\widehat{\mathbf{G}_1}\mathbf{C}_N & -\frac{L}{2}\widehat{\mathbf{G}_1}\mathbf{C}_N\widehat{\mathbf{G}_1} & \mathbf{0} \\ \mathbf{0} & \mathbf{0} & \frac{2}{L}\mathbf{C}_M \end{bmatrix} \begin{bmatrix} J_i \mathbf{I} \\ \mathbf{0} \\ \mathbf{0} \end{bmatrix} d\xi \mathbf{u}_j$$

$$+ \sum_{i=1}^{N} \delta \mathbf{u}_i^T \sum_{q=1}^{M} \int_{-1}^{1} [J_i' \mathbf{I} \;\; \mathbf{0} \;\; \mathbf{0}] \begin{bmatrix} \frac{2}{L}\mathbf{C}_N \widehat{\mathbf{G}_1} & \mathbf{C}_N \widehat{\mathbf{G}_1} & \mathbf{0} \\ -\widehat{\mathbf{G}_1}\mathbf{C}_N\widehat{\mathbf{G}_1} & -\frac{L}{2}\widehat{\mathbf{G}_1}\mathbf{C}_N\widehat{\mathbf{G}_1} & \mathbf{0} \\ \mathbf{0} & \mathbf{0} & \frac{2}{L}\mathbf{C}_M \end{bmatrix} \begin{bmatrix} K_q' \mathbf{I} \\ I_q \mathbf{I} \\ I_q' \mathbf{I} \end{bmatrix} d\xi \boldsymbol{\theta}_q$$

$$+\sum_{p=1}^{M}\delta\boldsymbol{\theta}_p^T\sum_{j=1}^{N}\int_{-1}^{1}[K_p'\mathbf{I}\;\; I_p\mathbf{I}\;\; I_p'\mathbf{I}]\begin{bmatrix}-\frac{2}{L}\widehat{\mathbf{G}_1}\mathbf{C}_N & -\widehat{\mathbf{G}_1}\mathbf{C}_N\widehat{\mathbf{G}_1} & \mathbf{0}\\ -\widehat{\mathbf{G}_1}\mathbf{C}_N & -\frac{L}{2}\widehat{\mathbf{G}_1}\mathbf{C}_N\widehat{\mathbf{G}_1} & \mathbf{0}\\ \mathbf{0} & \mathbf{0} & \frac{2}{L}\mathbf{C}_M\end{bmatrix}\begin{bmatrix}J_j'\mathbf{I}\\ \mathbf{0}\\ \mathbf{0}\end{bmatrix}d\xi\mathbf{u}_j$$

$$+\sum_{p=1}^{M}\delta\boldsymbol{\theta}_p^T\sum_{q=1}^{M}\int_{-1}^{1}[K_p'\mathbf{I}\;\; I_p\mathbf{I}\;\; I_p'\mathbf{I}]\begin{bmatrix}-\frac{2}{L}\widehat{\mathbf{G}_1}\mathbf{C}_N\widehat{\mathbf{G}_1} & -\widehat{\mathbf{G}_1}\mathbf{C}_N\widehat{\mathbf{G}_1} & \mathbf{0}\\ -\widehat{\mathbf{G}_1}\mathbf{C}_N\widehat{\mathbf{G}_1} & -\frac{L}{2}\widehat{\mathbf{G}_1}\mathbf{C}_N\widehat{\mathbf{G}_1} & \mathbf{0}\\ \mathbf{0} & \mathbf{0} & \frac{2}{L}\mathbf{C}_M\end{bmatrix}\begin{bmatrix}K_q'\mathbf{I}\\ I_q\mathbf{I}\\ I_q'\mathbf{I}\end{bmatrix}d\xi\boldsymbol{\theta}_q$$

and

$$\delta U=\sum_{i=1}^{N}\delta\mathbf{u}_i^T\left(\frac{L}{2}\int_{-1}^{1}J_i\mathbf{n}d\xi+\mathbf{F}_i\right)$$
$$+\sum_{p=1}^{M}\delta\boldsymbol{\theta}_p^T\left[\frac{L}{2}\int_{-1}^{1}\left(-K_p\widehat{\mathbf{G}_1}\mathbf{n}+I_p\mathbf{m}\right)d\xi+\left(-K_p(\xi_p)\widehat{\mathbf{G}_1}\mathbf{F}_p+\mathbf{M}_p\right)\right]. \quad (116)$$

This leads to the standard finite–element equilibrium

$$\delta\mathbf{p}^T(\mathbf{K}\mathbf{p}-\mathbf{R})=\mathbf{0}\;\;\Longrightarrow\;\;\mathbf{K}\mathbf{p}-\mathbf{R}=\mathbf{0},$$

where $\mathbf{p}$ is the vector of N unknown nodal displacements $\mathbf{u}_j$ and M unknown nodal rotations $\boldsymbol{\theta}_p$, $\mathbf{K}$ and $\mathbf{R}$ are the element stiffness matrix and the vector of the equivalent nodal loading.

If the same nodes are chosen for the unknown displacements and rotations ($M=N\Leftrightarrow J_i=I_i$ and $K_i=-\frac{1}{N}\frac{L}{2}I_i(\xi-\xi_i)$), the stationarity principle becomes

$$\sum_{p=1}^{N}\delta\mathbf{p}_i^T\sum_{j=1}^{M}(\mathbf{K}_{ij}\mathbf{p}_j-\mathbf{R}_i)=0\;\Longrightarrow\;\sum_{j=1}^{M}\mathbf{K}_{ij}\mathbf{p}_j=\mathbf{R}_i,$$

where $\mathbf{p}_i^T=\langle\mathbf{u}_i^T\;\;\boldsymbol{\theta}_i^T\rangle$,

$$\mathbf{R}_i=\frac{L}{2}\int_{-1}^{1}\begin{bmatrix}I_i\mathbf{I} & \mathbf{0}\\ -K_i\widehat{\mathbf{G}_1} & I_i\mathbf{I}\end{bmatrix}\begin{Bmatrix}\mathbf{n}\\ \mathbf{m}\end{Bmatrix}d\xi+\begin{Bmatrix}\mathbf{F}_i\\ \mathbf{M}_i\end{Bmatrix},$$

$$\mathbf{K}_{ij}=\frac{2}{L}\int_{-1}^{1}\begin{bmatrix}I_i'I_j'\mathbf{C}_N & I_i'\mathbf{C}_N(K_j'\mathbf{I}+\frac{L}{2}I_j\widehat{\mathbf{G}_1})\\ (K_i'\mathbf{I}-\frac{L}{2}I_i\widehat{\mathbf{G}_1})I_j'\mathbf{C}_N & (K_i'\mathbf{I}-\frac{L}{2}I_i\widehat{\mathbf{G}_1})\mathbf{C}_N(K_j'\mathbf{I}+\frac{L}{2}I_j\widehat{\mathbf{G}_1})+I_i'I_j'\mathbf{C}_M\end{bmatrix}d\xi.$$

It is instructive to compare these results with the corresponding expressions for

the residual force vector and the material stiffness matrix in [34] evaluated in the undeformed configuration. The only difference arises from the presence of the linked interpolation.

For the beams with the internal degrees of freedom (that are written within a part of the vector of the nodal unknowns $\mathbf{p}$ denoted as $\mathbf{p}_a$) it is always possible to perform static condensation of these degrees of freedom in order to reduce the size of the global problem. This is performed by suitable ordering of the degrees of freedom so that the element equilibrium $\mathbf{K}\mathbf{p} = \mathbf{R}$ may be written in a block-matrix form as

$$\begin{bmatrix} \mathbf{K}_{aa} & \mathbf{K}_{ab} \\ \mathbf{K}_{ba} & \mathbf{K}_{bb} \end{bmatrix} \begin{Bmatrix} \mathbf{p}_a \\ \mathbf{p}_b \end{Bmatrix} = \begin{Bmatrix} \mathbf{R}_a \\ \mathbf{R}_b \end{Bmatrix},$$

where $\mathbf{p}_b$ contains only the unknown rotations and displacements of the boundary nodes $\mathbf{p}_b^T = \langle \mathbf{u}_1^T \;\; \boldsymbol{\theta}_1^T \;\; \mathbf{u}_N^T \;\; \boldsymbol{\theta}_N^T \rangle$. Further we have

$$\mathbf{p}_a = \mathbf{K}_{aa}^{-1}(\mathbf{R}_a - \mathbf{K}_{ab}\mathbf{p}_b), \tag{117}$$

which allows us to compute the internal degrees of freedom once the global unknowns $\mathbf{p}_b$ have been determined. These global unknowns are computed from

$$\overbrace{(\mathbf{K}_{bb} - \mathbf{K}_{ba}\mathbf{K}_{aa}^{-1}\mathbf{K}_{ab})}^{\mathbf{K}}\,\mathbf{p}_b = \overbrace{\mathbf{R}_b - \mathbf{K}_{ba}\mathbf{K}_{aa}^{-1}\mathbf{R}_a}^{\mathbf{R}}. \tag{118}$$

The condensed stiffness matrix and load vector indicated above are identical to those given in (62) and (67) since the interpolation employed here has been designed to provide the exact solution to the problem. The proof to this follows from the variation of the strain energy, which for a problem–independent formulation reads

$$\delta V_{def} = \langle \delta\mathbf{p}_a^T \;\; \delta\mathbf{p}_b^T \rangle \begin{bmatrix} \mathbf{K}_{aa} & \mathbf{K}_{ab} \\ \mathbf{K}_{ba} & \mathbf{K}_{bb} \end{bmatrix} \begin{Bmatrix} \mathbf{p}_a \\ \mathbf{p}_b \end{Bmatrix}. \tag{119}$$

With $\mathbf{p}_a$ given in (117), variation of this internal degrees of freedom is

$$\delta\mathbf{p}_a = -\mathbf{K}_{aa}^{-1}\mathbf{K}_{ab}\delta\mathbf{p}_b. \tag{120}$$

Substituting (120) into the variation of the strain energy (119) gives

$$\delta V_{def} = \mathbf{p}_b^T(\mathbf{K}_{bb} - \mathbf{K}_{ba}\mathbf{K}_{aa}^{-1}\mathbf{K}_{ab})\mathbf{p}_b, \tag{121}$$

where the term in the bracket presents the stiffness matrix which is identical to the $\mathbf{K}$ in expression (118).

The variation of the strain energy for a problem–dependent formulation reads

$$\delta V_{def} = \delta \mathbf{p}_b^T \, \overline{\mathbf{K}} \, \mathbf{p}_b, \tag{122}$$

where $\overline{\mathbf{K}}$ is the stiffness matrix given by (67). Since the strain energy is the same regardless of the formulation used, it follows that $\overline{\mathbf{K}} = \mathbf{K}_{bb} - \mathbf{K}_{ba}\mathbf{K}_{aa}^{-1}\mathbf{K}_{ab}$.

From the variation of the work of the applied loading, the same can be proven for load vector $\mathbf{R}$.

The exact analytical distribution of the displacement and the rotation field follows from the full problem–independent interpolation defined by (100) and (115). The exact analytical distribution of the strain measures and the stress and stress-couple resultants further follows from (10) and (25).

2.5 Examples

In this section we will consider a few problems with different distributed loading and apply the results derived in order to obtain a number of interpolations for the unknown quantities, all of which provide the exact theoretical result. In all examples the nodal points will be taken to be equally spaced along the element including element boundaries as the nodal points, i.e. $\xi_i = \dfrac{2i - M - 1}{M - 1}$ for $i = 1, ..., M$ and $\bar{\xi}_j = \dfrac{2j - N - 1}{N - 1}$ for $j = 1, ..., N$.

2.5.1 Thick beam element with no distributed loading

For a beam without distributed loading ($\mathbf{m} = \mathbf{0}$ and $\mathbf{n} = \mathbf{0}$) the dimensionless loading functions vanish ($\boldsymbol{\mu} = \mathbf{0}$ and $\boldsymbol{\nu} = \mathbf{0}$) and, as stated earlier, the exact solution is returned by the proposed interpolation provided $M \geq 3$ and $N \geq 2$. In what follows we take the interpolation for the rotation field of a minimum order, i.e. $M = 3$, for which the equally spaced nodal points are $\xi_1 = -1$, $\xi_2 = 0$ and $\xi_3 = 1$ with the corresponding nodal rotations $\boldsymbol{\theta}_1$, $\boldsymbol{\theta}_2$ and $\boldsymbol{\theta}_3$ and the Lagrangian interpolation

$$I_1 = \frac{1}{2}\xi(\xi - 1), \quad I_2 = -(\xi + 1)(\xi - 1), \quad I_3 = \frac{1}{2}(\xi + 1)\xi, \tag{123}$$

while for the position field we take different number of nodes: minimum ($N = 2$), equal to the number of nodes for the rotation field ($N = 3$) or larger than the number of nodes for the rotation field by one ($N = 4$). This will result in different expressions for the position field, which are all however equivalent to one another. For the rotation field, (123) in conjunction with (100) always leads to

$$\boldsymbol{\theta}(\xi) = \frac{1}{2}\xi(\xi - 1)\boldsymbol{\theta}_1 - (\xi + 1)(\xi - 1)\boldsymbol{\theta}_2 + \frac{1}{2}(\xi + 1)\xi\boldsymbol{\theta}_3. \tag{124}$$

Element with a minimum number of nodal parameters

For $N = 2$ the nodal points to interpolate the position field are $\bar{\xi}_1 = -1$ and $\bar{\xi}_2 = 1$, with the corresponding nodal positions $\mathbf{r}_1$ and $\mathbf{r}_2$ and the Lagrangian interpolation polynomials

$$J_1 = -\frac{1}{2}(\xi - 1), \quad J_2 = \frac{1}{2}(\xi + 1). \tag{125}$$

Substituting this into (101) gives

$$\mathbf{r}(\xi) = -\frac{1}{2}(\xi - 1)\mathbf{r}_1 + \frac{1}{2}(\xi + 1)\mathbf{r}_2 + \frac{L}{4}(1 - \xi^2)\mathbf{G}_1 \times \left[\frac{\xi}{3}(\boldsymbol{\theta}_1 - 2\boldsymbol{\theta}_2 + \boldsymbol{\theta}_3) + \frac{1}{2}(\boldsymbol{\theta}_3 - \boldsymbol{\theta}_1)\right], \tag{126}$$

which evaluated, for example, at $\xi = -\frac{1}{3}$, $\xi = 0$, $\xi = \frac{1}{3}$ gives

$$\mathbf{r}(-\frac{1}{3}) = \frac{1}{3}(2\mathbf{r}_1 + \mathbf{r}_2) + \frac{L}{81}\mathbf{G}_1 \times (-11\boldsymbol{\theta}_1 + 4\boldsymbol{\theta}_2 + 7\boldsymbol{\theta}_3) \tag{127}$$

$$\mathbf{r}(0) = \frac{1}{2}(\mathbf{r}_1 + \mathbf{r}_2) + \frac{L}{8}\mathbf{G}_1 \times (\boldsymbol{\theta}_3 - \boldsymbol{\theta}_1) \tag{128}$$

$$\mathbf{r}(\frac{1}{3}) = \frac{1}{3}(\mathbf{r}_1 + \mathbf{r}_2) + \frac{L}{81}\mathbf{G}_1 \times (-7\boldsymbol{\theta}_1 - 4\boldsymbol{\theta}_2 + 11\boldsymbol{\theta}_3). \tag{129}$$

It is known from elementary engineering beam theory that in the absence of distributed loadings the beam is exposed to constant extensional and shear strains. This results is confirmed by the present interpolation and becomes obvious upon substitution of (124) and (126) into (10):

$$\begin{aligned}\boldsymbol{\Gamma} = \frac{d\mathbf{u}}{dx_1} + \widehat{\mathbf{G}_1\boldsymbol{\theta}} &= \frac{2}{L}(\mathbf{r} - \mathbf{R})' + \mathbf{G}_1 \times \boldsymbol{\theta} = \frac{2}{L}\mathbf{r}' - \mathbf{G}_1 + \mathbf{G}_1 \times \boldsymbol{\theta} \\ = \frac{\mathbf{r}_2 - \mathbf{r}_1}{L} + \frac{1}{2}\mathbf{G}_1 \times \left[\frac{1 - 3\xi^2}{3}(\boldsymbol{\theta}_1 - 2\boldsymbol{\theta}_2 + \boldsymbol{\theta}_3) - \xi(\boldsymbol{\theta}_3 - \boldsymbol{\theta}_1)\right] - \mathbf{G}_1 + \mathbf{G}_1 \times \boldsymbol{\theta} \\ = \frac{\mathbf{r}_2 - \mathbf{r}_1}{L} + \frac{1}{6}\mathbf{G}_1 \times (\boldsymbol{\theta}_1 + 4\boldsymbol{\theta}_2 + \boldsymbol{\theta}_3) - \mathbf{G}_1.\end{aligned} \tag{130}$$

Element with same nodes for positions and rotations

Introducing an additional node to interpolate the position vector in the middle of the beam we obtain redundant nodal degrees of freedom, which, however, make a particularly convenient option as the nodes used to interpolate the position and the rotation vector coincide.

In other words, $N = M = 3$ and the nodal points to interpolate the position field

are the same as the nodal points for rotations, with the corresponding nodal positions $\mathbf{r}_1,\ \mathbf{r}_2$ and $\mathbf{r}_3$. The Lagrangian interpolation is the same as the one used in (123). In conjunction with the solution for position field for the elements with equidistant nodes given in (106) gives

$$\mathbf{r}(\xi) = \frac{1}{2}\xi(\xi-1)\mathbf{r}_1 - (\xi^2-1)\mathbf{r}_2 + \frac{1}{2}\xi(\xi+1)\mathbf{r}_3 + \frac{L}{12}\xi(1-\xi^2)\mathbf{G}_1\times(\boldsymbol{\theta}_1 - 2\boldsymbol{\theta}_2 + \boldsymbol{\theta}_3). \quad (131)$$

This result can be obtained from the solution with minimum number of nodal parameters (126) that is given for $\mathbf{r}(-1)=\mathbf{r}_1$ and $\mathbf{r}(1)=\mathbf{r}_2$, where in this case ($N=M=3$) $\mathbf{r}(-1)=\mathbf{r}_1$, $\mathbf{r}(0)=\mathbf{r}_2$ and $\mathbf{r}(1)=\mathbf{r}_3$. Also, we introduce $\dfrac{L}{8}\mathbf{G}_1\times(\boldsymbol{\theta}_3-\boldsymbol{\theta}_1)$ from (128) with the same nodal renumeration.

Element with independent interpolation for positions and rotations

Introducing two internal nodes to interpolate the position vector we get another set of redundant nodal degrees of freedom which is also interesting since the interpolations for the position and the rotation vector turn out to be independent.

Now, $N = M+1 = 4$ and the nodal points to interpolate the position field are $\bar{\xi}_1 = -1,\ \bar{\xi}_2 = -\dfrac{1}{3},\ \bar{\xi}_3 = \dfrac{1}{3}$ and $\bar{\xi}_4 = 1$, with the nodal positions $\mathbf{r}_1,\ \mathbf{r}_2,\ \mathbf{r}_3$ and $\mathbf{r}_4$. The Lagrangian interpolation functions are

$$J_1 = -\frac{9}{16}(\xi+\frac{1}{3})(\xi-\frac{1}{3})(\xi-1), \quad J_2 = \frac{27}{16}(\xi+1)(\xi-\frac{1}{3})(\xi-1),$$
$$J_3 = -\frac{27}{16}(\xi+1)(\xi+\frac{1}{3})(\xi-1), \quad J_4 = \frac{9}{16}(\xi+1)(\xi+\frac{1}{3})(\xi-1) \quad (132)$$

and the interpolation for the position vector is simply given by (103). The same result would be obtained from the solution with minimum number of nodal parameters (126) upon expressing $\mathbf{G}_1\times(\boldsymbol{\theta}_1-2\boldsymbol{\theta}_2+\boldsymbol{\theta}_3)$ by the difference of (129) and (127) and expressing $\mathbf{G}_1\times(\boldsymbol{\theta}_3-\boldsymbol{\theta}_1)$ from the sum of the same expressions. Nodes $\mathbf{r}(-1)=\mathbf{r}_1,\ \mathbf{r}(1)=\mathbf{r}_2$ from (126) are renumbered as $\mathbf{r}(-1)=\mathbf{r}_1$, $\mathbf{r}(-\dfrac{1}{3})=\mathbf{r}_2$, $\mathbf{r}(\dfrac{1}{3})=\mathbf{r}_3$ and $\mathbf{r}(1)=\mathbf{r}_4$. The result is given here:

$$\mathbf{r}(\xi) = -\frac{1}{2}(\xi-1)\mathbf{r}_1 + \frac{1}{2}(\xi+1)\mathbf{r}_4 + (1-\xi^2)\frac{9}{16}\left[\xi(3\mathbf{r}_3 - 3\mathbf{r}_2 - \mathbf{r}_4 + \mathbf{r}_1) + (\mathbf{r}_2 + \mathbf{r}_3 - \mathbf{r}_1 - \mathbf{r}_4)\right]$$
$$= -\frac{1}{2}(\xi-1)\left[\frac{9}{8}(\xi^2-1)+1\right]\mathbf{r}_1 + \frac{9}{16}(3\xi-1)(\xi^2-1)\mathbf{r}_2 - \frac{9}{16}(3\xi+1)(\xi^2-1)\mathbf{r}_3 + \frac{1}{2}(\xi+1)\left[\frac{9}{8}(\xi^2-1)+1\right]\mathbf{r}_4 = \sum_{j=1}^{4} J_j(\xi)\mathbf{r}_j. \quad (133)$$

2.5.2 Thick beam element with constant distributed loading n and m

Constant distributed loading ($\mathbf{m}$ and $\mathbf{n}$) results in constant dimensionless loading functions $\boldsymbol{\mu}$ and $\boldsymbol{\nu}$ and the exact solution is obtained by the proposed interpolation with $M \geq 4$ and $N \geq 3$. The interpolation of the rotation field is of a minimum order, i.e. $M = 4$, for which the equally spaced nodal points ξ_i ($i = 1, ..., 4$) are the same as the nodal points $\bar{\xi}_j$ ($j = 1, ..., 4$) in the previous part, $\xi_2 = 0,\ \xi_3 = 1$ with the corresponding nodal rotations $\boldsymbol{\theta}_1,\ \boldsymbol{\theta}_2,\ \boldsymbol{\theta}_3$ and $\boldsymbol{\theta}_4$ and the Lagrangian interpolation functions $I_i(\xi)\ \ i = 1, ..., 4$ the same as the interpolation functions $J_j(\xi),\ \ j = 1, ..., 4$ also given in the previous part by (132). This leads to the same interpolation for the rotation field $\boldsymbol{\theta}(\xi) = \sum_{i=1}^{4} I_i(\xi)\boldsymbol{\theta}_i$.
For the position field, we take different number of nodes: minimum ($N = 3$), equal to the number of nodes for the rotation field ($N = 4$) or larger than the number of nodes for the rotation field by one ($N = 5$). This will result in different expressions of the position field equivalent to one another.

Element with a minimum number of nodal parameters
For $N = 3$ the nodal points used to interpolate the position field are $\bar{\xi}_1 = -1,\ \bar{\xi}_2 = 0,\ \bar{\xi}_3 = 1$, with the corresponding nodal positions $\mathbf{r}_1,\ \mathbf{r}_2$ and $\mathbf{r}_3$ and the Lagrangian interpolation functions

$$J_1 = \frac{1}{2}\xi(\xi-1),\ \ J_2 = -(\xi+1)(\xi-1),\ \ J_3 = \frac{1}{2}(\xi+1)\xi. \quad (134)$$

In conjunction with (101) this leads to

$$\mathbf{r}(\xi) = \frac{1}{2}\xi(\xi-1)\mathbf{r}_1 - (\xi+1)(\xi-1)\mathbf{r}_2 + \frac{1}{2}(\xi+1)\xi\mathbf{r}_3 + \frac{L}{2}\xi(\xi^2-1)\mathbf{G}_1 \times \frac{9}{16}\left[\frac{\xi}{4}(\boldsymbol{\theta}_1 - 3\boldsymbol{\theta}_2 + 3\boldsymbol{\theta}_3 - \boldsymbol{\theta}_4) - \frac{1}{3}(\boldsymbol{\theta}_1 - \boldsymbol{\theta}_2 - \boldsymbol{\theta}_3 + \boldsymbol{\theta}_4)\right], \quad (135)$$

which, evaluated, for example, at $\xi = -\frac{1}{2}$, $\xi = -\frac{1}{3}$, $\xi = \frac{1}{3}$ and $\xi = \frac{1}{2}$, gives

$$\mathbf{r}(-\frac{1}{2}) = \frac{3}{8}\mathbf{r}_1 + \frac{3}{4}\mathbf{r}_2 - \frac{1}{8}\mathbf{r}_3 + \frac{3}{8}\frac{L}{2}\mathbf{G}_1 \times \frac{9}{16}\left(-\frac{11}{24}\boldsymbol{\theta}_1 + \frac{17}{24}\boldsymbol{\theta}_2 - \frac{1}{24}\boldsymbol{\theta}_3 - \frac{5}{24}\boldsymbol{\theta}_4\right) \quad (136)$$

$$\mathbf{r}(-\frac{1}{3}) = \frac{2}{9}\mathbf{r}_1 + \frac{8}{9}\mathbf{r}_2 - \frac{1}{9}\mathbf{r}_3 + \frac{8}{27}\frac{L}{2}\mathbf{G}_1 \times \frac{9}{16}\left(-\frac{5}{12}\boldsymbol{\theta}_1 + \frac{7}{12}\boldsymbol{\theta}_2 + \frac{1}{12}\boldsymbol{\theta}_3 - \frac{1}{4}\boldsymbol{\theta}_4\right) \quad (137)$$

$$\mathbf{r}(\frac{1}{3}) = -\frac{1}{9}\mathbf{r}_1 + \frac{8}{9}\mathbf{r}_2 + \frac{2}{9}\mathbf{r}_3 - \frac{8}{27}\frac{L}{2}\mathbf{G}_1 \times \frac{9}{16}\left(-\frac{1}{4}\boldsymbol{\theta}_1 + \frac{1}{12}\boldsymbol{\theta}_2 + \frac{7}{12}\boldsymbol{\theta}_3 - \frac{5}{12}\boldsymbol{\theta}_4\right) \quad (138)$$

$$\mathbf{r}(\frac{1}{2}) = -\frac{1}{8}\mathbf{r}_1 + \frac{3}{4}\mathbf{r}_2 + \frac{3}{8}\mathbf{r}_3 - \frac{3}{8}\frac{L}{2}\mathbf{G}_1 \times \frac{9}{16}\left(-\frac{5}{24}\boldsymbol{\theta}_1 - \frac{1}{24}\boldsymbol{\theta}_2 + \frac{17}{24}\boldsymbol{\theta}_3 - \frac{11}{24}\boldsymbol{\theta}_4\right) \quad (139)$$

For constant distributed loadings the beam is exposed to linearly varying direct and shearing strains, which is confirmed by the present interpolation upon substitution of $\boldsymbol{\theta} = \sum_{i=1}^{4} I_i(\xi)\boldsymbol{\theta}_i$ in (10):

$$\boldsymbol{\Gamma} = \frac{2}{L}\mathbf{r}' + \mathbf{G}_1 \times \boldsymbol{\theta} - \mathbf{G}_1 = \frac{2}{L}\left[(\xi - \frac{1}{2})\mathbf{r}_1 - 2\xi\mathbf{r}_2 + (\xi + \frac{1}{2}\mathbf{r}_3)\right]$$
$$+\frac{9}{16}\mathbf{G}_1 \times \left[\left(\xi^3 - \frac{\xi}{2}\right)(\boldsymbol{\theta}_1 - 3\boldsymbol{\theta}_2 + 3\boldsymbol{\theta}_3 - \boldsymbol{\theta}_4) - \left(\xi^2 - \frac{1}{3}\right)(\boldsymbol{\theta}_1 - \boldsymbol{\theta}_2 - \boldsymbol{\theta}_3 + \boldsymbol{\theta}_4)\right]$$
$$-\frac{9}{16}\mathbf{G}_1 \times \left[\left(\xi^3 - \xi^2 - \frac{1}{9}\xi + \frac{1}{9}\right)\boldsymbol{\theta}_1 - 3\left(\xi^3 - \frac{1}{3}\xi^2 - \xi + \frac{1}{3}\right)\boldsymbol{\theta}_2\right.$$
$$\left.+3\left(\xi^3 + \frac{1}{3}\xi^2 - \xi - \frac{1}{3}\right)\boldsymbol{\theta}_3 - \left(\xi^3 + \xi^2 - \frac{1}{9}\xi - \frac{1}{9}\right)\boldsymbol{\theta}_4\right] - \mathbf{G}_1$$

$$= \frac{\mathbf{r}_3 - \mathbf{r}_1}{L} + \frac{2\xi}{L}(\mathbf{r}_1 - 2\mathbf{r}_2 + \mathbf{r}_3)$$
$$+ \frac{9}{16}\mathbf{G}_1 \times \left[-\frac{\xi}{2}(\boldsymbol{\theta}_1 - 3\boldsymbol{\theta}_2 + 3\boldsymbol{\theta}_3 - \boldsymbol{\theta}_4) + \frac{1}{3}(\boldsymbol{\theta}_1 - \boldsymbol{\theta}_2 - \boldsymbol{\theta}_3 + \boldsymbol{\theta}_4) \right]$$
$$+ \frac{9}{16}\mathbf{G}_1 \times \left[\frac{\xi}{9}(\boldsymbol{\theta}_1 - 27\boldsymbol{\theta}_2 + 27\boldsymbol{\theta}_3 - \boldsymbol{\theta}_4) - \frac{1}{9}(\boldsymbol{\theta}_1 - 9\boldsymbol{\theta}_2 - 9\boldsymbol{\theta}_3 + \boldsymbol{\theta}_4) \right] - \mathbf{G}_1$$
$$= \frac{\mathbf{r}_3 - \mathbf{r}_1}{L} + \frac{2\xi}{L}(\mathbf{r}_1 - 2\mathbf{r}_2 + \mathbf{r}_3)$$
$$+ \frac{1}{32}\mathbf{G}_1 \times [4(\boldsymbol{\theta}_1 + 3\boldsymbol{\theta}_2 + 3\boldsymbol{\theta}_3 + \boldsymbol{\theta}_4) + \xi(-7\boldsymbol{\theta}_1 - 27\boldsymbol{\theta}_2 + 27\boldsymbol{\theta}_3 + 7\boldsymbol{\theta}_4)] - \mathbf{G}_1. \quad (140)$$

Element with same nodes for positions and rotations

Introducing an additional node to interpolate the position vector and setting the nodes to coincide with the nodes used to interpolate the rotation vector, we arrive at a set of redundant nodal degrees of freedom with $N = M = 4,\ \bar{\xi}_i = \xi_i,\ i = 1, ..., 4,$ $\mathbf{r}_1 = \mathbf{r}(-1),\ \mathbf{r}_2 = \mathbf{r}(-\frac{1}{3}),\ \mathbf{r}_3 = \mathbf{r}(\frac{1}{3})$ and $\mathbf{r}_4 = \mathbf{r}(1)$ and the Lagrangian interpolation as in (132). This gives the following expression for the displacement field

$$\mathbf{r}(\xi) = -\frac{9}{16}(\xi^2 - \frac{1}{9})(\xi - 1)\mathbf{r}_1 + \frac{27}{16}(\xi - \frac{1}{3})(\xi^2 - 1)\mathbf{r}_2 - \frac{27}{16}(\xi + \frac{1}{3})(\xi^2 - 1)\mathbf{r}_3$$
$$+ \frac{9}{16}(\xi + 1)(\xi^2 - \frac{1}{9})\mathbf{r}_4 + \frac{9L}{128}(\xi^2 - 1)(\xi^2 - \frac{1}{9})\mathbf{G}_1 \times (\boldsymbol{\theta}_1 - 3\boldsymbol{\theta}_2 + 3\boldsymbol{\theta}_3 - \boldsymbol{\theta}_4), \quad (141)$$

which is again exactly the result obtained from the solution with minimum number of nodal parameters (135) upon noting that $\mathbf{r}(-\frac{1}{3}),\ \mathbf{r}(\frac{1}{3})$ and $\mathbf{r}_3 = \mathbf{r}(1)$ in (135) respectively correspond to $\mathbf{r}_2 = \mathbf{r}(-\frac{1}{3}),\ \mathbf{r}_3 = \mathbf{r}(\frac{1}{3})$ and $\mathbf{r}_4 = \mathbf{r}(1)$ here. To show this, it is necessary to express $\frac{1}{3}\frac{L}{2}\mathbf{G}_1 \times \frac{9}{16}(\boldsymbol{\theta}_1 - \boldsymbol{\theta}_2 - \boldsymbol{\theta}_3 + \boldsymbol{\theta}_4)$ and $\mathbf{r}(0)$ from the difference of the sum of (137) and (138), respectively, and substitute the result in (135).

Element with independent interpolation for positions and rotations

Now $N = M + 1 = 5$ and the nodal points to interpolate the position field are $\bar{\xi}_1 = -1,\ \bar{\xi}_2 = -\frac{1}{2},\ \bar{\xi}_3 = 0,\ \bar{\xi}_4 = \frac{1}{2}$ and $\bar{\xi}_5 = 1$, with the nodal positions $\mathbf{r}_1,\ \mathbf{r}_2,\ \mathbf{r}_3,\ \mathbf{r}_4$ and $\mathbf{r}_5$. The corresponding Lagrangian interpolation functions are

$$J_1 = \frac{2}{3}(\xi+\frac{1}{2})\xi(\xi-\frac{1}{2})(\xi-1), \qquad J_2 = -\frac{8}{3}(\xi+1)\xi(\xi-\frac{1}{2})(\xi-1),$$
$$J_3 = 4(\xi+1)(\xi+\frac{1}{2})(\xi-\frac{1}{2})(\xi-1), \qquad J_4 = -\frac{8}{3}(\xi+1)(\xi+\frac{1}{2})\xi(\xi-1),$$
$$J_5 = \frac{2}{3}(\xi+1)(\xi+\frac{1}{2})\xi(\xi-\frac{1}{2}) \tag{142}$$

and the interpolation for the position vector is simply given by (103). As expected, the same result would be obtained from the solution with minimum number of nodal parameters (135) upon introduction of $\frac{L}{2}\mathbf{G}_1 \times \frac{9}{16}\frac{1}{4}(\boldsymbol{\theta}_1 - 3\boldsymbol{\theta}_2 + 3\boldsymbol{\theta}_3 - \boldsymbol{\theta}_4) = \frac{2}{3}(\mathbf{r}_1 - 4\mathbf{r}_2 + 6\mathbf{r}_3 - 4\mathbf{r}_4 + \mathbf{r}_5)$ and $\frac{L}{2}\mathbf{G}_1 \times \frac{9}{16}\frac{1}{3}(\boldsymbol{\theta}_1 - \boldsymbol{\theta}_2 - \boldsymbol{\theta}_3 + \boldsymbol{\theta}_4) = \frac{2}{3}(\mathbf{r}_1 - 2\mathbf{r}_2 + 2\mathbf{r}_4 - \mathbf{r}_5)$ from the sum of the difference of (139) and (137), respectively, and noting that $\mathbf{r}(-\frac{1}{2}),\ \mathbf{r}_2 = \mathbf{r}(0),\ \mathbf{r}(\frac{1}{2})$ and $\mathbf{r}_3 = \mathbf{r}(1)$ in the previous part respectively correspond to $\mathbf{r}_2 = \mathbf{r}(-\frac{1}{2}), \mathbf{r}_3 = \mathbf{r}(0), \mathbf{r}_4 = \mathbf{r}(\frac{1}{2})$ and $\mathbf{r}_5 = \mathbf{r}(1)$ here:

$$\begin{aligned}\mathbf{r}(\xi) &= \frac{1}{2}\xi(\xi-1)\mathbf{r}_1 - (\xi+1)(\xi-1)\mathbf{r}_3 + \frac{1}{2}(\xi+1)\xi\mathbf{r}_5 \\ &\quad + \frac{2}{3}\xi(\xi^2-1)[\xi(\mathbf{r}_1 - 4\mathbf{r}_2 + 6\mathbf{r}_3 - 4\mathbf{r}_4 + \mathbf{r}_5) - (\mathbf{r}_1 - 2\mathbf{r}_2 + 2\mathbf{r}_4 - \mathbf{r}_5)] \\ &= \xi(\xi-1)\left[\frac{2}{3}\xi(\xi+1) - \frac{2}{3}(\xi+1) + \frac{1}{2}\right]\mathbf{r}_1 - \frac{4}{3}\xi(\xi^2-1)(2\xi-1)\mathbf{r}_2 + (\xi^2-1)(4\xi^2-1)\mathbf{r}_3 \\ &\quad - \frac{4}{3}\xi(\xi^2-1)(2\xi+1)\mathbf{r}_4 + \xi(\xi+1)\left[\frac{2}{3}\xi(\xi-1) + \frac{2}{3}(\xi-1) + \frac{1}{2}\right]\mathbf{r}_5 = \sum_{j=1}^{5} J_j(\xi)\mathbf{r}_j.\end{aligned} \tag{143}$$

3 Static non–linear analysis of beam elements and configuration–dependent interpolation of arbitrary order

In this chapter, numerical approaches for solving governing equations of the geometrically non-linear Reissner–Simo beam theory will be studied. We will present an original novel configuration–dependent interpolation [28] for the kinematic quantities of the Reissner–Simo beam.

3.1 Introduction to non–linear beam problems

Geometrically exact beam theory and its finite element implementation have been the subject of extensive research in the recent past(see e.g. [9, 19, 21, 33, 35, 43]). We are concerned with the geometrically exact 3D beam theory of Reissner [32] and Simo [33] which has provided the basis for many of the recent finite element formulations for 3D beams (e.g. [9, 17]). The geometrically exact theory provides the relationship between the configuration and the adopted strain measures which are fully consistent with the virtual work principle and the differential equations of motion, regardless of the magnitude of displacements, rotations and strains involved [33].

Standard procedures in the finite element method use Lagrangian polynomials as interpolation functions to describe unknown functions approximately. Since non–linear analysis employs Newton–Raphson solution procedure to solve the system of equations iteratively, this allows us to generalise the interpolation procedure without additional computational efforts apart from the changes made on the element level.

When dealing with 3D problems, rotations in space can present very serious problems. These are the problems of additivity and objectivity (invariance). The geometrically exact theory says that the strain measures are objective which means that they have the ability to remain unaffected by a constant motion of the configuration. However, this is not necessarily automatically satisfied when the problem is implemented into a finite element method environment. The reason for this is the additive character of the interpolation functions that are used in the finite element method, whereas the rotations in space cannot be presented in this way.

Jelenić and Crisfield [18] introduced a strain–invariant and path–independent ge-

ometrically exact isoparametric 3D beam element with arbitrary number of nodes. The key to the formulation is found in the interpolation of current local rotations. A different approach, aimed at resolving a more general type of non-objectivity of the numerical results with respect to the chosen definition of the beam reference line, is given in [4] by Borri and Bottasso. The resulting formulation in the process returns exactly the same solution for the interpolation of the rotation field as [18], and it additionally eliminates the problem of shear locking by design. However, the formulation is only applicable to two–noded elements and the given methodology has been strictly limited to that case. Both of these formulations [4, 5, 18] present a problem dependent on the configuration of the beam, hence configuration–dependent interpolation term can be used.

In non–linear 3D beam theory with rotational degrees of freedom [33] configuration–dependent interpolation therefore may be utilised to provide a result invariant to the choice of the beam reference axis [5] or invariant to a rigid–body rotation [18]. For 2D beam elements, the latter issue vanishes, and such elements are more illustrative for the study of accuracy of the configuration–dependent interpolation in higher–order elements.

When choosing new interpolation functions we demand they result in exact solution where such exists, such as linear analysis and pure bending in non–linear analysis. In order to define the new configuration–dependent interpolation, existing configuration–dependent interpolations are used as a template [5, 18].

In the first three subsections of the second chapter we present the three basic ingredients on which we build our family of elements with configuration–dependent interpolation.

The first of these is the family of generalised interpolation functions for the rotation increments which, for a two–noded element, coincides with the interpolation for the same quantity in the helicoidal interpolation, our second basic ingredient. Since the helicoidal interpolation is only applicable to two–noded elements and it utilises the same interpolation also for the position vector, it appears to be a natural idea to use the generalised interpolation from our first ingredient when attempting to generalise the helicoidal interpolation to higher–order elements. This interpolation is next fine–tuned to provide the exact solution in linear analysis, our third ingredient.

In the following subsection we constrain this interpolation to satisfy the strain–

invariance condition. Results for the 2D case are given as well as the graphical representation of the proposed functions.

3.1.1 Summary of the strain–invariant 3D beam formulation

A strain–invariant path–independent formulation for geometrically exact higher–order beam element has been derived in [18]. In this formulation the position vector of the beam reference axis, taken to coincide with the line of centroids, in the deformed state $\mathbf{r}(x_1)$ has been interpolated in a standard Lagrangian manner as

$$\mathbf{r}(x_1) \approx \mathbf{r}^h(x_1) = \sum_{i=1}^{N} I_i(x_1)\mathbf{r}_i \ , \tag{144}$$

where $x_1 \in [0, L]$ is the material–point position parameter, N is the number of element nodes, $I_i(x_1)$ are the Lagrangian polynomials of order $N-1$ satisfying $I_i(x_{1j}) = \delta_{ij}$ and $\mathbf{r}_i = \mathbf{r}^h(x_{1i})$, where index h denotes an interpolated field, and δ_{ij} is the Kronecker symbol ($\delta_{ij} = 1$ if $i = j$ and $\delta_{ij} = 0$ otherwise).
The rotations have been treated in a very specific manner. The rotation matrix $\mathbf{\Lambda}(x_1)$ has been decomposed into a part which is constant for the whole beam and rigidly attached to a node ($\mathbf{\Lambda}_r$), and the part due to a local $\mathbf{\Psi}^l$ rotation with respect to $\mathbf{\Lambda}_r$:

$$\mathbf{\Lambda}(x_1) = \mathbf{\Lambda}_r \exp \mathbf{\Psi}^l(x_1) \approx \mathbf{\Lambda}^h(x_1) = \mathbf{\Lambda}_r \exp \hat{\mathbf{\Psi}}^{lh}(x_1) \ , \tag{145}$$

with

$$\exp \hat{\mathbf{\Psi}}^{lh} = \mathbf{I} + \frac{\sin \Psi^{lh}}{\Psi^{lh}} \ \hat{\mathbf{\Psi}}^{lh} + \frac{1 - \cos \Psi^{lh}}{(\Psi^{lh})^2} \ (\hat{\mathbf{\Psi}}^{lh})^2 \ , \tag{146}$$

where $\Psi^{lh} = \| \ \mathbf{\Psi}^{lh} \ \|$ and $\mathbf{\Lambda}_r$ may be taken to coincide with a particular node I or may be related to two chosen nodes I and J via

$$\mathbf{\Lambda}_r = \mathbf{\Lambda}_I \ \exp(\frac{1}{2}\hat{\boldsymbol{\phi}}) \ , \tag{147}$$

where $\boldsymbol{\phi}$ is the relative material rotation between the nodes I and J extracted from

$$\exp \hat{\boldsymbol{\phi}} = \mathbf{\Lambda}_I^T \ \mathbf{\Lambda}_J \tag{148}$$

and index l denotes a local value of a rotation taken with respect to the reference triad $\mathbf{\Lambda}_r$. Note that for $I = J$, $\exp \hat{\boldsymbol{\phi}} = \mathbf{I}$ or, in other words, there is no relative rotation ϕ.

The local rotation $\boldsymbol{\Psi}^l(x_1)$ is next interpolated in the standard Lagrangian way

$$\boldsymbol{\Psi}^l(x_1) \approx \boldsymbol{\Psi}^{lh}(x_1) = \sum_{i=1}^{N} I_i(x_1)\boldsymbol{\Psi}_i^l \,, \tag{149}$$

where the local nodal rotations $\boldsymbol{\Psi}_i^l$ are extracted from

$$\exp \hat{\boldsymbol{\Psi}}_i^{\,l} = \boldsymbol{\Lambda}_r^T \boldsymbol{\Lambda}_i \,. \tag{150}$$

For the non–linear finite–element solution procedure it is necessary to interpolate the Newton–Raphson increments $\Delta\mathbf{r}$ and $\Delta\boldsymbol{\vartheta}$ in $\Delta\boldsymbol{\Lambda} = \widehat{\Delta\boldsymbol{\vartheta}}\boldsymbol{\Lambda}$. Obviously

$$\Delta\mathbf{r} \approx \Delta\mathbf{r}^h = \sum_{i=1}^{N} I_i \, \Delta\mathbf{r}_i \,, \tag{151}$$

while $\Delta\boldsymbol{\vartheta}$ has been closely investigated in [18] and the result found in the form

$$\Delta\boldsymbol{\vartheta} \approx \Delta\boldsymbol{\vartheta}^h = \sum_{i=1}^{N} \tilde{\mathbf{I}}^i(\boldsymbol{\Lambda}^h)\Delta\boldsymbol{\vartheta}_i \,, \tag{152}$$

with

$$\tilde{\mathbf{I}}^i = \sum_{j=1}^{N}\sum_{k=1}^{N} \Delta_k^{ij}\boldsymbol{\Lambda}_r \Big\{ (\delta_{Ik} + \delta_{Jk}) \left[\mathbf{I} - \mathbf{H}(\boldsymbol{\Psi}^{lh}) \sum_{m=1}^{N} I_m \mathbf{H}^{-1}(\boldsymbol{\Psi}_m^l) \right] \mathbf{V}_j + \mathbf{H}(\boldsymbol{\Psi}^{lh}) I_k \mathbf{H}^{-1}(\boldsymbol{\Psi}_j^l) \Big\} \boldsymbol{\Lambda}_r^T \,, \tag{153}$$

$$\mathbf{V}_I = \frac{1}{2}(\mathbf{I} + \frac{1}{\phi}\tan\frac{\phi}{4}\hat{\boldsymbol{\phi}}) \,, \tag{154}$$

$$\mathbf{V}_J = \frac{1}{2}(\mathbf{I} - \frac{1}{\phi}\tan\frac{\phi}{4}\hat{\boldsymbol{\phi}}) \tag{155}$$

and

$$\mathbf{H}(\boldsymbol{\Psi}^l) = \mathbf{I} + \frac{1-\cos\Psi^l}{(\Psi^l)^2}\,\hat{\boldsymbol{\Psi}}^{\,l} + \frac{\Psi^l - \sin\Psi^l}{(\Psi^l)^3}\,(\hat{\boldsymbol{\Psi}}^{\,l})^2 \,, \tag{156}$$

$$\mathbf{H}^{-1}(\boldsymbol{\Psi}^l) = \mathbf{I} - \frac{1}{2}\,\hat{\boldsymbol{\Psi}}^{\,l} - \frac{1}{2}\,\frac{\Psi^l\,\sin\Psi^l + 2\cos\Psi^l - 2}{(\Psi^l)^2(1-\cos\Psi^l)}\,(\hat{\boldsymbol{\Psi}}^{\,l})^2 \,, \tag{157}$$

while

$$\Delta_k^{ij} = \begin{cases} 1 & \text{for } i = j = k \\ 0 & \text{otherwise} \end{cases} . \tag{158}$$

3.1.2 Summary of the helicoidal 3D beam formulation

The helicoidal interpolation presented and developed in many different aspects in [4, 5, 7, 6, 8] may be thought of as originating from a requirement that the finite-element solution should be invariant to the choice of the beam reference line and kinematically consistent in the sense that it should belong to the solution space including the orthogonality group $SO(3)$.

The first of these requirements boils down simply to the condition that both the position vector of the reference line ($\mathbf{r}$) and the rotation tensor ($\mathbf{\Lambda}$) should be interpolated using the same interpolation functions. For instance, using the standard Lagrangian polynomials this yields [8]

$$\mathbf{r}^h(x_1) = \sum_{i=1}^{N} I_i(x_1)\mathbf{r}_i \tag{159}$$

$$\mathbf{\Lambda}^h(x_1) = \sum_{i=1}^{N} I_i(x_1)\mathbf{\Lambda}_i. \tag{160}$$

The above interpolation of the rotation tensor, however, is clearly kinematically inconsistent, i.e. $\mathbf{\Lambda}^h(x_1)$ is in general neither orthogonal nor unimodular (see Subsection 2.2.1 for definitions). To satisfy this requirement, an alternative interpolation has been proposed in [4] which reads

$$\mathbf{r}^h(x_1) = \sum_{i=1}^{2} \tilde{\mathbf{N}}_i\mathbf{r}_i \tag{161}$$

$$\mathbf{\Lambda}^h(x_1) = \sum_{i=1}^{2} \tilde{\mathbf{N}}_i\mathbf{\Lambda}_i \quad \Rightarrow \quad \Delta\boldsymbol{\vartheta}^h(x_1) = \sum_{i=1}^{2} \tilde{\mathbf{N}}_i\Delta\boldsymbol{\vartheta}_i, \tag{162}$$

where the generalised interpolation functions $\tilde{\mathbf{N}}_i$ are identical to $\tilde{\mathbf{I}}_i$ in (153) for two–noded element $N = 2$ (see Appendix B). It is important to note that the proposed helicoidal interpolation makes sense only for two–noded elements.

Linearised model

If we attempted to apply this result to a higher–order element, we would realise that the exact result, even in the limit case of the analysis becoming linear, cannot be

achieved. To show this let us first note that

$$\mathbf{\Lambda}_r \mathbf{\Lambda}_r^T = \mathbf{I} \,, \tag{163}$$

$$\mathbf{\Lambda}_r \mathbf{H}(\mathbf{\Psi}^{lh}) \mathbf{\Lambda}_r^T = \mathbf{H}(\mathbf{\Lambda}_r \mathbf{\Psi}^{lh}) \,, \tag{164}$$

$$\mathbf{\Lambda}_r \mathbf{H}^{-1}(\mathbf{\Psi}_i^l) \mathbf{\Lambda}_r^T = \mathbf{H}^{-1}(\mathbf{\Lambda}_r \mathbf{\Psi}_i^l) \,, \tag{165}$$

$$\mathbf{\Lambda}_r \mathbf{V}_J \mathbf{\Lambda}_r^T = \frac{1}{2} \, (\mathbf{I} - \frac{1}{\phi} \, \tan \frac{\phi}{4} \, \widehat{\mathbf{\Lambda}_r \boldsymbol{\phi}}) \,, \tag{166}$$

$$\mathbf{\Lambda}_r \mathbf{V}_I \mathbf{\Lambda}_r^T = \frac{1}{2} \, (\mathbf{I} + \frac{1}{\phi} \, \tan \frac{\phi}{4} \, \widehat{\mathbf{\Lambda}_r \boldsymbol{\phi}}) \tag{167}$$

and also that $\mathbf{\Lambda}_r \mathbf{\Psi}_i^l$ and $\mathbf{\Lambda}_r \boldsymbol{\phi}$ are the spatial counterparts of $\mathbf{\Psi}_i^l$ and $\boldsymbol{\phi}$:

$$\boldsymbol{\psi}_i^l = \mathbf{\Lambda}_r \mathbf{\Psi}_i^l \,, \tag{168}$$

$$\boldsymbol{\varphi} = \mathbf{\Lambda}_r \boldsymbol{\phi} \,. \tag{169}$$

Now, for linearised model, the rotations become infinitesimally small which means that $\mathbf{\Lambda}_r = \mathbf{\Lambda}_0$, where $\mathbf{\Lambda}_0$ is a matrix of initial undeformed orientation. If we want to write $\mathbf{H}(\boldsymbol{\psi}^{lh})$ and $\mathbf{H}^{-1}(\psi_i^l)$ as linear functions of their arguments, we build up a Taylor series of the trigonometric functions involved and keep the linear terms only. This gives us linear functions

$$\mathbf{H}(\boldsymbol{\psi}^{lh}) = \mathbf{I} + \frac{1}{2} \, \hat{\boldsymbol{\psi}}^{lh} \,, \tag{170}$$

$$\mathbf{H}^{-1}(\boldsymbol{\psi}_i^l) = \mathbf{I} - \frac{1}{2} \, \hat{\boldsymbol{\psi}}_i^{\,l} \,. \tag{171}$$

Also

$$\mathbf{\Lambda}_0 \mathbf{V}_I \mathbf{\Lambda}_0^T = \frac{1}{2} \, \mathbf{I} + \frac{1}{2} \, \lim_{\varphi \to 0} (\frac{\tan \frac{\varphi}{4}}{\varphi}) \, \hat{\boldsymbol{\varphi}} = \frac{1}{2} \, (\mathbf{I} + \frac{1}{4} \, \hat{\boldsymbol{\varphi}}) \,, \tag{172}$$

$$\mathbf{\Lambda}_0 \mathbf{V}_J \mathbf{\Lambda}_0^T = ... = \frac{1}{2} \, (\mathbf{I} - \frac{1}{4} \, \hat{\boldsymbol{\varphi}}) \,, \tag{173}$$

$$\boldsymbol{\varphi} = \boldsymbol{\psi}_J^l - \boldsymbol{\psi}_I^l \,, \tag{174}$$

and, owing to $\mathbf{\Lambda}_r = \mathbf{\Lambda}_0$, the rotations cease to be local i.e. $\boldsymbol{\psi}_i^l = \boldsymbol{\psi}_i$.

For linearised model we thus have

$$\tilde{\mathbf{I}}^i = \sum_{j=1}^{N}\sum_{k=1}^{N} \Delta_k^{ij}(\delta_{Ik}+\delta_{Jk}) \left[\mathbf{I} - (\mathbf{I}+\frac{1}{2}\hat{\boldsymbol{\psi}}^h) \sum_{m=1}^{N} I_m(\mathbf{I}-\frac{1}{2}\hat{\boldsymbol{\psi}}_m)\right] \mathbf{\Lambda}_0\mathbf{V}_j\mathbf{\Lambda}_0^T + \sum_{j=1}^{N}\sum_{k=1}^{N} \Delta_k^{ij} I_k(\mathbf{I}+\frac{1}{2}\,\hat{\boldsymbol{\psi}}^h)(\mathbf{I}-\frac{1}{2}\,\hat{\boldsymbol{\psi}}_j) = I_i(\mathbf{I}+\frac{1}{2}\widehat{\boldsymbol{\psi}^h - \boldsymbol{\psi}_i}) \,. \quad (175)$$

The results from (161) and (162) now become

$$\mathbf{r}^h = \sum_{i=1}^{N} I_i(\mathbf{I}+\frac{1}{2}\widehat{\boldsymbol{\psi}^h - \boldsymbol{\psi}_i})\mathbf{r}_i = \sum_{i=1}^{N} I_i(\mathbf{I}+\frac{1}{2}\widehat{\boldsymbol{\psi}^h - \boldsymbol{\psi}_i})(\mathbf{R}_i+\mathbf{u}_i) \,, \quad (176)$$

$$\Delta\boldsymbol{\vartheta}^h = \sum_{i=1}^{N} I_i(\mathbf{I}+\frac{1}{2}\widehat{\boldsymbol{\psi}^h - \boldsymbol{\psi}_i})\Delta\boldsymbol{\vartheta}_i \,, \quad (177)$$

where $\mathbf{R}_i$ is the vector of initial nodal positions and $\mathbf{u}_i$ is the vector of nodal displacements. Since $\mathbf{r}^h = \mathbf{R}^h + \mathbf{u}^h$ and $\mathbf{R}^h = \sum_{i=1}^{N} I_i\mathbf{R}_i$ and because for linearised model $\Delta\boldsymbol{\vartheta}_i = \boldsymbol{\psi}_i$, we further have

$$\sum_{i=1}^{N} I_i\mathbf{R}_i + \mathbf{u}^h = \sum_{i=1}^{N} I_i\mathbf{R}_i + \sum_{i=1}^{N} I_i\mathbf{u}_i + \frac{1}{2}\sum_{i=1}^{N} I_i\hat{\boldsymbol{\psi}}^h\mathbf{R}_i - \frac{1}{2}\sum_{i=1}^{N} I_i\hat{\boldsymbol{\psi}}_i\mathbf{R}_i \,, \quad (178)$$

$$\boldsymbol{\psi}^h = (\mathbf{I}+\frac{1}{2}\hat{\boldsymbol{\psi}}^h) \sum_{i=1}^{N} I_i\boldsymbol{\psi}_i \,, \quad (179)$$

i.e.

$$(\mathbf{I}-\frac{1}{2}\,\hat{\boldsymbol{\psi}}^h)\boldsymbol{\psi}^h = \sum_{i=1}^{N} I_i\boldsymbol{\psi}_i \quad \Rightarrow \boldsymbol{\psi}^h = \sum_{i=1}^{N} I_i\boldsymbol{\psi}_i \quad (180)$$

and

$$\mathbf{u}^h = \sum_{i=1}^{N} I_i\mathbf{u}_i + \frac{1}{2}\hat{\boldsymbol{\psi}}^h \sum_{i=1}^{N} I_i\mathbf{R}_i - \frac{1}{2}\sum_{i=1}^{N} I_i\hat{\boldsymbol{\psi}}_i\mathbf{R}_i = \sum_{i=1}^{N} I_i(\mathbf{u}_i + \frac{1}{2}\widehat{\mathbf{R}_i - \mathbf{R}^h}\boldsymbol{\psi}_i) \,. \quad (181)$$

3.1.3 Exact interpolation in linear 3D beam theory

In the first chapter of the thesis it has been shown that in linear analysis the exact result follows from the interpolation

$$\boldsymbol{\psi}^h = \sum_{i=1}^{N} I_i \boldsymbol{\psi}_i \,, \tag{182}$$

$$\mathbf{u}^h = \sum_{i=1}^{N} I_i \bigg(\mathbf{u}_i + \frac{1}{N} (\boldsymbol{\psi} - \boldsymbol{\psi}_i) \times \mathbf{R}_i \bigg). \tag{183}$$

With cross product being anticommutative operator, equation (183) can be rewritten as

$$\mathbf{u}^h = \sum_{i=1}^{N} I_i \bigg(\mathbf{u}_i - \frac{1}{N} \mathbf{R}_i \times (\boldsymbol{\psi} - \boldsymbol{\psi}_i) \bigg),$$

which can further be written as

$$\mathbf{u}^h = \sum_{i=1}^{N} I_i \bigg(\mathbf{u}_i + \frac{1}{N} \widehat{\mathbf{R}_i - \mathbf{R}}^h \boldsymbol{\psi}_i \bigg), \tag{184}$$

which coincides with the result in (180) and (181) only for two–noded element where $N = 2$. In other words, an attempt to generalise the helicoidal interpolation from (161) and (162) to higher–order elements by using the generalised interpolation from (153) would fail to provide the exact linear result.

In order to generalise the formulation from (161) and (162) to higher–order elements, the generalised interpolation from (153) may still be used if accordingly modified. In particular, to achieve the desired interpolation for $\mathbf{u}^h$ in (183), we have to have a generalised interpolation which will result in the linearised form which is

$$\tilde{\mathbf{I}}^i = I_i (\mathbf{I} + \frac{1}{N} \widehat{\boldsymbol{\psi}^h - \boldsymbol{\psi}_i}) \,, \tag{185}$$

rather than the result obtained in (175). This is possible if the generalised interpolation in (153) is modified into

$$\tilde{\mathbf{I}}^i = \sum_{j=1}^{N} \sum_{k=1}^{N} \Delta_k^{ij} \boldsymbol{\Lambda}_r \bigg\{ (\delta_{Ik} + \delta_{Jk}) \left[\mathbf{I} - \mathbf{H}(\boldsymbol{\Psi}^{lh}) \sum_{m=1}^{N} I_m \mathbf{H}^{-1}(\boldsymbol{\Psi}^l_m) \right] \mathbf{V}_j + \mathbf{H}(\underbrace{\frac{2}{N}} \boldsymbol{\Psi}^{lh}) I_k \mathbf{H}^{-1}(\underbrace{\frac{2}{N}} \boldsymbol{\Psi}^l_j) \bigg\} \boldsymbol{\Lambda}_r^T \,, \tag{186}$$

with the modifications indicated.

Obviously, the above modification is in a sense artificial, since the original $\tilde{\mathbf{I}}^i$ in (153) has been derived from the strain-invariance condition. Nevertheless, the latter condition is needed for the rotational, not translational interpolation, i.e. there are no principal objections to applying the result from (186) to the interpolation for the position vector. Given the basic requirement, however, i.e. that its linearised form should reduce to $\tilde{\mathbf{I}}^i = I_i(\mathbf{I} + \frac{1}{N}\widehat{\boldsymbol{\psi}^h - \boldsymbol{\psi}_i})$, it makes sense to apply a more general modification of the form

$$\mathbf{J}_i = \sum_{j=1}^{N}\sum_{k=1}^{N} \Delta_k^{ij} \boldsymbol{\Lambda}_r \Big\{ (\delta_{Ik} + \delta_{Jk}) \left[\mathbf{I} - \mathbf{H}(\beta\boldsymbol{\Psi}^{lh}) \sum_{m=1}^{N} I_m \mathbf{H}^{-1}(\beta\boldsymbol{\Psi}^l{}_m) \right] \mathbf{V}_{\alpha j} + \mathbf{H}(\gamma\ \boldsymbol{\Psi}^{lh}) I_k \mathbf{H}^{-1}(\gamma\ \boldsymbol{\Psi}^l_j) \Big\} \boldsymbol{\Lambda}_r^T \ , \quad (187)$$

with

$$\mathbf{V}_{\alpha I,J} = \frac{1}{2}(\mathbf{I} \pm \frac{1}{\phi} \tan\frac{\alpha\phi}{4}\ \hat{\boldsymbol{\phi}}) \quad (188)$$

and α, β, γ as free parameters. For $\alpha = \beta = \gamma = 1$ we thus recover the original interpolation from (153), while for $\alpha = \beta = 1$ and $\gamma = \frac{2}{N}$ we recover the modified interpolation from (186).

As mentioned in Section 3.1.1, to keep the formulation strain invariant and at the same time make it reduce to the exact form in linear analysis regardless of the number of nodes, it turns out to be necessary to interpolate the rotational changes exactly as in (152), with $\tilde{\mathbf{I}}^i$ given in (153). It has to be remembered, however, that such duality goes against the logic of the idea in [5] (see expressions (161) and (162)), which was motivated by a desire to make the formulation independent of the choice of the beam reference axis.

3.1.4 Strain invariance of the proposed formulation

Furthermore, as stated earlier, the strain invariant interpolation is given as $\Delta\boldsymbol{\vartheta}^h = \sum_{i=1}^{N} \tilde{\mathbf{I}}^i \Delta\boldsymbol{\vartheta}_i$ and $\mathbf{r}^h = \sum_{i=1}^{N} I_i \mathbf{r}_i$, not $\mathbf{r}^h = \sum_{i=1}^{N} \tilde{\mathbf{I}}_i \mathbf{r}_i$, or in this case the modified interpolation $\mathbf{r}^h = \sum_{i=1}^{N} \mathbf{J}_i \mathbf{r}_i$. In other words, the latter interpolation is acceptable only if we can prove that it also gives a strain–invariant solution.
To check this, we recall from [18] that a strain invariant interpolation $\mathbf{r}^h$ must satisfy

$$\underline{\mathbf{r}}^h = \boldsymbol{\Lambda}_R(\mathbf{r}_R + \mathbf{r}^h) \ , \quad (189)$$

where Λ_R and $\mathbf{r}_R$ are arbitrary constant rotation and translation and $\underline{\mathbf{r}}^h$ is the interpolated position of a configuration rotated by $\mathbf{\Lambda}_R$ and displaced by $\mathbf{r}_R$, such that

$$\underline{\mathbf{\Lambda}}_i = \mathbf{\Lambda}_R \mathbf{\Lambda}_i \ , \tag{190}$$

$$\underline{\mathbf{r}}_i = \mathbf{\Lambda}_R(\mathbf{r}_R + \mathbf{r}_i) \ . \tag{191}$$

For the interpolation given in (187) we thus have to check if

$$\sum_{i=1}^{N} \underline{\mathbf{J}}_i \ \underline{\mathbf{r}}_i = \mathbf{\Lambda}_R(\mathbf{r}_R + \sum_{i=1}^{N} \mathbf{J}_i \mathbf{r}_i) \ . \tag{192}$$

Since $\mathbf{\Psi}^l$ and $\boldsymbol{\phi}$ in $\mathbf{J}_i$ in (187) are local rotations, which are by definition not affected by any constant rotation it follows that $\underline{\mathbf{J}}_i = \mathbf{J}_i(\mathbf{\Lambda}_R \mathbf{\Lambda}) = \mathbf{\Lambda}_R \mathbf{J}_i \mathbf{\Lambda}_R^T$ and we are left to check if

$$\sum_{i=1}^{N} \mathbf{\Lambda}_R \mathbf{J}_i \mathbf{\Lambda}_R^T \mathbf{\Lambda}_R(\mathbf{r}_R + \mathbf{r}_i) = \mathbf{\Lambda}_R(\mathbf{r}_R + \sum_{i=1}^{N} \mathbf{J}_i \mathbf{r}_i) \ , \tag{193}$$

i.e.

$$\sum_{i=1}^{N} \mathbf{\Lambda}_R \mathbf{J}_i \mathbf{r}_R + \sum_{i=1}^{N} \mathbf{\Lambda}_R \mathbf{J}_i \mathbf{r}_i = \mathbf{\Lambda}_R \mathbf{r}_R + \mathbf{\Lambda}_R \sum_{i=1}^{N} \mathbf{J}_i \mathbf{r}_i \ . \tag{194}$$

Since $\mathbf{\Lambda}_R$ and $\mathbf{r}_R$ are constant,

$$\mathbf{\Lambda}_R \sum_{i=1}^{N} \mathbf{J}_i \ \mathbf{r}_R + \cancel{\mathbf{\Lambda}_R \sum_{i=1}^{N} \mathbf{J}_i \mathbf{r}_i} = \mathbf{\Lambda}_R \mathbf{r}_R + \cancel{\mathbf{\Lambda}_R \sum_{i=1}^{N} \mathbf{J}_i \mathbf{r}_i} \ .$$

After premultiplying by $\mathbf{\Lambda}_R^T$ we are thus left to check if $(\sum_{i=1}^{N} \mathbf{J}_i - \mathbf{I})\mathbf{r}_R = \mathbf{0}$ i.e. if $\sum_{i=1}^{N} \mathbf{J}_i$ has a single arbitrary eigenvector and all the eigenvalues equal to unity. In other, simpler words, the interpolation functions $\mathbf{J}_i$ will provide a strain–invariant solution only if $\sum_{i=1}^{N} \mathbf{J}_i = \mathbf{I}$ i.e. only if they are complete.

The condition for a strain-invariant solution is therefore (note that $\boldsymbol{\psi}^l = \mathbf{\Lambda}_r \mathbf{\Psi}^l$)

$$\begin{aligned} \textstyle\sum_{i=1}^{N} \mathbf{J}_i = \textstyle\sum_{i=1}^{N} \{ & \delta_{Ii} \left[\mathbf{I} - \mathbf{H}(\beta \boldsymbol{\psi}^{lh}) \textstyle\sum_{m=1}^{N} I_m \mathbf{H}^{-1}(\beta \boldsymbol{\psi}_m^l) \right] \frac{1}{2} (\mathbf{I} + \frac{1}{\phi} \ \tan \frac{\alpha \phi}{4} \ \hat{\boldsymbol{\phi}}) \\ & + \delta_{Ji} \left[\mathbf{I} - \mathbf{H}(\beta \boldsymbol{\psi}^{lh}) \textstyle\sum_{m=1}^{N} I_m \mathbf{H}^{-1}(\beta \boldsymbol{\psi}_m^l) \right] \frac{1}{2} (\mathbf{I} - \frac{1}{\phi} \ \tan \frac{\alpha \phi}{4} \ \hat{\boldsymbol{\phi}}) \\ & + \mathbf{H}(\gamma \boldsymbol{\psi}^{lh}) I_i \mathbf{H}^{-1}(\gamma \boldsymbol{\psi}_i^l) \} = \mathbf{I} \ , \end{aligned}$$

i.e. $(\frac{1}{2}+\frac{1}{2})\left[\mathbf{I}-\mathbf{H}(\beta\boldsymbol{\psi}^{lh})\sum_{m=1}^{N} I_m\mathbf{H}^{-1}(\beta\boldsymbol{\psi}^{l}_{m})\right]$

$$+\,\mathbf{H}(\gamma\boldsymbol{\psi}^{lh})\sum_{i=1}^{N} I_i\mathbf{H}^{-1}(\gamma\boldsymbol{\psi}^{l}_{i})=\mathbf{I}\,,$$

leading to

$$\mathbf{H}(\beta\boldsymbol{\psi}^{lh})\sum_{i=1}^{N} I_i\mathbf{H}^{-1}(\beta\boldsymbol{\psi}^{l}_{i})=\mathbf{H}(\gamma\boldsymbol{\psi}^{lh})\sum_{i=1}^{N} I_i\mathbf{H}^{-1}(\gamma\boldsymbol{\psi}^{l}_{i})\,.$$

The strain–invariance condition therefore requires that $\beta=\gamma$ and, given the structure of $\mathbf{H}$ and $\mathbf{H}^{-1}$ in (156) and (157), this appears to be the only condition. The resulting interpolation, therefore, has only two free parameters (α,β):

$$\begin{aligned}\mathbf{J}_i=&\frac{1}{2}\delta_{Ii}\left[\mathbf{I}-\mathbf{H}(\beta\boldsymbol{\psi}^{lh})\sum_{m=1}^{N} I_m\mathbf{H}^{-1}(\beta\boldsymbol{\psi}^{l}_{m})\right](\mathbf{I}+\frac{1}{\phi}\,\tan\frac{\alpha\phi}{4}\,\hat{\boldsymbol{\phi}})\\&+\frac{1}{2}\delta_{Ji}\left[\mathbf{I}-\mathbf{H}(\beta\boldsymbol{\psi}^{lh})\sum_{m=1}^{N} I_m\mathbf{H}^{-1}(\beta\boldsymbol{\psi}^{l}_{m})\right](\mathbf{I}-\frac{1}{\phi}\,\tan\frac{\alpha\phi}{4}\,\hat{\boldsymbol{\phi}})\\&+\mathbf{H}(\beta\boldsymbol{\psi}^{lh})I_i\mathbf{H}^{-1}(\beta\boldsymbol{\psi}^{l}_{i})\,.\end{aligned}\tag{195}$$

In conclusion, the helicoidal interpolation may be generalised to higher–order elements in the following two ways:
1) $\beta=1$, which provides a same interpolation for the position vector and the rotation matrix and thus gives a solution which is independent to the position of the beam reference axis; this solution, however, does not represent the exact field distribution in the linear limit;
2) $\beta=\dfrac{2}{N}$, which provides the exact field distribution in the linear limit, but fails to provide the solution which is independent of the position of the beam reference axis.

3.1.5 Application to 2D beam problems

It is obvious from the above presentation that one of the principal motivations for the development of the generalised interpolation (195) lies in the analysis of the conditions for objectivity of the numerical solution [18], which is a problem that exists only in 3D and is solved by introducing the generalised interpolation (152). However, since we here study the implications of applying this result to the interpolation of translations, it makes sense to limit our attention only to 2D, where the complexities of implementation of the kinematics of 3D rotations vanish.
In 2D these results simplify considerably since all the rotations are coaxial. Owing to the structure of matrices $\mathbf{H}$ and $\mathbf{H}^{-1}$, which contain the skew–symmetric matrices of

rotational components, it turns out simply that

$$\Delta\boldsymbol{\vartheta}^h = \sum_{i=1}^{N} \tilde{\mathbf{I}}^i \Delta\boldsymbol{\vartheta}_i = \sum_{i=1}^{N} I_i \Delta\boldsymbol{\vartheta}_i \,, \tag{196}$$

which means that the total rotations in 2D (let us denote them as $\boldsymbol{\varphi}$ rather than $\boldsymbol{\vartheta}$) are interpolated simply as $\boldsymbol{\varphi} \approx \boldsymbol{\varphi}^h = \sum_{i=1}^{N} I_i \boldsymbol{\varphi}_i$.
After the nodes I and J have been chosen, the rigid rotation from $\boldsymbol{\Lambda}_r$ in (147) is simply

$$\boldsymbol{\varphi}_r = \frac{\boldsymbol{\varphi}_I + \boldsymbol{\varphi}_J}{2} \tag{197}$$

and the local nodal rotations are obtained as

$$\boldsymbol{\varphi}_i^l = \boldsymbol{\varphi}_i - \boldsymbol{\varphi}_r \,, \tag{198}$$

while the interpolated local rotations are

$$\boldsymbol{\varphi}^{lh} = \boldsymbol{\varphi}^h - \boldsymbol{\varphi}_r = \sum_{i=1}^{N} I_i \boldsymbol{\varphi}_i - \sum_{i=1}^{N} I_i \boldsymbol{\varphi}_r = \sum_{i=1}^{N} I_i \boldsymbol{\varphi}_i^l \,. \tag{199}$$

Since all the rotations are planar, note that $\boldsymbol{\psi}^l$ and $\boldsymbol{\Psi}^l$ in $\mathbf{J}_i$ are the same, and in 2D we have denoted them as $\boldsymbol{\varphi}^l$.

Since all the rotations are coaxial, $\boldsymbol{\varphi}^h = \varphi^h \mathbf{e}_3$, $\boldsymbol{\varphi}_i = \varphi_i \mathbf{e}_3$, $\boldsymbol{\varphi}_r = \varphi_r \mathbf{e}_3$, $\boldsymbol{\varphi}^{lh} = \varphi^{lh} \mathbf{e}_3$, $\boldsymbol{\varphi}_i^l = \varphi_i^l \mathbf{e}_3$, $\boldsymbol{\phi} = \phi \mathbf{e}_3$, where $\mathbf{e}_3$ is a unit vector orthogonal to the plane of the problem, the products of matrices $\mathbf{H}(\beta\boldsymbol{\varphi}^{lh})$ and $\mathbf{H}^{-1}(\beta\boldsymbol{\varphi}_m^l)$ in $\mathbf{J}_i$ in (195) simplify.

Denoting

$$\mathbf{e}_3 = \begin{Bmatrix} 0 \\ 0 \\ 1 \end{Bmatrix} \Longleftrightarrow \hat{\mathbf{e}}_3 = \begin{bmatrix} 0 & -1 & 0 \\ 1 & 0 & 0 \\ 0 & 0 & 0 \end{bmatrix} \,,$$

these matrices become

$$\mathbf{H}(\beta\varphi^{lh}) = \mathbf{I} + \frac{1 - \cos\beta\varphi^{lh}}{\beta\varphi^{lh}} \hat{\mathbf{e}}_3 + \frac{\beta\varphi^{lh} - \sin\beta\varphi^{lh}}{\beta\varphi^{lh}} (\hat{\mathbf{e}}_3)^2 \,, \tag{200}$$

$$\mathbf{H}^{-1}(\beta\varphi_m^l) = \mathbf{I} - \frac{\beta\varphi_m^l}{2} \hat{\mathbf{e}}_3 - \frac{1}{2} \frac{\beta\varphi_m^l \sin\beta\varphi_m^l + 2\cos\beta\varphi_m^l - 2}{1 - \cos\beta\varphi_m^l} (\hat{\mathbf{e}}_3)^2 \tag{201}$$

and noting that $\mathbf{J}_i$ only ever multiplies the position vector, which only has the first two components different from zero, we may introduce $\hat{\mathbf{e}} = \begin{bmatrix} 0 & -1 \\ 1 & 0 \end{bmatrix}$, where $(\hat{\mathbf{e}})^2 = -\mathbf{I}$.

Finally matrices $\mathbf{H}(\beta\varphi^{lh})$ and $\mathbf{H}^{-1}(\beta\varphi^l_m)$ can be written as

$$\mathbf{H}(\beta\varphi^{lh}) = \frac{\sin\beta\varphi^{lh}}{\beta\varphi^{lh}}\mathbf{I} + \frac{1-\cos\beta\varphi^{lh}}{\beta\varphi^{lh}}\hat{\mathbf{e}}\,, \tag{202}$$

$$\mathbf{H}^{-1}(\beta\varphi^l_m) = \frac{\beta\varphi^l_m}{2}\frac{\sin\beta\varphi^l_m}{1-\cos\beta\varphi^l_m}\mathbf{I} - \frac{\beta\varphi^l_m}{2}\hat{\mathbf{e}}\,. \tag{203}$$

Let us analyse the product $\mathbf{H}(\beta\varphi^{lh})\mathbf{H}^{-1}(\beta\varphi^l_m)$ in expression (195). From (202) and (203) it follows

$$\mathbf{H}(\beta\varphi^{lh})\mathbf{H}^{-1}(\beta\varphi^l_m) = \frac{\beta\varphi^l_m}{2}\,(\frac{\sin\beta\varphi^{lh}}{\beta\varphi^{lh}}\mathbf{I} + \frac{1-\cos\beta\varphi^{lh}}{\beta\varphi^{lh}}\hat{\mathbf{e}})(\frac{\sin\beta\varphi^l_m}{1-\cos\beta\varphi^l_m}\mathbf{I} - \hat{\mathbf{e}})\,. \tag{204}$$

Using the double angle trigonometric transformations, and the relations $\varphi^{lh} = \varphi^h - \varphi_r$ and $\varphi^l_m = \varphi_m - \varphi_r$ with $\varphi_r = \dfrac{\varphi_I + \varphi_J}{2}$, we finally have the following result expressed in terms of the actual rotational unknowns $\varphi_1, ..., \varphi_N$:

$$\mathbf{H}(\beta\varphi^{lh})\mathbf{H}^{-1}(\beta\varphi^l_m) = \frac{\dfrac{\sin\dfrac{\beta\varphi^{lh}}{2}}{\dfrac{\beta\varphi^{lh}}{2}}}{\dfrac{\sin\dfrac{\beta\varphi^l_m}{2}}{\dfrac{\beta\varphi^l_m}{2}}}\left[\cos(\beta\frac{\varphi^h-\varphi_m}{2})\mathbf{I} + \sin(\beta\frac{\varphi^h-\varphi_m}{2})\hat{\mathbf{e}}\right]\,. \tag{205}$$

Taking the above result and substituting it into (195), along with $\phi = \varphi_J - \varphi_I$, thus gives

$$\mathbf{J}_i = (\mathbf{I} - \sum_{m=1}^{N}\mathbf{N}_m)(\frac{\delta_{Ii}+\delta_{Ji}}{2}\mathbf{I} + \frac{\delta_{Ii}-\delta_{Ji}}{2}\frac{\tan(\alpha\dfrac{\varphi_J-\varphi_I}{4})}{\varphi_J-\varphi_I}\hat{\mathbf{e}}) + \mathbf{N}_i\,, \tag{206}$$

with

$$\mathbf{N}_i = I_i\frac{\dfrac{\sin(\beta\dfrac{\varphi^h-\varphi_r}{2})}{\beta\dfrac{\varphi^h-\varphi_r}{2}}}{\dfrac{\sin(\beta\dfrac{\varphi_i-\varphi_r}{2})}{\beta\dfrac{\varphi_i-\varphi_r}{2}}}\left[\cos(\beta\frac{\varphi^h-\varphi_i}{2})\mathbf{I} + \sin(\beta\frac{\varphi^h-\varphi_i}{2})\hat{\mathbf{e}}\right] \tag{207}$$

and $\varphi_r = \dfrac{\varphi_I + \varphi_J}{2}$. Introducing substitutions $\psi^h = \beta\dfrac{\varphi^h - \varphi_r}{2}$ and $\psi_i = \beta\dfrac{\varphi_i - \varphi_r}{2}$ this may be further compacted to

$$\mathbf{N}_i = I_i \frac{\dfrac{\sin\psi^h}{\psi^h}}{\dfrac{\sin\psi_i}{\psi_i}} \left[\cos(\psi^h - \psi_i)\mathbf{I} + \sin(\psi^h - \psi_i)\hat{\mathbf{e}}\right] , \tag{208}$$

where the result in the brackets is the 2D orthogonal tensor of rotation $\psi^h - \psi_i$.
Note that the above result is well defined in the limit when $\varphi_i \to \varphi_r \Longleftrightarrow \psi_i \to 0$:

$$\lim_{\psi_i \to 0} \mathbf{N}_i = I_i \frac{\sin\psi^h}{\psi^h}(\cos\psi^h \mathbf{I} + \sin\psi^h \hat{\mathbf{e}}) .$$

If $\psi^h \to 0$, too, $\mathbf{N}_i$ obviously reduces to the Lagrangian interpolation. In the case when $I = J$:

$$\mathbf{J}_i|_{I=J} = \delta_{Ii}(\mathbf{I} - \sum_{m=1}^{N} \mathbf{N}_m) + \mathbf{N}_i .$$

3.1.6 Kinematically consistent interpolation

Here we derive the conditions under which the solution of the beam problem does not depend on the chosen reference axis. Two different reference axes will be considered, denoted as p_0 and p_c in Figure 3.1.

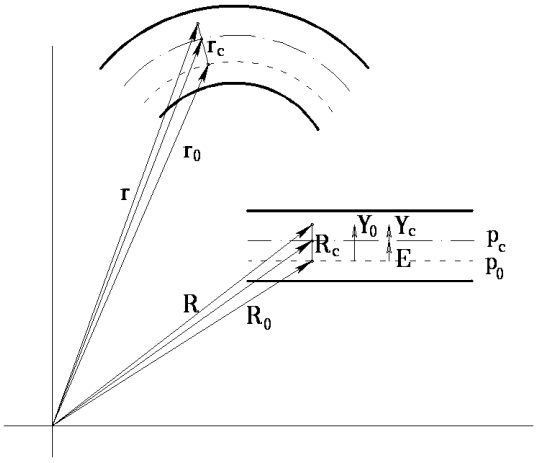

Figure 3.1: Multiple reference axes.

The position vector in the undeformed state $\mathbf{R}$ can be defined with respect to both reference lines as

$$\mathbf{R}(x) = \mathbf{R}_0(x_1) + \mathbf{\Lambda}_0\mathbf{Y}_0(x_2, x_3) = \mathbf{R}_c(x_1) + \mathbf{\Lambda}_0\mathbf{Y}_c(x_2, x_3), \tag{209}$$

where $\mathbf{R}_0$ is the position vector of the point on the reference line p_0 in a cross–section, $\mathbf{R}_c$ is the position vector of the point on the reference line p_c in the cross-section considered, $\mathbf{E}$ is the position vector of the point on reference line p_c with respect to the point on p_0, $\mathbf{\Lambda}_0$ is the initial rotation matrix defining orientation of the cross–section, $\mathbf{Y}_0$ is the position vector of the observed point in the cross–section with respect to the point on p_0, and $\mathbf{Y}_c$ is the position vector of the observed point with respect to the point on p_c.

From (209) there follows

$$\mathbf{Y}_0 - \mathbf{Y}_c = \mathbf{\Lambda}_0^T(\mathbf{R}_c - \mathbf{R}_0). \tag{210}$$

Further, the position vector in the deformed state can also be written with respect to both of these axes as follows

$$\mathbf{r}(x) = \mathbf{r}_0(x_1) + \mathbf{\Lambda}\mathbf{Y}_0(x_2, x_3) = \mathbf{r}_c(x_1) + \mathbf{\Lambda}\mathbf{Y}_c(x_2, x_3). \tag{211}$$

Let us now assume an orientation–dependent interpolation $\tilde{\mathbf{C}}^i(\mathbf{\Lambda}^h(x_1), x_1)$ for the position of a chosen reference line, i.e.

$$\mathbf{r}_0(x_1) = \sum_{i=1}^{N} \tilde{\mathbf{C}}^i \mathbf{r}_{0,i} \tag{212}$$

$$\mathbf{r}_c(x_1) = \sum_{i=1}^{N} \tilde{\mathbf{C}}^i \mathbf{r}_{c,i}\ . \tag{213}$$

Using (212) and (213), (211) can be written as

$$\sum_{i=1}^{N} \tilde{\mathbf{C}}^i(x_1)\mathbf{r}_{0,i} + \mathbf{\Lambda}(x_1)\mathbf{Y}_0(x_2, x_3) = \sum_{i=1}^{N} \tilde{\mathbf{C}}^i(x_1)\mathbf{r}_{c,i} + \mathbf{\Lambda}(x_1)\mathbf{Y}_c(x_2, x_3)$$

Since $\mathbf{r}_{0,i} = \mathbf{r}_{c,i} - \mathbf{\Lambda}_i\mathbf{E}$ and $\mathbf{Y}_0 = \mathbf{E} + \mathbf{Y}_c$, the above expression reduces to

$$(\mathbf{\Lambda} - \sum_{i=1}^{N} \tilde{\mathbf{C}}^i \mathbf{\Lambda}_i)\mathbf{E} = \mathbf{0}. \tag{214}$$

This expression has to be satisfied for any $\mathbf{E}$, therefore

$$\mathbf{\Lambda} = \sum_{i=1}^{N} \tilde{\mathbf{C}}^i \mathbf{\Lambda}_i. \tag{215}$$

This is the condition that has to be satisfied if a solution is to be independent of the choice of the beam reference axis. In other words, such a solution is possible only if the same interpolation functions are used to interpolate both the position vector field

and the rotation tensor field.

If the interpolation from [18] is used as $\tilde{\mathbf{C}}^i$ in (215), the result is an orthogonal matrix even though the nodal rotation matrices are interpolated in an additive manner. The proof is given in Appendix C.

3.2 Reissner beam theory and finite–element formulation

Kinematic of the beam is given in the subsection 2.2.1 of the second chapter of the thesis.

3.2.1 Total potential energy

To apply the interpolation derived in the previous section, we consider the Reissner–Simo beam [34] with the strain energy

$$\phi = \frac{1}{2}\int_0^L \langle \boldsymbol{\Gamma}^T \boldsymbol{\kappa}^T \rangle \begin{Bmatrix} \mathbf{N} \\ \mathbf{M} \end{Bmatrix} dx_1 \tag{216}$$

and the potential of the applied loading

$$U = \int_0^L \langle \mathbf{u}^T \boldsymbol{\vartheta}^T \rangle \begin{Bmatrix} \mathbf{n} \\ \mathbf{m} \end{Bmatrix} dx_1 + \langle \mathbf{u}_0^T \boldsymbol{\vartheta}_0^T \rangle \begin{Bmatrix} \mathbf{F}_0 \\ \mathbf{T}_0 \end{Bmatrix} + \langle \mathbf{u}_L^T \boldsymbol{\vartheta}_L^T \rangle \begin{Bmatrix} \mathbf{F}_L \\ \mathbf{T}_L \end{Bmatrix} , \tag{217}$$

where $\mathbf{n}, \mathbf{m}$ are the distributed force and moment loading, and $\mathbf{F}_0$, $\mathbf{T}_0$, $\mathbf{F}_L$, $\mathbf{T}_L$ are the endpoint concentrated force and moment loadings. Here $\mathbf{u}_0, \mathbf{u}_L$ denote endpoint displacement vectors, while $\boldsymbol{\vartheta}_0, \boldsymbol{\vartheta}_L$ denote endpoint rotation vectors. Note that the potential in (217) makes sense only for conservative loading and in 3D the applied moments are very often non–conservative.
For conservative loading, the equilibrium follows from the requirement that the variation of the total potential energy should be zero:

$$\delta(\phi - U) = 0 \Longleftrightarrow \int_0^L \langle \delta\boldsymbol{\Gamma}^T \delta\boldsymbol{\kappa}^T \rangle \begin{Bmatrix} \mathbf{N} \\ \mathbf{M} \end{Bmatrix} dx_1 - \delta U = 0 \,, \tag{218}$$

with

$$\delta U = \int_0^L \langle \delta\mathbf{r}^T \; \delta\boldsymbol{\vartheta}^T \rangle \begin{Bmatrix} \mathbf{n} \\ \mathbf{m} \end{Bmatrix} dx_1 + \langle \delta\mathbf{r}_0^T \; \delta\boldsymbol{\vartheta}_0^T \rangle \begin{Bmatrix} \mathbf{F}_0 \\ \mathbf{T}_0 \end{Bmatrix} + \langle \delta\mathbf{r}_L^T \; \delta\boldsymbol{\vartheta}_L^T \rangle \begin{Bmatrix} \mathbf{F}_L \\ \mathbf{T}_L \end{Bmatrix} . \tag{219}$$

3.2.2 2D application

Strain measures of a 2D problem contain only one shear strain $\gamma_2 = \gamma$ and one bending strain $\kappa_3 = \kappa$, hence the strain measures given in (8) and (9) can be simplified and written in an expanded form as

$$\begin{Bmatrix} \epsilon \\ \gamma \\ \kappa \end{Bmatrix} = \begin{bmatrix} \cos(\varphi_0+\varphi) & \sin(\varphi_0+\varphi) & 0 \\ -\sin(\varphi_0+\varphi) & \cos(\varphi_0+\varphi) & 0 \\ 0 & 0 & 1 \end{bmatrix} \begin{Bmatrix} \cos\varphi_0 + u' \\ \sin\varphi_0 + v' \\ \varphi' \end{Bmatrix} - \begin{Bmatrix} 1 \\ 0 \\ 0 \end{Bmatrix} . \tag{220}$$

The variation of the strain energy is

$$\delta\phi \approx \delta\phi^h = \int_0^L \langle \delta\mathbf{r}^T \ \delta\varphi \rangle \begin{bmatrix} \mathbf{I}_2 \dfrac{d}{dx_1} & \mathbf{0}_2 \\ \mathbf{r}'^T \hat{\mathbf{e}} & \dfrac{d}{dx_1} \end{bmatrix} \begin{bmatrix} \mathbf{\Lambda} & \mathbf{0}_2 \\ \mathbf{0}_2^T & 1 \end{bmatrix} \begin{Bmatrix} \mathbf{N} \\ M \end{Bmatrix} dx_1 , \tag{221}$$

with $\mathbf{0}_2$ as the two–dimensional null–vector and matrix $\hat{\mathbf{e}} = \begin{bmatrix} 0 & -1 \\ 1 & 0 \end{bmatrix}$. After application of interpolation of $\delta\mathbf{r}$ and $\delta\varphi$, the above becomes

$$\delta\phi = \delta\mathbf{p}^T\mathbf{q}_i = \langle \delta\mathbf{p}_1^T ... \ \delta\mathbf{p}_N^T \rangle \begin{Bmatrix} \mathbf{q}_{i,1} \\ \vdots \\ \mathbf{q}_{i,N} \end{Bmatrix} = \sum_{j=1}^{N} \delta\mathbf{p}_j^T \mathbf{q}_{i,j} ,$$

where

$$\delta\mathbf{p}_j = \begin{Bmatrix} \delta\mathbf{r}_j \\ \delta\varphi_j \end{Bmatrix} .$$

To find the internal force vector at a node j, $\mathbf{q}_{i,j}$, our interpolation will be introduced

$$\mathbf{r} \approx \mathbf{r}^h = \sum_{i=1}^{N} \mathbf{J}_i \mathbf{r}_i , \tag{222}$$

$$\varphi \approx \varphi^h = \sum_{i=1}^{N} I_i \varphi_i , \tag{223}$$

with $\mathbf{J}_i$ given in (206). Obviously,

$$\delta\varphi \approx \delta\varphi^h = \sum_{i=1}^{N} I_i \delta\varphi_i ,$$

while

$$\delta\mathbf{r} \approx \delta\mathbf{r}^h = \sum_{i=1}^{N}(\delta\mathbf{J}_i\mathbf{r}_i + \mathbf{J}_i\delta\mathbf{r}_i) = \sum_{i=1}^{N}\mathbf{J}_i\delta\mathbf{r}_i + \sum_{i=1}^{N}\delta\mathbf{J}_i\mathbf{r}_i \ .$$

Since the expression for $\delta\mathbf{J}_i$ will be needed in order to calculate the variation of the total potential energy, variation of this interpolation and some parts of it will be given here.

In order to write the complete variation of $\mathbf{J}_i$ given by (206), variation of the function $\mathbf{N}_i$ and the coefficient $(\dfrac{1}{\varphi_J - \varphi_I}\tan\alpha\dfrac{\varphi_J - \varphi_I}{4})$ will be needed.

Variation of the function $\mathbf{N}_i$ is

$$\delta\mathbf{N}_i = \frac{\beta}{2}\mathbf{N}_i\sum_{k=1}^{N}\mathbf{M}_{ik}\delta\varphi_k \ , \tag{224}$$

where (see Appendix D for the derivation)

$$\mathbf{M}_{ik} = I_k(-f^h\mathbf{I} + \hat{\mathbf{e}}) + (f_i\mathbf{I} - \hat{\mathbf{e}})\delta_{ik} - \frac{\delta_{Ik} + \delta_{Jk}}{2}(f_i - f^h)\mathbf{I} \ , \tag{225}$$

with $f_i = \dfrac{1}{\psi_i} - \dfrac{\cos\psi_i}{\sin\psi_i}$ and $f^h = \dfrac{1}{\psi^h} - \dfrac{\cos\psi^h}{\sin\psi^h}$.

Variation of the coefficient $\dfrac{\tan\alpha\dfrac{\varphi_J - \varphi_I}{4}}{\varphi_J - \varphi_I}$ is

$$\delta\left(\frac{\tan\alpha\dfrac{\varphi_J - \varphi_I}{4}}{\varphi_J - \varphi_I}\right) = \sum_{k=1}^{N}(\delta_{Jk} - \delta_{Ik})m\ \delta\varphi_k \ ,$$

where

$$m = \frac{\alpha}{4(\varphi_J - \varphi_I)\cos^2\alpha\dfrac{\varphi_J - \varphi_I}{4}} - \frac{\tan\alpha\dfrac{\varphi_J - \varphi_I}{4}}{(\varphi_J - \varphi_I)^2} \ . \tag{226}$$

Finally

$$\delta\mathbf{J}_i = \sum_{k=1}^{N}\mathbf{P}_{ik}\delta\varphi_k \ , \tag{227}$$

where

$$\mathbf{P}_{ik} = \frac{\beta}{2}\left[\mathbf{N}_i\mathbf{M}_{ik} - \left(\frac{\delta_{Ii}+\delta_{Ji}}{2}\mathbf{I} + \frac{\delta_{Ii}-\delta_{Ji}}{2}\frac{\tan\alpha\dfrac{\varphi_J-\varphi_I}{4}}{\varphi_J-\varphi_I}\hat{\mathbf{e}}\right)\sum_{m=1}^{N}\mathbf{N}_m\mathbf{M}_{mk}\right] + (\mathbf{I}-\sum_{m=1}^{N}\mathbf{N}_m)\frac{\delta_{Ii}-\delta_{Ji}}{2}(\delta_{Jk}-\delta_{Ik})m\,\hat{\mathbf{e}}\,. \quad (228)$$

Further

$$\delta\mathbf{J}_i\mathbf{r}_i = \sum_{k=1}^{N}\mathbf{P}_{ik}\mathbf{r}_i\delta\varphi_k = [\mathbf{P}_{i1}\mathbf{r}_i \quad \mathbf{P}_{i2}\mathbf{r}_i \quad ... \quad \mathbf{P}_{iN}\mathbf{r}_i]\begin{Bmatrix}\delta\varphi_1\\ \delta\varphi_2\\ \vdots\\ \delta\varphi_N\end{Bmatrix}$$

and

$$\delta\mathbf{r} \approx \delta\mathbf{r}^h = \sum_{i=1}^{N}(\mathbf{J}_i\delta\mathbf{r}_i + \delta\mathbf{J}_i\mathbf{r}_i) = [[\mathbf{J}_1 \quad \mathbf{j}_1] \quad ... \quad [\mathbf{J}_N \quad \mathbf{j}_N]]\begin{Bmatrix}\begin{Bmatrix}\delta\mathbf{r}_1\\ \delta\varphi_1\end{Bmatrix}\\ \vdots\\ \begin{Bmatrix}\delta\mathbf{r}_N\\ \delta\varphi_N\end{Bmatrix}\end{Bmatrix}, \quad (229)$$

where

$$\mathbf{j}_k = \sum_{i=1}^{N}\mathbf{P}_{ik}\mathbf{r}_i\,.$$

Let us introduce the following notation

$$\begin{Bmatrix}\delta\mathbf{r}\\ \delta\varphi\end{Bmatrix} = \sum_{j=1}^{N}\mathbf{K}_j\delta\mathbf{p}_j\,, \quad (230)$$

where

$$\delta\mathbf{p}_j = \begin{Bmatrix}\delta\mathbf{r}_j\\ \delta\varphi_j\end{Bmatrix} \quad (231)$$

and

$$\mathbf{K}_j = \begin{bmatrix}\mathbf{J}_j & \mathbf{j}_j\\ \mathbf{0}_2^T & I_j\end{bmatrix}\,, \quad (232)$$

as well as the matrices of Reissner's beam theory [36]

$$\mathbf{D} = \begin{bmatrix} \mathbf{I}_2 \dfrac{d}{dx_1} & -\hat{\mathbf{e}}\mathbf{r}' \\ \mathbf{0}_2^T & \dfrac{d}{dx_1} \end{bmatrix}, \quad \mathbf{L} = \begin{bmatrix} \mathbf{\Lambda} & \mathbf{0}_2 \\ \mathbf{0}_2^T & 1 \end{bmatrix}, \quad \mathbf{S} = \begin{Bmatrix} \mathbf{N} \\ M \end{Bmatrix}, \tag{233}$$

where $\mathbf{0}_2$ is a two–dimensional null vector and $\mathbf{I}_2$ is a two–dimensional unity matrix. With this notation, the strain–energy variation may be expressed as

$$\delta\phi \approx \delta\phi^h = \sum_{j=1}^{N} \delta\mathbf{p}_j^T \int_0^L (\mathbf{D}\mathbf{K}_j)^T \mathbf{L}\mathbf{S} dx_1 = \sum_{j=1}^{N} \delta\mathbf{p}_j^T \mathbf{q}_{i,j} \,, \tag{234}$$

where $\mathbf{q}_{i,j}$ is the vector of the internal forces at node j.

3.2.3 Special case for $I = J$

All the expressions written so far imply that nodes I and J may be different nodes ($I \neq J$). Let us from now on take that $I = J$ and calculate expressions needed to evaluate the variation of the interpolation functions of the position vector $\delta\mathbf{J}_i$. In this case rotation in the reference state $\varphi_r = \dfrac{\varphi_I + \varphi_{I=J}}{2} = \varphi_I$ and from (206), (225) and (228)

$$\mathbf{J}_i = \mathbf{N}_i + \delta_{Ii}(\mathbf{I} - \sum_{m=1}^{N} \mathbf{N}_m) \,, \tag{235}$$

$$\mathbf{M}_{ik} = I_k(-f^h\mathbf{I} + \hat{\mathbf{e}}) + (f_i\mathbf{I} - \hat{\mathbf{e}})\delta_{ik} - \delta_{Ik}(f_i - f^h)\mathbf{I} \,, \tag{236}$$

$$\mathbf{P}_{ik} = \frac{\beta}{2}\left(\mathbf{N}_i\mathbf{M}_{ik} - \delta_{Ii}\sum_{m=1}^{N}\mathbf{N}_m\mathbf{M}_{mk}\right) \,, \tag{237}$$

$$\mathbf{j}_k = \sum_{i=1}^{N} \mathbf{P}_{ik}\mathbf{r}_i = \frac{\beta}{2}\sum_{i=1}^{N} \mathbf{N}_i \, \mathbf{M}_{ik}(\mathbf{r}_i - \mathbf{r}_I) \,. \tag{238}$$

The function $\mathbf{N}_i$ remains the same as given in (208) but ψ^h and ψ_i in it now simplify to $\psi^h = \beta\dfrac{\varphi^h - \varphi_I}{2}$ and $\psi_i = \beta\dfrac{\varphi_i - \varphi_I}{2}$.

Note that, in linear analysis, (229) reads

$$\delta\mathbf{r}^h = \sum_{i=1}^{N} I_i \left[\delta\mathbf{r}_i + \frac{\beta}{2}\hat{\mathbf{e}}\left(\mathbf{R}^h - \mathbf{R}_i\right)\delta\varphi_i\right], \tag{239}$$

which for $\beta = \dfrac{2}{N}$ coincides with the variation of (183) thus confirming that the linked interpolation is a limiting case of the configuration–dependent interpolation with $\beta = \dfrac{2}{N}$ in linear analysis.

Vector of the internal forces for $I = J$ follows from (221) and (230)

$$\mathbf{q}_{i,j} = \int_0^L \mathbf{B}_j^T \mathbf{L}\mathbf{S} dx_1 \,, \tag{240}$$

with

$$\mathbf{B}_j = \mathbf{D}\mathbf{K}_j = \begin{bmatrix} \mathbf{J}'_j & \sum_{i=1}^N \mathbf{P}'_{ij}\mathbf{r}_i - \hat{\mathbf{e}} I_j \mathbf{r}' \\ \mathbf{0}_2^T & I'_j \end{bmatrix} = \begin{bmatrix} \mathbf{J}'_j & \mathbf{j}'_j - \hat{\mathbf{e}} I_j \mathbf{r}' \\ \mathbf{0}_2^T & I'_j \end{bmatrix} \,, \tag{241}$$

$$\mathbf{J}'_j = \mathbf{N}'_j - \delta_{Ij} \sum_{m=1}^N \mathbf{N}'_m \,, \tag{242}$$

$$\mathbf{N}'_j = \mathbf{N}_j \left[\left(\frac{I'_j}{I_j} - f^h \psi^{h'} \right) \mathbf{I} + \psi^{h'} \hat{\mathbf{e}} \right] \,, \tag{243}$$

$$\psi^{h'} = \frac{\beta}{2} \sum_{p=1}^N I'_p \varphi_p \,, \tag{244}$$

$$\mathbf{P}'_{ij} = \frac{\beta}{2} \left[\mathbf{N}'_i \mathbf{M}_{ij} + \mathbf{N}_i \mathbf{M}'_{ij} - \delta_{Ii} \sum_{m=1}^N \left(\mathbf{N}'_m \mathbf{M}_{mj} + \mathbf{N}_m \mathbf{M}'_{mj} \right) \right] \,, \tag{245}$$

$$\mathbf{M}'_{ij} = I'_j \left(-f^h \mathbf{I} + \hat{\mathbf{e}} \right) + (\delta_{Ij} - I_j) f^{h'} \mathbf{I} \,, \tag{246}$$

$$f^{h'} = -\left(\frac{1}{(\psi^h)^2} - \frac{1}{\sin^2 \psi^h} \right) \psi^{h'} = -\tilde{g}^h \, \psi^{h'} \,, \tag{247}$$

$$\tilde{g}^h = \frac{1}{(\psi^h)^2} - \frac{1}{\sin^2 \psi^h} \,, \tag{248}$$

$$\mathbf{r}' = \sum_{j=1}^N \mathbf{J}'_j \mathbf{r}_j \,, \tag{249}$$

$$\mathbf{j}'_j = \sum_{i=1}^N \mathbf{P}'_{ij} \, \mathbf{r}_i \,. \tag{250}$$

3.3 Graphical presentation of the proposed configuration–dependent interpolation functions

The configuration–dependent interpolation derived will be now illustrated for a 2D problem and compared to the Lagrangian interpolation polynomials for a two–noded and a three–noded element.

3.3.1 Two–noded element

If a reference node I is chosen to be the left node of a two–noded element ($I = 1$), interpolation matrices $\mathbf{J}_1$ and $\mathbf{J}_2$ are obtained from (206) as

$$\mathbf{J}_1 = \mathbf{I} - \mathbf{N}_2 \quad \text{and} \quad \mathbf{J}_2 = \mathbf{N}_2 \ ,$$

where $\mathbf{N}_2$ is calculated from (208) for $\psi_1 = 0$, $\psi^h = I_2\psi_2$, $I_1 = 1 - \dfrac{x_1}{L}$ and $I_2 = \dfrac{x_1}{L}$ and various values of $\psi_2 = \dfrac{\beta}{2}(\varphi_2 - \varphi_1)$. The matrix function $\mathbf{N}_2$ is for a planar problem a two–dimensional tensor with its components given in Figure 3 as functions of x_1. Different line–types are used to illustrate these functions for different values of ψ_2 (0, $\dfrac{\pi}{3}$ and $\dfrac{\pi}{2}$). As expected, for $\psi_2 = 0$, $\mathbf{J}_1$ and $\mathbf{J}_2$ coincide with the Lagrangian polynomials I_1 and I_2. As the local rotation ψ_2 increases the diagonal terms in $\mathbf{N}_2$ increasingly deviate from $I_2 = \dfrac{x_1}{L}$, while the off–diagonal terms also grow from the initial zero value.

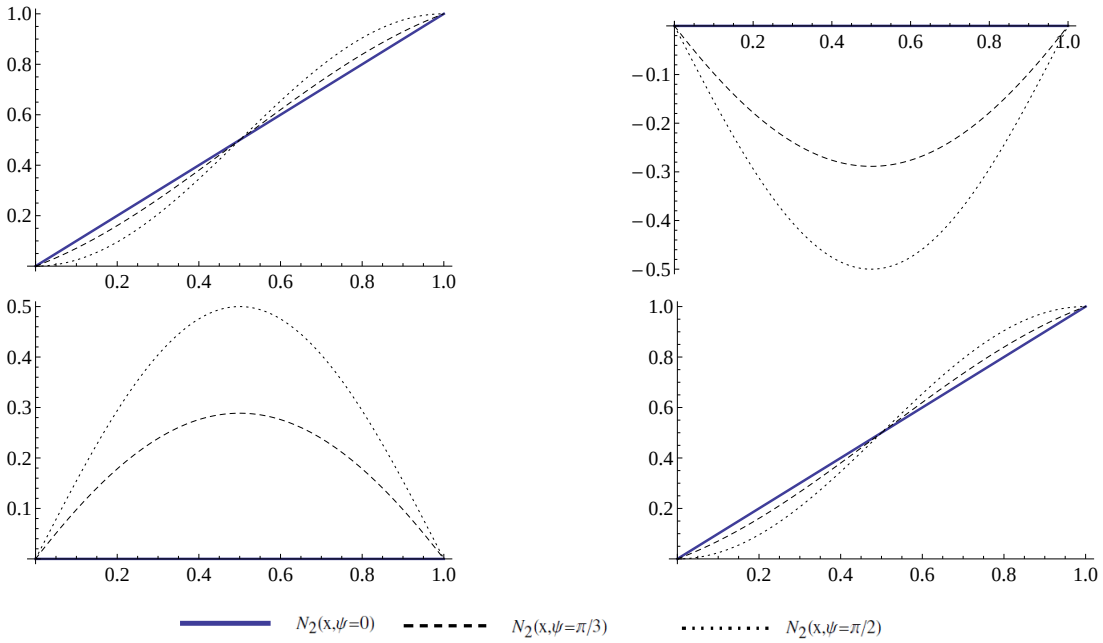

Figure 3.2: Function $\mathbf{N}_2(x_1, \psi_2 = 0, \dfrac{\pi}{3}, \dfrac{\pi}{2})$.

3.3.2 Three–noded element

In this case the reference node is chosen to be the middle node of the element ($I = 2$). The configuration–dependent interpolation $\mathbf{J}_1$, $\mathbf{J}_2$ and $\mathbf{J}_3$ follow from (206) as

$$\mathbf{J}_1 = \mathbf{N}_1, \ \mathbf{J}_2 = \mathbf{I} - \mathbf{N}_1 - \mathbf{N}_3 \text{ and } \mathbf{J}_3 = \mathbf{N}_3,$$

where matrices $\mathbf{N}_1$ and $\mathbf{N}_3$ are calculated from (208). To simplify the calculation, the local rotations of the first and the last node are taken to be equal in magnitude and of an opposite sign.

The components of $\mathbf{J}_1$, $\mathbf{J}_2$ and $\mathbf{J}_3$ are shown in Figures 4-6 for three different values of $\psi_1 = -\psi_3$ $(0, \ \frac{\pi}{6}, \ \frac{\pi}{4})$. Again, it can be observed that, for a zero local rotation, the proposed interpolation functions coincide with the Lagrangian polynomials $I_1 = 1 - 3\frac{x_1}{L} + 2\frac{x_1^2}{L^2}$, $I_2 = 4\frac{x_1}{L} - 4\frac{x_1^2}{L^2}$ and $I_3 = -\frac{x_1}{L} + 2\frac{x_1^2}{L^2}$. Obviously, the departure of the proposed interpolation from the Lagrangian interpolation is in this element far smaller than in the two–node element.

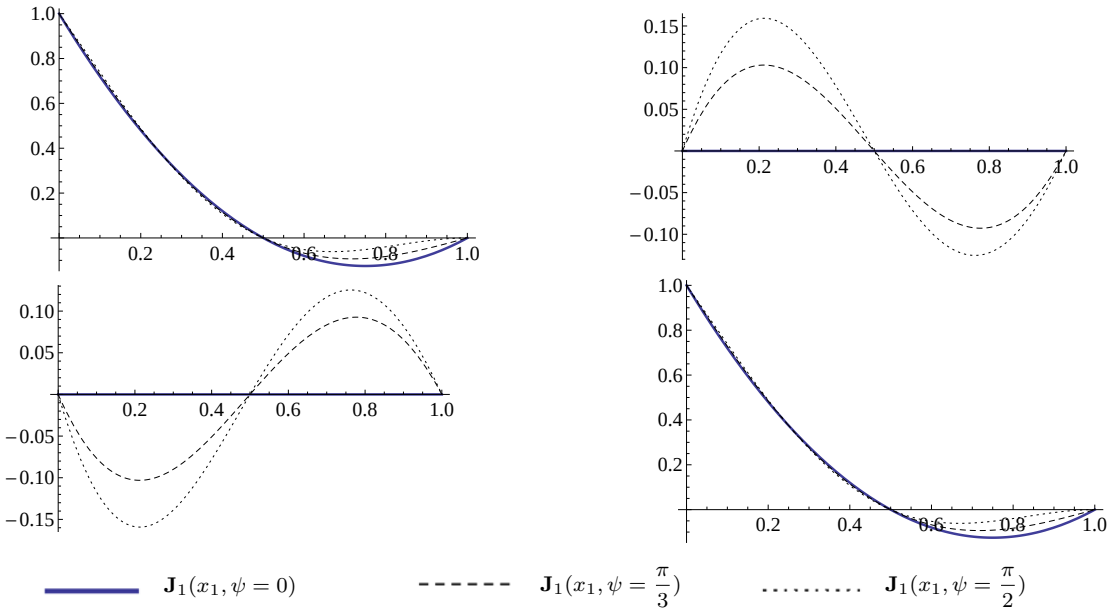

Figure 3.3: Function $\mathbf{J}_1(x_1, \psi = 0, \frac{\pi}{3}, \frac{\pi}{2})$.

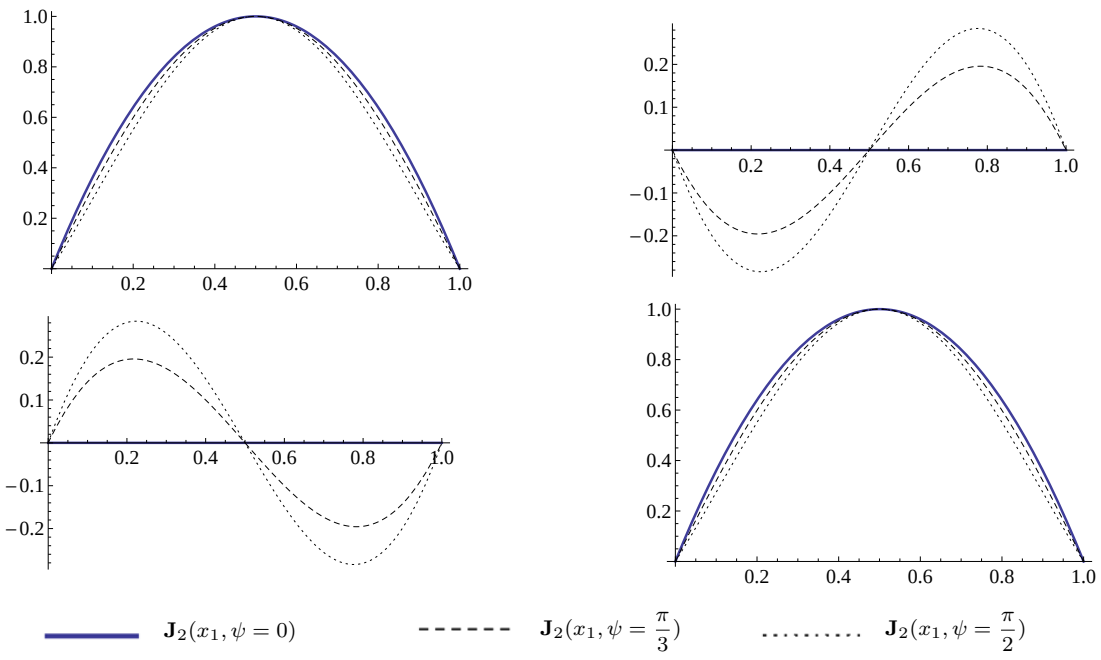

Figure 3.4: Function $\mathbf{J}_2(x_1, \psi = 0, \frac{\pi}{3}, \frac{\pi}{2})$.

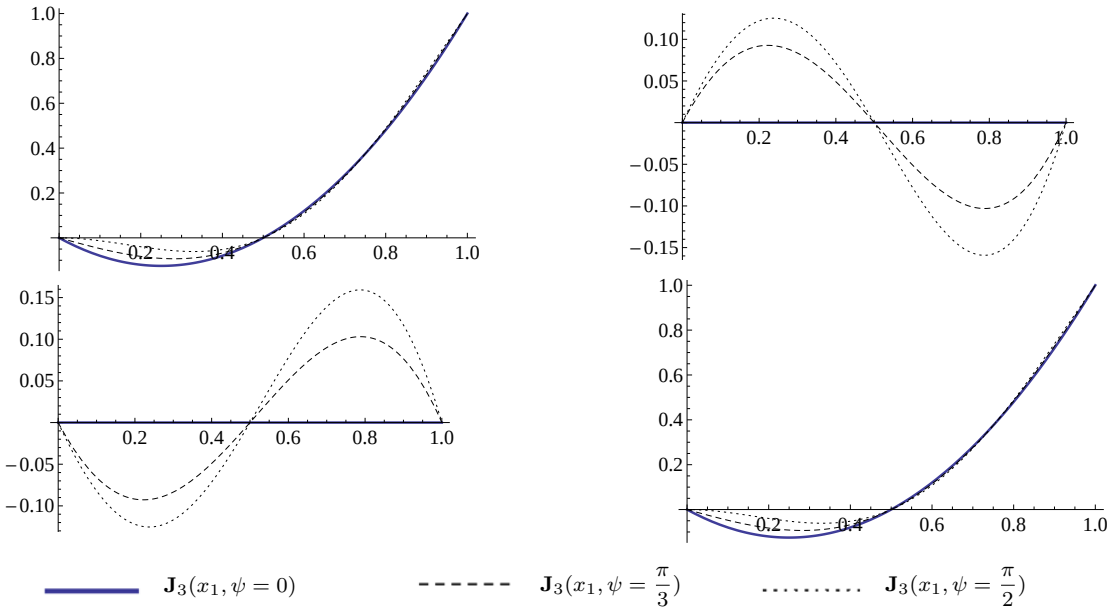

Figure 3.5: Function $\mathbf{J}_3(x_1, \psi = 0, \frac{\pi}{3}, \frac{\pi}{2})$.

3.3.3 Linearisation of the vector of the internal forces

The nodal equilibrium

$$\mathbf{g}_j \equiv \mathbf{q}_{i,j} - \mathbf{q}_{e,j} = \mathbf{0} \tag{251}$$

is to be established iteratively via

$$\sum_{k=1}^{N} \mathbf{K}_{jk}\, \Delta\mathbf{p}_k = -\mathbf{g}_j, \tag{252}$$

where $\mathbf{q}_{i,j}$ is the vector of the internal forces at node j, $\mathbf{q}_{e,j}$ is the vector of the external forces at node j and $\mathbf{K}_{jk}$ is the stiffness matrix relating the change in $\mathbf{p}_k$ to the change of $\mathbf{q}_{i,j}$.

In order to obtain the stiffness matrix of the finite element, it is necessary to carry out the linearisation of the vector of the internal forces $\mathbf{q}_{i,j}$ given by (240).

Linearisation of the vector of the internal forces can be performed as follows:

$$\Delta\mathbf{q}_{i,j} = \int_0^L \left(\Delta\mathbf{B}_j^T\mathbf{L}\,\mathbf{S} + \mathbf{B}_j^T\Delta\mathbf{L}\,\mathbf{S} + \mathbf{B}_j^T\mathbf{L}\,\Delta\mathbf{S}\right) dx_1. \tag{253}$$

Denoting $\Delta\mathbf{B}_j$ as $\Delta\mathbf{B}_j = \Delta\mathbf{B}_{1j} + \Delta\mathbf{B}_{2j}$ with

$$\Delta\mathbf{B}_{1j} = \begin{bmatrix} \Delta\mathbf{J}_j' & \Delta\mathbf{j}_j' \\ \mathbf{0}_2^T & 0 \end{bmatrix}, \tag{254}$$

$$\Delta\mathbf{B}_{2j} = \begin{bmatrix} \mathbf{0} & -\hat{\mathbf{e}}I_j\Delta\mathbf{r}' \\ \mathbf{0}_2^T & 0 \end{bmatrix}, \tag{255}$$

we may separate the geometric from the configuration–dependent influences in $\mathbf{B}_j$ i.e.

$$\Delta\mathbf{q}_{i,j} = \int_0^L \Delta\mathbf{B}_{1j}^T\mathbf{L}\,\mathbf{S}dx_1 + \int_0^L \Delta\mathbf{B}_{2j}^T\mathbf{L}\,\mathbf{S}dx_1 + \int_0^L \mathbf{B}_j^T\Delta\mathbf{L}\,\mathbf{S}dx_1 + \int_0^L \mathbf{B}_j^T\mathbf{L}\,\Delta\mathbf{S}dx_1 = \sum_{k=1}^{N}\mathbf{K}_{jk}^{CD}\Delta\mathbf{p}_k + \sum_{k=1}^{N}\mathbf{K}_{jk}^{G}\Delta\mathbf{p}_k + \sum_{k=1}^{N}\mathbf{K}_{jk}^{M}\Delta\mathbf{p}_k. \tag{256}$$

The first term in the above expression is the configuration–dependent part, the next two terms make the geometric part and the last term is the material part of the stiffness matrix. $\mathbf{K}_{jk}^M$ and $\mathbf{K}_{jk}^G$ are the standard material and geometric nodal stiffness matrix blocks where, however, the strain measures are computed from the interpolated position vector $\mathbf{r}$ as given in (222).

Since $\mathbf{S}$ depends linearly on the strain measures, the last term in $\Delta\mathbf{q}_{i,j}$ turns out to

be

$$\int_0^L \mathbf{B}_j^T \mathbf{L} \Delta \mathbf{S} dx_1 = \sum_{k=1}^{N} \int_0^L \mathbf{B}_j^T \mathbf{L} \mathbf{C} \mathbf{L}^T \mathbf{B}_k dx_1 \, \Delta \mathbf{p}_k \ ,$$

where $\mathbf{C} = diag(EA, GA_s, EI)$ is a constitutive matrix for a 2D problem and the material part of the stiffness matrix block is given as

$$\mathbf{K}_{jk}^M = \int_0^L \mathbf{B}_j^T \mathbf{L} \mathbf{C} \mathbf{L}^T \mathbf{B}_k dx_1. \tag{257}$$

Matrix $\mathbf{B}_j$ in expression (257) is the same as $\mathbf{D}\mathbf{K}_j$ where $\mathbf{D}$ is a differentiation matrix from [35] given as

$$\mathbf{D} = \begin{bmatrix} \dfrac{d}{dx_1} & 0 & v' + \sin\varphi_0 \\ 0 & \dfrac{d}{dx_1} & -(u' + \cos\varphi_0) \\ 0 & 0 & \dfrac{d}{dx_1} \end{bmatrix} \tag{258}$$

and $\mathbf{K}_j$ given in (232).

The geometric part of the stiffness matrix block also follows using the standard procedure (see Appendix E):

$$\mathbf{K}_{jk}^G = \int_0^L (\mathbf{D}_2 \mathbf{K}_j)^T \mathbf{G} (\mathbf{D}_2 \mathbf{K}_k) \, dx_1 \ , \tag{259}$$

where matrices $\mathbf{D}_2$ and $\mathbf{G}$ introduced in [35] are given as

$$\mathbf{D}_2 = \begin{bmatrix} \dfrac{d}{dx_1} & 0 & 0 \\ 0 & \dfrac{d}{dx_1} & 0 \\ 0 & 0 & 1 \end{bmatrix} , \tag{260}$$

$$\mathbf{G} = \begin{bmatrix} 0 & 0 & -t \\ 0 & 0 & n \\ -t & n & -t(v' + \sin\varphi_0) - n(u' + \cos\varphi_0) \end{bmatrix} , \tag{261}$$

with spatial stress resultants n, t defined as

$$\overline{\mathbf{n}} = \begin{Bmatrix} n \\ t \end{Bmatrix} = \mathbf{\Lambda} \begin{bmatrix} EA & 0 \\ 0 & GA_s \end{bmatrix} \begin{Bmatrix} \epsilon \\ \gamma \end{Bmatrix} . \tag{262}$$

The configuration–dependent part of the stiffness matrix block given by the first term in (256) will be derived from (254) .

From (242), $\Delta \mathbf{J}_j'$ follows as

$$\Delta \mathbf{J}'_j = \Delta \mathbf{N}'_j - \delta_{Ij} \sum_{m=1}^{N} \Delta \mathbf{N}'_m \ , \tag{263}$$

$$\Delta \mathbf{N}_j = \frac{\beta}{2} \mathbf{N}_j \sum_{k=1}^{N} \mathbf{M}_{jk} \Delta \varphi_k \ , \tag{264}$$

$$\Delta \mathbf{N}'_j = \frac{\beta}{2} \sum_{k=1}^{N} \left(\mathbf{N}'_j \mathbf{M}_{jk} + \mathbf{N}_j \mathbf{M}'_{jk} \right) \Delta \varphi_k = \frac{\beta}{2} \mathbf{N}_j \sum_{k=1}^{N} \mathbf{T}_{jk} \Delta \varphi_k \ , \tag{265}$$

with

$$\mathbf{T}_{jk} = \left(\frac{I'_j}{I_j} + \psi^{h'} (-f^h \mathbf{I} + \hat{\mathbf{e}}) \right) \mathbf{M}_{jk} + \mathbf{M}'_{jk} \tag{266}$$

where $\mathbf{M}'_{jk}$ is given by (246).

Linearisation of the derivative of the interpolation function $\mathbf{J}_j$ is given by

$$\Delta \mathbf{J}'_j = \frac{\beta}{2} \sum_{k=1}^{N} (\mathbf{N}_j \mathbf{T}_{jk} - \delta_{Ij} \sum_{m=1}^{N} \mathbf{N}_m \mathbf{T}_{mk}) \Delta \varphi_k = \sum_{k=1}^{N} \mathbf{Z}_{jk} \Delta \varphi_k \ , \tag{267}$$

with

$$\begin{aligned} \mathbf{Z}_{jk} = \frac{\beta}{2} (\mathbf{N}_j \mathbf{T}_{jk} - \delta_{Ij} \sum_{m=1}^{N} \mathbf{N}_m \mathbf{T}_{mk}) \\ = \frac{\beta}{2} \left[(\mathbf{N}_j \mathbf{M}_{jk})' - \delta_{Ij} \sum_{m=1}^{N} (\mathbf{N}_m \mathbf{M}_{mk})' \right] \ . \end{aligned} \tag{268}$$

From (245) and (250), $\Delta \mathbf{j}'_j$ follows as

$$\begin{aligned} \Delta \mathbf{j}'_j = \frac{\beta}{2} \sum_{p=1}^{N} (\Delta \mathbf{N}'_p \mathbf{M}_{pj} + \mathbf{N}'_p \Delta \mathbf{M}_{pj} + \Delta \mathbf{N}_p \mathbf{M}'_{pj} + \mathbf{N}_p \Delta \mathbf{M}'_{pj}) (\mathbf{r}_p - \mathbf{r}_I) \\ + \frac{\beta}{2} \sum_{p=1}^{N} (\mathbf{N}'_p \mathbf{M}_{pj} + \mathbf{N}_p \mathbf{M}'_{pj}) (\Delta \mathbf{r}_p - \Delta \mathbf{r}_I) \ , \end{aligned} \tag{269}$$

with

$$\Delta \mathbf{M}_{pj} = \frac{\beta}{2} \sum_{k=1}^{N} \mathbf{V}^p_{jk} \Delta \varphi_k \ , \tag{270}$$

where

$$\mathbf{V}_{jk}^{p} = \left[(I_j - \delta_{Ij})g^h(I_k - \delta_{Ik}) - g_p(\delta_{pj} - \delta_{Ij})(\delta_{pk} - \delta_{Ik})\right]\mathbf{I} \tag{271}$$

and

$$\Delta\mathbf{M}'_{pj} = \frac{\beta}{2}\sum_{k=1}^{N}\mathbf{V}_{jk}^{p'}\Delta\varphi_k \ , \tag{272}$$

with

$$\mathbf{V}_{jk}^{p'} = \left[(I'_j g^h + I_j g^{h'} - \delta_{Ij}g^{h'})(I_k - \delta_{Ik}) + (I_j - \delta_{Ij})I'_k g^h)\right]\mathbf{I} \ . \tag{273}$$

In the above equation $g^{h'} = -2\psi^{h'}h^h$, where $h^h = \dfrac{1}{(\psi^h)^3} - \dfrac{\cos\psi^h}{\sin^3\psi^h}$.
Equation (269) now turns into

$$\Delta\mathbf{j}'_j = \sum_{k=1}^{N}\mathbf{f}_{jk}\Delta\varphi_k + \sum_{k=1}^{N}\mathbf{R}_{jk}\Delta\mathbf{r}_k \tag{274}$$

with

$$\mathbf{f}_{jk} = \frac{\beta^2}{4}\sum_{p=1}^{N}\left[\mathbf{N}_p\left(\mathbf{T}_{pk}\mathbf{M}_{pj} + \mathbf{M}_{pk}\mathbf{M}'_{pj} + \mathbf{V}_{jk}^{p'}\right) + \mathbf{N}'_p\mathbf{V}_{jk}^{p}\right](\mathbf{r}_p - \mathbf{r}_I) \tag{275}$$

and

$$\mathbf{R}_{jk} = \frac{\beta}{2}\left[(\mathbf{N}_k\mathbf{M}_{kj})' - \delta_{Ik}\sum_{m=1}^{N}(\mathbf{N}_m\mathbf{M}_{mj})'\right] . \tag{276}$$

Finally, the configuration–dependent part of the stiffness matrix block is given as

$$\mathbf{K}_{jk}^{CD} = \int_0^L \begin{bmatrix} \mathbf{0}_{2x2} & \mathbf{Z}_{jk}^T\overline{\boldsymbol{n}} \\ \overline{\boldsymbol{n}}^T\mathbf{R}_{jk} & f \end{bmatrix} dx_1 \tag{277}$$

where $\overline{\mathbf{n}} = \boldsymbol{\Lambda}\mathbf{N}$, with vector $\mathbf{N}$ from $\mathbf{S} = \begin{Bmatrix} \mathbf{N} \\ M \end{Bmatrix}$ and $f = \mathbf{f}_{jk}^T\overline{\mathbf{n}}$.

4 Numerical examples

All numerical examples will be calculated using three different interpolations: the standard Lagrangian interpolation, linked interpolation introduced in [20] and the new configuration-dependent interpolation (CDI) proposed here. To summarise, between themselves, these interpolations differ inasmuch as they assume different approximation of the position field as follows:

Lagrangian: $\mathbf{r}^h = \sum_{i=1}^{N} I_i \mathbf{r}_i$

Linked: $\mathbf{r}^h = \sum_{i=1}^{N} I_i [\mathbf{r}_i + \frac{1}{N} \hat{\mathbf{e}} (\mathbf{R}^h - \mathbf{R}_i) \varphi_i]$

CDI: $\mathbf{r}^h = \sum_{i=1}^{N} \left[\delta_{iI} (\mathbf{I} - \sum_{m=1}^{N} \mathbf{N}_m) + \mathbf{N}_i \right] \mathbf{r}_i$,

with $\mathbf{R}^h = \sum_{i=1}^{N} I_i \mathbf{R}_i$, $\varphi^h = \sum_{i=1}^{N} I_i \varphi_i$ and $\mathbf{N}_i$ given in (208).

In the tables with results, the number behind the name of the interpolation is the number of nodes per element, i.e *Lagrangian 2* is the 2 noded element which uses Lagrangian interpolation polynomials, *Linked 3* is the 3 noded element with linked interpolation employed etc.. The stiffness matrix and the internal force vector will be calculated using the full integration as well as the reduced integration. The full integration uses N points, where N is the number of nodes per element, while reduced integration uses $N-1$ points to calculate all terms. Note that the linked interpolation was originally conceived for application in linear analysis. Here, its application will be tested on examples in non–linear analysis.
When configuration-dependent interpolation is employed, examples will be calculated with both $\beta = 1$ and $\beta = \frac{2}{N}$. In the first case, the interpolation takes the form of the one introduced in [18], but here employed for interpolation of the position vector $\mathbf{r}$, and gives results which are independent of the choice of the beam reference line. When $\beta = \frac{2}{N}$ the interpolation function takes the form which provides exact solution in the linear analysis. In order to conduct numerical analysis, an algorithm for a non–linear 2D beam finite element calculation has been written in the program package Wolfram Mathematica.

4.1 Standard shear locking test

This example [3] demonstrated in Figure 4.1 was taken to study the effect of the shear forces on displacements when beam thickness changes from small (thin beam) to large (thick beam). This effect was introduced at the beginning of the first part as the problem that arises when standard Lagrangian interpolation is used in low-order elements, and becomes exceedingly large as the beam thickness becomes smaller.

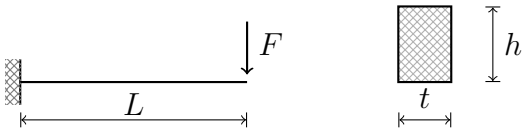

Figure 4.1: Cantilever under a vertical tip load.

This problem was analysed in [44] with the geometric and material properties of the beam given as: $L = 1$, $t = 0.1$, $E = 10^7$, $G = 10^{13}$ and the tip load $F = 1$. Since locking is directly related to the beam height h, this dimension is varied from very small 0.1 to very large 10. Vertical displacement results are compared with the reference solution obtained by discretising beam with 100 quadratic elements in the form of a quotient v/v_{ref}. Results are presented graphically with respect to parameter GL^2/Eh^2 in the logarithmic scale and demonstrated in the following figures for the linked interpolation and the configuration–dependent interpolation. The cantilever is modelled by one, five and ten elements.

The results presented in Figure 4.2 demonstrate that vertical displacements do not depend on the thickness of the beam when linked interpolation is used. Hence, we can say that this interpolation is insensitive to *shear locking* both for linear and quadratic elements. As expected, linear elements show better results as the number of the elements used to model the beam increases. On the other hand, quadratic elements show excellent behaviour with one element only. Behaviour of a two–noded element with configuration–dependent interpolation employed is presented in Figure 4.3 and is identical to first graph presented in Figure 4.2. The reason for this identical behaviour between these two interpolations is in the problem analysed, which is a problem of small displacements (very close to linear analysis), and the linked interpolation is a special case of the configuration dependent interpolation with $\beta = \frac{2}{N}$ when displacements and rotations become small.

Especially interesting property of a configuration–dependent interpolation becomes evident when quadratic and higher–order ($N \geq 3$) elements are used. Depending on the coefficient β, the results are quite different and this is shown in Figure 4.4. The

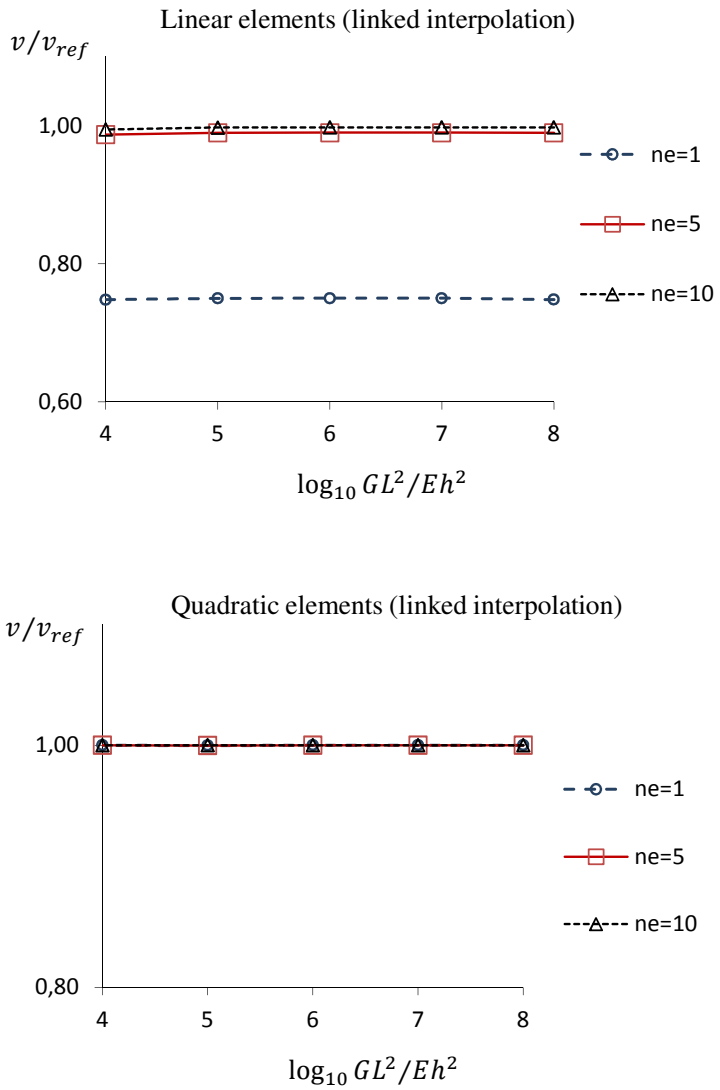

Figure 4.2: Normalised vertical displacement at free end versus parameter GL^2/Eh^2 with linked interpolation employed.

results with $\beta = 2/N$ are better that the ones obtained with $\beta = 1$. This is so because the problem is in a domain of small displacements and rotations and for this special case the configuration–dependent interpolation reduces to linked interpolation, for $\beta = 2/N$. This distinction does not exist in linear (two–noded) elements because $N = 2$ and $\beta = 2/N = 1$. This conclusion will be analysed further and confirmed in the following examples. Again it is shown here that the elements with configuration-dependent interpolation do not suffer from *shear locking*.

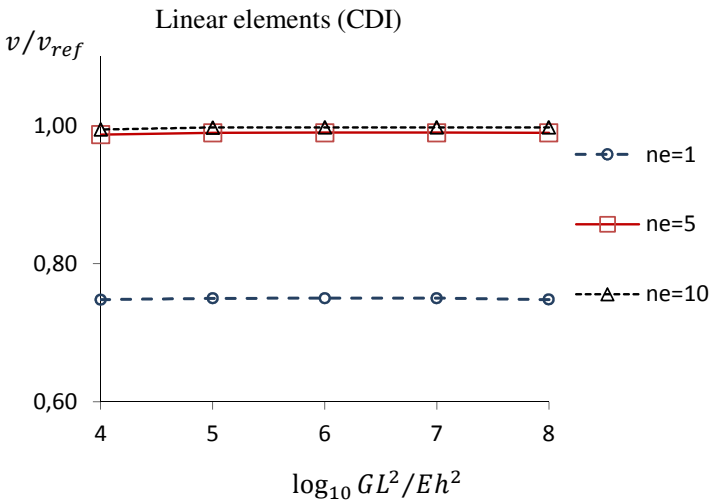

Figure 4.3: Normalised vertical displacement at free end versus parameter GL^2/Eh^2 with configuration–dependent interpolation employed for two–noded element.

4.2 Pinned fixed diamond frame

This example was solved analytically by Jenkins et al. [22] using elliptic integrals. Mattiasson [24] performed the numerical evaluation of the elliptic integrals thus providing a valuable test for finite element formulations considering large deflections.
The problem is shown in Figure 4.5 and has been solved using two elements only, one per each leg. The number of nodes per element is variable and the stiffness matrix and the internal force vector are calculated using both full and reduced integration. The Newton–Raphson iterative solution procedure is considered to have converged when the displacement norm has become less than 10^{-12}. Geometrical and material characteristics are given as follows: length of each leg is $L = 1$, Young's modulus $E = 1$, the shear modulus $G = 10E$, the second moment of area $I = 1$ and the area of the cross section as well as the shear area is $A = 1000$. The results are compared to the exact ones given in [24] for the maximum ratio $PL^2/EI = 10$ with n load steps employed, as shown in Table 4.1.

Mattiasson [24] gave results for the horizontal displacement of the middle node (node 2 in Figure 4.5) and the vertical displacement and rotation of the loaded node (node 3 in Figure 4.5). Table 4.1 shows the reference solution as well as our results. The reference node in the configuration–dependent interpolation has been set to $I = 1$ for CDI2, $I = 2$ for CDI3 and CDI4 and $I = 3$ for CDI5. It has to be mentioned that the reference solution has been obtained for Euler's elastica ($A \to \infty, A_s \to \infty$), while the results obtained here can only model this properties approximately. As a result, the

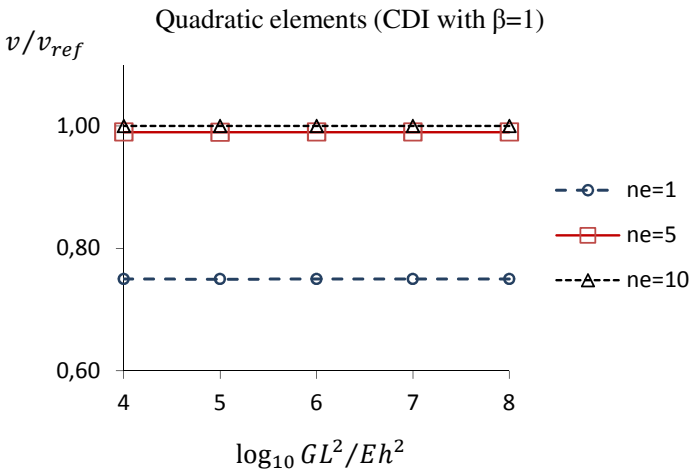

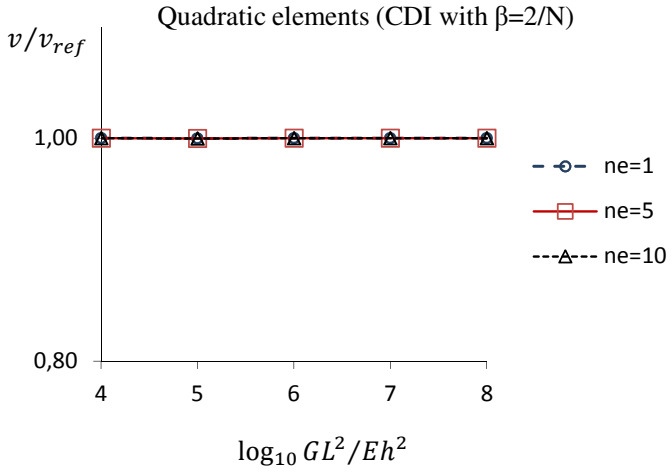

Figure 4.4: Normalised vertical displacement at free end versus parameter GL^2/Eh^2 with configuration–dependent interpolation employed.

extension dominated displacement v does not converge towards the reference solution.

From Table 4.1 it can be seen that the results for Lagrangian and linked interpolation are identical when reduced integration is employed. This induces us to conclude that the value of the functions in integrals which define the stiffness matrix and the internal force vector in these Gaussian points are identical. An interesting property occurs with linear configuration–dependent element (CDI2) which shows no sensitivity to the number of the integration points, meaning that the reduced and the full integration give identical result which is a known result [7]. As expected, the accuracy increases as the number of nodes increases. Also, all elements, except Lagrangian 2 with full integration, show certain resistance to shear locking. CDI elements show very little difference between full and reduced integration. The difference in cases when $\beta = 1$ and $\beta = 2/N$ reduces as the number of nodes per element increases.

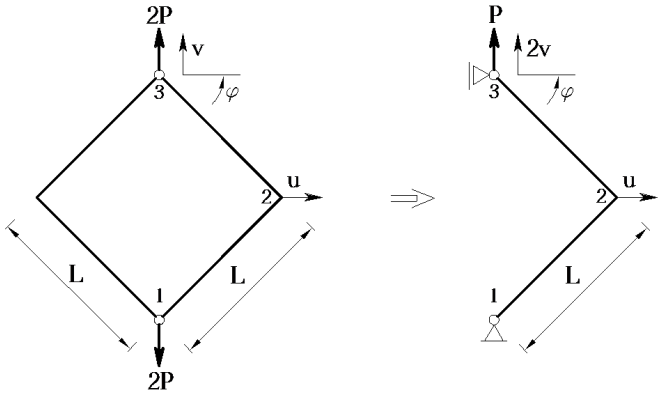

Figure 4.5: Diamond frame.

Table 4.1: Horizontal displacement of the middle node and the vertical displacement and rotation of the loaded node.

	Reduced integration				**Full integration**			
Interpolation	u	v	φ	n	u	v	φ	n
Lagrangian 2	0.48270	0.55478	1.90744	4	0.00261	0.01478	0.79043	1
Lagrangian 3	0.46444	0.50682	1.45607	12	0.28537	0.37490	1.46635	4
Lagrangian 4	0.46440	0.50585	1.50705	8	0.42523	0.47790	1.49034	12
Lagrangian 5	0.46500	0.50633	1.50431	11	0.45982	0.50147	1.50424	11
Linked 2	0.48270	0.55478	1.90744	4	0.14187	0.23793	1.15110	2
Linked 3	0.46444	0.50682	1.45607	12	0.40523	0.45938	1.52972	7
Linked 4	0.46440	0.50585	1.50705	8	0.45967	0.50286	1.51093	12
Linked 5	0.46500	0.50633	1.50431	11	0.46417	0.50624	1.50280	11
CDI2	0.38676	0.42829	1.68613	4	0.38676	0.42829	1.68613	4
CDI3 ($\beta = 1$)	0.45438	0.48723	1.49583	7	0.38976	0.43174	1.67810	9
CDI3 ($\beta = 2/3$)	0.45951	0.49677	1.47566	11	0.44959	0.49087	1.46847	12
CDI4 ($\beta = 1$)	0.46427	0.50426	1.50410	11	0.45836	0.49417	1.48360	8
CDI4 ($\beta = 2/4$)	0.46444	0.50547	1.50623	12	0.45848	0.50258	1.50322	11
CDI5 ($\beta = 1$)	0.46503	0.50628	1.50444	11	0.46463	0.50534	1.50582	11
CDI5 ($\beta = 2/5$)	0.46502	0.50634	1.50434	11	0.46329	0.50524	1.50365	11
Reference solution [24]	**u=0.46601**		**v=0.48760**		**φ=1.50351**			

4.3 Lee's frame

Problem of buckling of a hinged right–angle frame was considered in [34, 1]. The second moment of area, the area and the shear area of the cross section are $I = 2$, $A = 6$, $A_s = A/1.2$ and the length of each leg is $l = 120$. The value of Young's modulus is $E = 7.2 \times 10^6$ and the Poisson's ratio is 0.3. The frame is modelled using ten elements,

five per leg, and the number of nodes per element is variable from two to five nodes. The horizontal leg of the frame is loaded with a point force $P = 15000$ at $l/5$ applied in one load step only. Figure 4.6 shows deformation lines for various values of loading force $P = 8000,\ 15000,\ 17000$.

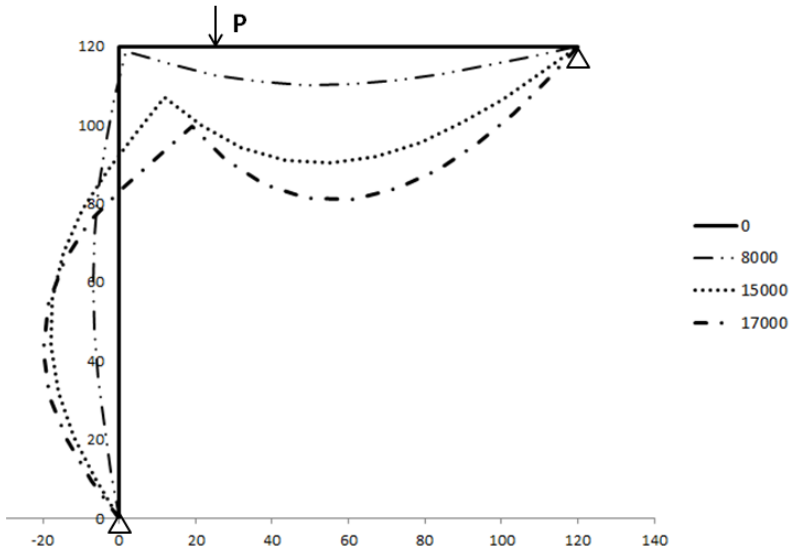

Figure 4.6: Lee's frame [34].

The reference solution for this example is obtained using 100 standard Lagrangian quadratic elements [36], 50 per leg with reduced Gaussian integration employed for evaluation of the stiffness matrix and the internal force vector. The displacements of the loaded node are given in the Table 4.2. The Newton–Raphson solution procedure tolerance is set to 10^{-12} for the displacement norm.

As expected, reduced integration shows good behaviour in case when Lagrangian and linked interpolation is applied on three–to–five–noded elements, while full integration shows quite poor behaviour for both of these interpolations in case when the number of nodes on an element is two or three. Naturally, higher–order elements give better results.

When CDI2 is applied, full and reduced integration give identical results as shown in the previous example. Also, for higher–order elements the difference between these two integrations becomes smaller as the number of nodes increases.

When comparing the CDI results for a higher–order element with different β between themselves, let us recall that $\beta = 1$ gives a solution independent of the position of the beam reference axis, but fails to provide the exact field distribution in linear analysis, while $\beta = \dfrac{2}{N}$ has exactly the opposite properties. It turns out that for highly non–linear problems like the present one, the former option is preferable. For the problems

Table 4.2: Displacements of the loaded node.

	Reduced integration			**Full integration**		
Interpolation	u	v	φ	u	v	φ
Lagrangian 2	6.4607277	-22.4863863	-0.3939265	0.0032633	-0.2281249	-0.0064778
Lagrangian 3	8.0163768	-25.8624736	-0.3929177	3.3400045	-14.3642921	-0.3026289
Lagrangian 4	8.0281657	-25.8924636	-0.3928227	7.8883600	-25.4463336	-0.3940329
Lagrangian 5	8.0282220	-25.8926334	-0.3928215	8.0266232	-25.8883396	-0.3923843
Linked 2	6.4607277	-22.4863387	-0.3939266	0.4216992	-4.5682100	-0.1444455
Linked 3	8.0163768	-25.8624736	-0.3929177	5.4241565	-19.4069233	-0.3308647
Linked 4	8.0281657	-25.8924636	-0.3928227	7.985295	-25.7133556	-0.3927950
Linked 5	8.0282220	-25.8926334	-0.3928215	8.0274237	-25.8903288	-0.3928343
CDI2	7.2445778	-23.6173958	-0.3968412	7.2445778	-23.6173958	-0.3968412
CDI3($\beta = 1$)	8.0265498	-25.8883573	-0.3928296	7.4676069	-24.2866212	-0.3956893
CDI3 ($\beta = 2/3$)	8.0210611	-25.8745419	-0.3928771	7.2254171	-24.2366473	-0.3811429
CDI4 ($\beta = 1$)	8.0282182	-25.8926222	-0.3928216	8.0237235	-25.8819096	-0.3928529
CDI4 ($\beta = 2/4$)	8.0281837	-25.8925191	-0.3928223	8.0086297	-25.8293214	-0.3929931
CDI5 ($\beta = 1$)	8.0282222	-25.8926338	-0.3928215	8.0281793	-25.8925181	-0.3928221
CDI5 ($\beta = 2/5$)	8.0282220	-25.8926335	-0.3928215	8.0279227	-25.8917751	-0.3928267
Reference solution u=8.0282209 v=-25.8926306 φ=-0.3928215						

approaching the linear case, say with $P = 1000$ instead of $P = 15000$, it is expected that the latter option ($\beta = \frac{2}{N}$) is more accurate. Table 4.3 confirms that it really is so and that the results for $\beta = \frac{2}{N}$ approach these of the linked interpolation and are less affected by an application of the full integration. Only three–noded element has been reviewed since the higher order elements show less sensitivity to coefficient β.
It can be stated that the effect of coefficient β is also configuration–dependent, meaning that as the calculation is getting closer to linear analysis, the use of $\beta = 2/N$ is becoming increasingly justified. In contrast to the Lagrangian and linked interpolation, however, configuration–dependent interpolation shows very good behaviour when full integration is used, regardless of the choice of β and the order of element.

Table 4.3: Displacements of the loaded node for smaller force P=1000.

	Reduced integration			**Full integration**		
Interpolation	u	v	φ	u	v	φ
Linked 3	0.0097857	-0.6357238	-0.0213572	0.0097250	-0.6327330	-0.0212910
CDI3($\beta = 1$)	0.0097889	-0.6357313	-0.0213573	0.0094235	-0.5881441	-0.0214414
CDI3 ($\beta = 2/3$)	0.0097871	-0.6357271	-0.0213573	0.0097868	-0.6356997	-0.0213561
Reference solution u=0.0097877 v=-0.6357291 φ=-0.0213573						

On the basis of these results, it appears that an improvement in the definition of the configuration–dependent interpolation may be possible through redefinition of the coefficient β such that it would be equal to $2/N$ in the linear case and tend towards

the unity as the deformation overally progresses.

4.4 Clamped–hinged deep circular arch subject to point load

The problem of a deep circular hinged–clamped arch shown in Figure 4.7 has been considered by many authors [36, 11, 26] and the exact solution for the critical force, based on the Kirchhoff-Love theory is given by DaDeppo and Schmidt [11].

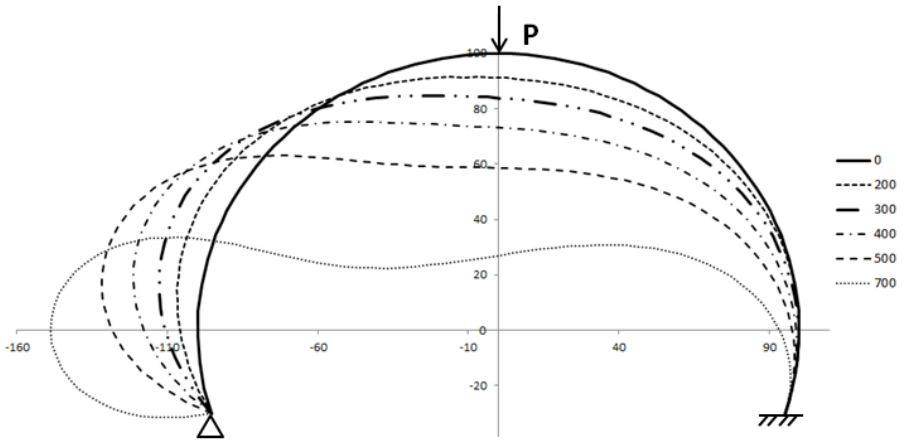

Figure 4.7: Deep circular arch subjected to a point load and the deformation lines caused by different values of the loading force P

The problem will be approximated using 40 straight beam elements of different order with the following characteristics: the value of Young's modulus $E = 1 \times 10^8$, Poisson's ratio $\nu = 0.5$, the second moment of area and the area of the cross section are respectively $I = 0.01$ and $A = 1$, the radius of the arch is $R = 100$ and the subtending angle of the arch is $\alpha = 215\,\text{deg}$. According to the Kirchoff-Love theory, the critical force that causes this arch to buckle matches the value of 897 [11]. Approximately 80 percent of the value of this critical force ($P = 700$) will be used as a loading force at the apex of the arch and the displacements and rotation of the loaded point will be compared using different interpolation functions with the reference solution obtained using 100 standard Lagrangian linear elements, with reduced Gaussian integration employed for evaluation of the stiffness matrix and the internal force vector. Results are obtained in two load steps and are given in Table 4.4. The Newton–Raphson tolerance has been set to 10^{-12} for the displacement norm.

The conclusions drawn from the previous two examples are confirmed by this example. The three–noded elements with different β are now again tested for a smaller value of the force $P = 150$. The results are shown in Table 4.5. The full integration

Table 4.4: Displacements of the apex.

	Reduced integration			**Full integration**		
Interpolation	u	v	φ	u	v	φ
Lagrangian 2	-50.9961799	-76.3623390	-0.1111182	-0.0757799	-0.1111479	-0.0002016
Lagrangian 3	-51.1053595	-77.0236301	-0.1093941	-37.4519073	-46.1934397	-0.1033123
Lagrangian 4	-51.1054127	-77.0240709	-0.1093922	-51.0850215	-76.9347624	-0.1097022
Lagrangian 5	-51.1054128	-77.0240712	-0.1093922	-51.1053798	-77.0239663	-0.1093926
Linked 2	-50.9961799	-76.3623390	-0.1111182	-2.8294271	-7.1527677	-0.0352417
Linked 3	-51.1053595	-77.0236301	-0.1093941	-46.9985542	-67.7505680	-0.1029238
Linked 4	-51.1054127	-77.0240709	-0.1093922	-51.0982901	-76.9967339	-0.1095222
Linked 5	-51.1054128	-77.0240712	-0.1093922	-51.1054013	-77.0240279	-0.1093923
CDI2	-50.9980130	-76.5599391	-0.1107745	-50.9980130	-76.5599391	-0.1107745
CDI3 ($\beta = 1$)	-51.1053317	-77.0239332	-0.1093925	-51.0076532	-76.6014917	-0.1106511
CDI3 ($\beta = 2/3$)	-51.1053531	-77.0237909	-0.1093933	-49.6844691	-72.9052221	-0.1121872
CDI4 ($\beta = 1$)	-51.1054128	-77.0240711	-0.1093922	-51.1053564	-77.0238795	-0.1093929
CDI4 ($\beta = 2/4$)	-51.1054128	-77.0240710	-0.1093922	-51.1023111	-77.0106158	-0.1094389
CDI5 ($\beta = 1$)	-51.1054129	-77.0240712	-0.1093922	-51.1054125	-77.0240698	-0.1093922
CDI5 ($\beta = 2/5$)	-51.1054129	-77.0240712	-0.1093922	-51.1054069	-77.0240511	-0.1093923
Reference solution u=-51.1918327 v=-77.1363559 φ=-0.1092019						

with $\beta = 2/N$ gives better results than when $\beta = 1$, while the reduced integration gives almost identical solutions for both coefficients.

Table 4.5: Displacements of the appex for smaller force P=150.

	Reduced integration			**Full integration**		
Interpolation	u	v	φ	u	v	φ
CDI3 ($\beta = 1$)	-4.504584	-5.934035	-0.0114678	-4.498577	-5.895356	-0.0115175
CDI3 ($\beta = 2/3$)	-4.504584	-5.934030	-0.0114678	-4.501265	-5.929965	-0.0114612
Reference solution u=-4.52286 v=-5.94521 φ=-0.0114624						

4.5 Cantilever beam loaded by two transversal forces

This example consists of a 2D cantilever beam loaded with two vertical forces, one applied at the free end and the other close to the mid–span, as shown in the Figure 4.8. This is a problem of large deflection behaviour, which demonstrates unlimited hardening behaviour, and has been considered by several authors [23, 10]. An analytic solution to this problem was given by Frisch–Fay [15].

The cross-sectional area of the beam is $A = 0.2$, the Young's modulus of elasticity is $E = 30 \times 10^6$, the shear modulus $G = 11538460$ and the second moment of area $I = 6 \times 10^{-3}$. The problem will be modelled using two elements of different length with number of nodes per element varying from two to five and the full load will be applied

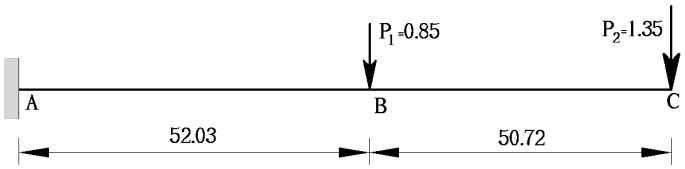

Figure 4.8: Cantilever beam loaded with two vertical forces.

in n load steps. Both reduced an full integration will be used and the Newton–Raphson iterative procedure is considered to have converged when the displacement norm has become less than 10^{-12}. Results for the end point C are given in the Table 4.6 and are compared to the reference solution. Analytic solution according to Frisch–Fay [15] says that the horizontal and vertical deflection of the end node C are $u_C = -31.01$ and $v_C = -67.32$ respectively and the results according to Manuel and Lee [23] using iterative procedure are $u_C = -30.75$ and $v_C = -66.96$. Since the results obtained here, using different interpolations need more decimal places to compare to one another, a reference solution in this case has been obtained using 100 quadratic standard Lagrangian elements with reduced integration employed and this solution is given in Table 4.6.

Table 4.6: Horizontal and vertical displacement of the end loaded node.

	Reduced integration			**Full integration**		
Interpolation	u	v	n	u	v	n
Lagrangian 2	-28.98611	-65.86169	1	-9.49 e-09	-0.00136	1
Lagrangian 3	-30.63686	-66.84291	2	-0.14422	-4.81456	2
Lagrangian 4	-30.74469	-66.95668	8	-28.80497	-63.48840	6
Lagrangian 5	-30.74577	-66.96151	8	-30.74660	-66.83158	8
Linked 2	-28.98611	-65.86169	1	-0.01638	-1.67411	1
Linked 3	-30.63686	-66.84291	2	-5.02053	-29.39257	2
Linked 4	-30.74469	-66.95668	8	-28.80497	-63.48840	6
Linked 5	-30.74577	-66.96151	8	-30.10605	-66.96148	8
CDI2	-28.83925	-63.46549	2	-28.83925	-63.46549	2
CDI3 ($\beta = 1$)	-30.77802	-66.91606	2	-28.83969	-63.46638	2
CDI3 ($\beta = 2/3$)	-30.70631	-66.88388	2	-1.15642	-13.97569	4
CDI4 ($\beta = 1$)	-30.74564	-66.96187	2	-29.91533	-65.24602	2
CDI4 ($\beta = 2/4$)	-30.74509	-66.95851	8	-21.26181	-56.05610	6
CDI5 ($\beta = 1$)	-30.74572	-66.96148	8	-30.52932	-66.42014	8
CDI5 ($\beta = 2/5$)	-30.74576	-66.96151	8	-29.05346	-64.58562	3
Reference solution	**u_C = -30.74573**			**v_C = -66.96151**		

From Table 4.6 it can be seen that the conclusions drawn from the previous exam-

ples are confirmed. Results for Lagrangian and linked interpolation are identical when reduced integration is used. Linear configuration–dependent element (CDI2) shows no sensitivity to the number of the integration points. Configuration-dependent interpolation with coefficient $\beta = 1$ shows better behaviour than when $\beta = \frac{2}{N}$ is used.

5 Conclusions

The theory given in the second and the third chapter of the thesis presents a very elegant form of a family of interpolation functions that interconnect linear and non–linear analysis of the beam problem.

In the second chapter a family of linked interpolation functions of arbitrary order for thick beam elements capable of providing exact solution has been derived and thoroughly analysed. Distinction is made between (i) the interpolation obtained solving the differential equations of the problem and introducing a full set of boundary conditions and (ii) the interpolation in which a number of internal kinematic conditions is used in addition to the kinematic boundary conditions.

In the first case, the kinematic boundary conditions alone are not sufficient for the solution of the thick beam problem (even though they are sufficient for the solution of the thin beam problem resulting in the standard Hermitean cubics) and they have to be supplemented by appropriate static boundary conditions. As a result, the interpolation for the position and the rotation field becomes heavily intertwined and dependent on the problem material and geometric properties. For both the thick and the thin beam, the part of the solution which is dependent on the boundary displacements and rotations involves standard quadratic and cubic polynomials well–known from the engineering beam theory. In the presence of arbitrary distributed loading it has been shown that this result is enhanced by the appropriate higher–order terms. Owing to its dependence on the material, geometric and loading characteristics of the problem analysed, this type of interpolation has been termed the *problem–dependent* interpolation.

In the second case we have eliminated all the material, geometric and loading parameters from the interpolation in order to arrive at a *problem–independent* result. Here, we have limited our attention to polynomial loading of arbitrary order and shown that with a sufficient finite number of internal nodes it is always possible to obtain the exact result. For a distributed force loading of arbitrary order three situations have been analysed in more detail:

(i) the problem–independent linked interpolation with a minimum number of parameters in which the number of nodes with translational degrees of freedom is smaller than the number of nodes with rotational degrees of freedom by one,

(ii) the problem–independent linked interpolation with the same nodal points for the translational and the rotational degrees of freedom and

(iii) the problem–independent interpolation in which the number of nodes with translational degrees of freedom is larger than the number of nodes with rotational degrees of freedom by one resulting in standard independent interpolation for the two field using Lagrangian polynomials of different order.

The second of these situations appears to be particularly elegant both mathematically and computationally and in this part of the thesis it has been presented in its general form of which some of the known linked interpolations reported in the literature have been shown to be special cases.

In the third chapter a new configuration–dependent interpolation has been introduced and applied to geometrically exact beam theory of Reissner [32]. The configuration–dependent interpolation uses the deformed state of a beam to describe the distribution of the field variables thus making interpolation non–linear in the unknown nodal parameters. The configuration–dependent interpolation derived originates from the helicoidal interpolation [4] and generalises it to higher–order elements using the relevant earlier results related to strain–invariant interpolation [18], and exact interpolation in linear analysis [20].

Two variations of the higher–order configuration–dependent interpolation have been derived in order to preserve an important underlying property of the mechanical problem. The first of these variations tend to be invariant to the beam reference axis, while the second variation provides exact field distribution in the limit of the analysis becoming linear. In the present work, these two properties cannot be preserved at the same time unless the element is of the lowest order, i.e. the original helicoidal element of [4]. A potential to do so, however, exists and will be investigated in our future work. The configuration–dependent interpolation has been derived for a 3D beam problem, but only implemented in 2D beam elements.

The forth chapter binds the first two theoretical chapters on a numerical level to demonstrate the behaviour of the interpolations proposed. The linked interpolation [20] designed for linear analysis has also been implemented and tested in non–linear analysis. The additional numerical overhead in the configuration–dependent interpolation is fully contained within the element formulation, does not introduce additional degrees of freedom, and only requires computation of an additional part of the element

tangent stiffness matrix.

Observing the numerical results, a few general conclusions may be drawn. It has been shown that the configuration–dependent interpolation does not suffer from shear locking regardless of the order of element and the order of numerical quadrature. In spite of that, the results obtained using a reduced integration are better than those using the full integration. The behaviour of the linked interpolation designed for linear analysis shows poor results when applied to non–linear analysis which is expected. Also, linked interpolation is more vulnerable to shear locking when using full integration than the configuration–dependent interpolation but less vulnerable than the Lagrangian interpolation. Very interesting property is that the linked interpolation with reduced integration gives the same nodal results as the Lagrangian interpolation with reduced integration. Generally, the configuration–dependent interpolation proposed gives only marginally better results for the nodal unknowns than the standard procedure. The variant of the configuration–dependent interpolation which gives the result independent of the position of the beam reference axis is generally more accurate than the variant which provides the exact field–distribution in linear analysis; the situation is reversed as the results become closer to the linear results, in particular with full integration. As the configuration–dependent interpolation is virtually free of shear locking, it has a great potential to be used in various problems in material non–linearity where higher–order quadrature may be needed.

References

[1] J.H. Argyris and S. Symeonidis. A sequel to: Nonlinear finite element analysis of elastic systems under nonconservative loading-Natural formulation. Part I. Quasistatic problems. *Computer Methods in Applied Mechanics and Engineering*, 26(3):377–383, 1981.

[2] F. Auricchio and R.L. Taylor. A shear deformable plate element with an exact thin limit. *Computer Methods in Applied Mechanics and Engineering*, 118:393–412, 1994.

[3] K.-J. Bathe. *Finite Element Procedures*. Prentice Hall, New Jersey, 1995.

[4] M. Borri and C. Bottasso. An intrinsic beam model based on a helicoidal approximation—Part I: Formulation. *International Journal for Numerical Methods in Engineering*, 37(13):2267–2289, 1994.

[5] M. Borri and C. Bottasso. An intrinsic beam model based on a helicoidal approximation—Part II: Linearization and finite element implementation. *International Journal for Numerical Methods in Engineering*, 37(13):2291–2309, 1994.

[6] M. Borri, L. Trainelli, and C.L. Bottasso. On representations and parameterizations of motion. *Multibody System Dynamics*, 4(2-3):129–193, 2000.

[7] C. L. Bottasso and M. Borri. Energy preserving/decaying schemes for non-linear beam dynamics using the helicoidal approximation. *Computer Methods in Applied Mechanics and Engineering*, 143(3-4):393–415, 1997.

[8] C.L. Bottasso, M. Borri, and L. Trainelli. Geometric invariance. *Computational Mechanics*, 29(2):163–169, 2002.

[9] A. Cardona and M. Geradin. A beam finite element non-linear theory with finite rotations. *International Journal for Numerical Methods in Engineering*, 26(11):2403–2438, 1988.

[10] L.A. Crivelli and C.A. Felippa. A three-dimensional non-linear Timoshenko beam based on the core-congruential formulation. *International Journal for Numerical Methods in Engineering*, 36:3647–3673, 1993.

[11] D.A. DaDeppo and R. Schmidt. Instability of clamped-hinged circular arches subjected to a point load. *Journal of Applied Mechanics*, 42(4):894–896, 1975.

[12] A. Eisinberg and G. Fedele. On the inverse of the Vandermonde matrix. *Applied Mathematics and Computation*, 174:1384–1397, 2006.

[13] A. Eisinberg, G. Fedele, and C. Imbrogno. Vandermonde systems on equidistant nodes in [0, 1]: accurate computation. *Applied Mathematics and Computation*, 172:971–984, 2006.

[14] M.E.A. El-Mikkawy. Explicit inverse of a generalized Vandermonde matrix. *Applied Mathematics and Computation*, 146:643–651, 2003.

[15] R. Frisch-Fay. A new approach to the analysis of the deflection of thin cantilevers. *Journal of Applied Mechanics*, 28:87–90, 1961.

[16] A. Ibrahimbegović. Quadrilateral finite-elements for analysis of thick and thin plates. *Computer Methods in Applied Mechanics and Engineering*, 110:195–209, 1993.

[17] A. Ibrahimbegović, F. Frey, and I. Kožar. Computational aspects of vector-like parametrization of three-dimensional finite rotations. *International Journal for Numerical Methods in Engineering*, 38(21):3653–3673, 1995.

[18] G. Jelenić and M.A. Crisfield. Geometrically exact 3D beam theory: implementation of a strain-invariant finite element for statics and dynamics. *Computer Methods in Applied Mechanics and Engineering*, 171(1-2):141–171, 1999.

[19] G. Jelenić and M.A. Crisfield. Objectivity of strain measures in geometrically exact 3D beam theory and its finite element implementation. *Proceedings of the Royal Society of London Series A - Mathematical Physical and Engineering Sciences*, 455:1125–1147, 1999.

[20] G. Jelenić and E. Papa. Exact solution of 3D Timoshenko beam problem using linked interpolation of arbitrary order. *Archive of Applied Mechanics*, 81(2):171–183, 2009.

[21] G. Jelenić and M. Saje. A kinematically exact space finite strain beam model finite element formulation by generalized virtual work principle. *Computer Methods in Applied Mechanics and Engineering*, 120(1-2):131–161, 1995.

[22] J.A. Jenkins, T.B. Seitz, and J.S. Przemieniecki. Large deflections of diamond-shaped frames. *International Journal of Solids and Structures*, 2(4):591–603, 1966.

[23] F.S. Manuel and S. Lee. Flexible bars subjected to arbitrary discrete loads and boundary conditions. *Journal of The Franklin Institute*, 285:452–474, 1968.

[24] K. Mattiasson. Numerical results from large deflection beam and frame problems analysed by means of elliptic integrals. *International Journal for Numerical Methods in Engineering*, 17(1):145–153, 1981.

[25] S. Mukherjee, J.N. Reddy, and C.S. Krishnamoorthy. Convergence properties and derivative extraction of the superconvergent Timoshenko beam finite element. *Computer Methods in Applied Mechanics and Engineering*, 190:3475–3500, 2001.

[26] A.K. Noor and J.M. Peters. Mixed models and reduced/selective integration displacement models for nonlinear analysis of curved beams. *International Journal for Numerical Methods in Engineering*, 17(4):615–631, 1981.

[27] E. Papa Dukić and G. Jelenić. Exact solution of 3D Timoshenko beam problem: problem–dependent formulation. *Archive of Applied Mechanics*, DOI 10.1007/s00419-013-0805-y.

[28] E. Papa Dukić, G. Jelenić, and M. Gaćeša. Configuration–dependent interpolation in higher–order 2D beam finite elements. *Finite Elements in Analysis and Design*, 78:47–61, 2014.

[29] J. Przemieniecki. *Theory of Matrix Structural Analysis*. McGraw-Hill, New York, 1968.

[30] J. Rakowski. The interpretation of the shear locking in beam elements. *Computers and Structures*, 37:769–776, 1990.

[31] J.N. Reddy. On locking-free shear deformable beam finite elements. *Computer Methods in Applied Mechanics and Engineering*, 149:113–132, 1997.

[32] E. Reissner. On one-dimensional finite-strain beam theory: The plane problem. *Zeitschrift für Angewandte Mathematik und Physik*, 23(5):795–804, 1972.

[33] J.C. Simo. A finite strain beam formulation. The three-dimensional dynamic problem. Part I. *Computer Methods in Applied Mechanics and Engineering*, 49(1):55–70, 1985.

[34] J.C. Simo and L. Vu-Quoc. A three-dimensional finite-strain rod model. Part II: Computational aspects. *Computer Methods in Applied Mechanics and Engineering*, 58(1):79–116, 1986.

[35] J.C. Simo and L. Vu-Quoc. On the dynamics of flexible beams under large overall motions—The plane case: Part I. *Journal of Applied Mechanics*, 53(4):849–854, 1986.

[36] J.C. Simo and L. Vu-Quoc. On the dynamics of flexible beams under large overall motions—The plane case: Part II. *Journal of Applied Mechanics*, 53(4):855–863, 1986.

[37] J.C. Simo and L. Vu-Quoc. On the dynamics in space of rods undergoing large motions—A geometrically exact approach. *Computer Methods in Applied Mechanics and Engineering*, 66(2):125–161, 1988.

[38] R.L. Taylor and S. Govindjee. A quadratic linked plate element with an exact thin plate limit. Technical report, University of California at Berkeley - Department of Civil and Environmental Engineering.

[39] A. Tessler and S.B. Dong. On a hierarchy of conforming Timoshenko beam elements. *Computers and Structures*, 14:335–344, 1981.

[40] L. Yunhua. Explanation and elimination of shear locking and membrane locking with field consistence approach. *Computer Methods in Applied Mechanics and Engineering*, 162:249–269, 1998.

[41] O.C. Zienkiewicz and R.L. Taylor. *The Finite Element Method for Solid and Structural Mechanics*. Elsevier Butterworth-Heinemann, Oxford, 2005.

[42] O.C. Zienkiewicz, R.L. Taylor, and J.Z. Zhu. *The Finite Element Method. Its Basis and Fundamentals*. Elsevier Butterworth-Heinemann, Oxford, 2005.

[43] D. Zupan and M. Saje. Finite-element formulation of geometrically exact three-dimensional beam theories based on interpolation of strain measures. *Computer Methods in Applied Mechanics and Engineering*, 192:5209–5248, 2003.

[44] E. Zupan, M. Saje, and D. Zupan. On a virtual work consistent three-dimensional Reissner-Simo beam formulation using the quaternion algebra. *Acta Mechanica*, 224:1709–1729, 2013.

List of Figures

List of Tables

Appendices

Appendix A. Inverse of a Vandermonde matrix

Over a domain $-1 \leq \xi \leq 1$ a function $f(\xi)$ may be approximated by a simple polynomial expansion

$$f(\xi) = \sum_{i=0}^{n-1} a_i \xi^i, \tag{278}$$

where the coefficients a_i are obtained by solving the so–called Vandermonde problem

$$\mathbf{Va} = \mathbf{f} \Longleftrightarrow \begin{bmatrix} 1 & \xi_2 & \xi_2^2 & \dots & \xi_2^{j-1} & \dots & \xi_2^{n-1} \\ 1 & \xi_3 & \xi_3^2 & \dots & \xi_3^{j-1} & \dots & \xi_3^{n-1} \\ \vdots & \vdots & \vdots & \ddots & \vdots & & \vdots \\ 1 & \xi_i & \xi_i^2 & \dots & \xi_i^{j-1} & \dots & \xi_i^{n-1} \\ \vdots & \vdots & \vdots & & \vdots & \ddots & \vdots \\ 1 & \xi_n & \xi_n^2 & \dots & \xi_n^{j-1} & \dots & \xi_n^{n-1} \end{bmatrix} \begin{Bmatrix} a_0 \\ a_1 \\ a_2 \\ \vdots \\ a_{j-1} \\ \vdots \\ a_{n-1} \end{Bmatrix} = \begin{Bmatrix} f_1 \\ f_2 \\ f_3 \\ \vdots \\ f_i \\ \vdots \\ f_n \end{Bmatrix} \tag{279}$$

with $f_i = f(\xi_i)$ and ξ_i are the chose nodal co–ordinates. Alternatively, the same function may also be approximated using the Lagrangian interpolation polynomials

$$I_j(\xi) = \prod_{k=1, k\neq j}^{n} \frac{\xi - \xi_k}{\xi_j - \xi_k} \tag{280}$$

as

$$f(\xi) = \sum_{j=1}^{n} I_j(\xi) f_j. \tag{281}$$

This result may be expanded into a power series of the type

$$I_j(\xi) = \sum_{i=0}^{n-1} d_{j,i} \xi^i \tag{282}$$

with known coefficients $d_{j,i}$ e.g.

$$d_{j,n-1} = \frac{1}{\prod_{k=1,k\neq j}^{n} (\xi_j - \xi_k)}, \quad d_{j,n-2} = -d_{j,n-1} \sum_{k=1,k\neq j}^{n} \xi_k, \text{ and } d_{j,0} = \prod_{k=1,k\neq j}^{n} \frac{-\xi_k}{\xi_j - \xi_k}.$$

Substituting (282) into (281) gives

$$f(\xi) = \sum_{j=1}^{n} \sum_{i=0}^{n-1} d_{j,i} \xi^i f_j = \sum_{i=0}^{n-1} \left(\sum_{j=1}^{n} d_{j,i} f_j \right) \xi^i, \tag{283}$$

which may be compared to (278) to provide the solution of the Vandermonde problem (279) as

$$a_i = \sum_{j=1}^{n} d_{j,i} f_j. \tag{284}$$

Since the Vandermonde problem implies $\mathbf{a} = \mathbf{W}\mathbf{f}$, where $\mathbf{W} = \mathbf{V}^{-1}$, from (284) it is obvious that the element w_{ij} of the inverse of the Vandermonde matrix is

$$w_{ij} = d_{j,i-1}, \tag{285}$$

where $d_{j,i}$ is the coefficient of the j^{th} Lagrangian polynomial of the order $n-1$ multiplying ξ^i as shown in (282). In other words, the columns of the inverse of the n^{th} order Vandermonde matrix are the Lagrangian polynomials of order $n-1$ written in the basis $\{\xi^0, ..., \xi^{n-1}\}$. For example, for a quadratic Lagrangian interpolation with equidistant nodes $I_1(\xi) = -\frac{1}{2}\xi(1-\xi)$, $I_2(\xi) = (1-\xi)(1+\xi)$ and $I_3(\xi) = \frac{1}{2}\xi(1+\xi)$, the inverse of the Vandermonde matrix reads

$$\mathbf{W} = \mathbf{V}^{-1} = \begin{bmatrix} 0 & 1 & 0 \\ -\frac{1}{2} & 0 & \frac{1}{2} \\ \frac{1}{2} & -1 & \frac{1}{2} \end{bmatrix}. \tag{286}$$

Since the elements of the Vandermonde matrix and its inverse are $v_{ij} = \xi_i^{j-1}$ and $w_{ij} = d_{j,i-1}$, the following results are obtained from $\mathbf{VW} = \mathbf{WV} = \mathbf{I}$:

$$\sum_{k=0}^{n-1} \xi_i^k d_{j,k} = \delta_{i,j} \quad \text{and} \quad \sum_{k=1}^{n} d_{k,i-1} \xi_k^{j-1} = \delta_{i,j}, \tag{287}$$

of which the first reproduces the well–known property $I_j(\xi_i) = \delta_{i,j}$ of the Lagrangian polynomials (282).

The second result in (287) is more interesting and perhaps not so well–known:
multiplying a chosen power (between 0 and $n-1$) of a nodal coordinate ξ_k with the coefficient in the k^{th} Lagrangian polynomial associated with a certain power of ξ, and summing over all the nodes $k = 1, ..., n$, gives a unity if the two powers are equal and zero otherwise.

A weaker but perhaps more illustrative conclusion follows by multiplying the second term in (287) with ξ^{i-1}, summing the result over $i = 1, ..., n$, and substituting (282):

$$\sum_{k=1}^{n} \xi_k^j I_k(\xi) = \xi^j, \quad j = 0, ..., n-1. \tag{288}$$

For $j = 0$ this of course turns into the standard completeness property of the Lagrangian polynomials $\sum_{k=1}^{n} I_k(\xi) = 1$.

Appendix B. Borri and Bottasso helicoidal interpolation $\tilde{\mathbf{N}}_i$

Here we will show that the generalised interpolation from (153) reduces to Borri and Bottasso helicoidal interpolation for a two–noded element and the assumptions for that particular case introduced in [4]. To that purpose, let us write the interpolation from (153) for each of two nodes as:

$$\tilde{\mathbf{I}}^1 = \mathbf{\Lambda}_r \left\{ 2\left[\mathbf{I} - \mathbf{H}(\psi^{lh}) \sum_{m=1}^{2} I_m \mathbf{H}^{-1}(\psi_m^l) \right] \mathbf{V}_{I=J} + \mathbf{H}(\psi^{lh}) I_1 \mathbf{H}^{-1}(\psi_1^l) \right\} \mathbf{\Lambda}_r^T \tag{289}$$

where for $I = J$, $\mathbf{V}_{I=J} = 1/2\mathbf{I}$. For a helicoidal interpolation, orientation of the local triad is expressed trough a rotation of the local triad at the beginning (for $\xi = 0$, where $0 \leq \xi \leq 1$), meaning that our $\mathbf{\Lambda} = \mathbf{I}$ and a local rotation of the first node $\psi_1^l = 0$. With this, expression (289) can be written as

$$\tilde{\mathbf{I}}^1 = \mathbf{I} - \mathbf{H}(\psi^{lh}) I_2 \mathbf{H}^{-1}(\psi_2^l). \tag{290}$$

The interpolation for the second node can be written with the same assumptions:

$$\tilde{\mathbf{I}}^2 = \mathbf{H}(\psi^{lh}) I_2 \mathbf{H}^{-1}(\psi_2^l). \tag{291}$$

This can be simplified as

$$\tilde{\mathbf{I}}^1 = \mathbf{I} - \mathbf{N}(\xi) \tag{292}$$

$$\tilde{\mathbf{I}}^2 = \mathbf{N}(\xi), \tag{293}$$

where $\xi = \frac{x}{L}$ and $\mathbf{N}(\xi)$ is the helicoidal interpolation from [4].

Appendix C. Strain–invariant interpolation

Strain–invariant interpolation has the general form given by expression (153).With the rotation matrix $\mathbf{\Lambda} = \mathbf{\Lambda}_r \, exp \, \hat{\boldsymbol{\psi}}^{lh}$, expression (215) can be written in a wider form as

$$\mathbf{\Lambda}_I \; exp\; \hat{\boldsymbol{\psi}}^{lh} = \sum_{i,j,k=1}^{N} \Delta_k^{ij} \mathbf{\Lambda}_I \{(\delta_I^k + \delta_J^k) \Big[\mathbf{I} - \mathbf{H}(\psi^{lh}) \sum_{m=1}^{N} I_m \mathbf{H}^{-1}(\psi_m^l) \Big] \mathbf{V}_j +$$

$$\mathbf{H}(\psi^{lh}) I_k \mathbf{H}^{-1}(\psi_j^l)\} \mathbf{\Lambda}_I^T \mathbf{\Lambda}_i$$

After the whole expression is multiplied by $\mathbf{\Lambda}_I^T$ from the left, we can write

$$exp\; \hat{\boldsymbol{\psi}}^{lh} = \sum_{i,j,k=1}^{N} \Delta_k^{ij} \{(\delta_I^k + \delta_J^k) \Big[\mathbf{I} - \mathbf{H}(\psi^{lh}) \sum_{m=1}^{N} I_m \mathbf{H}^{-1}(\psi_m^l) \Big] \mathbf{V}_j +$$

$$\mathbf{H}(\psi^{lh}) I_k \mathbf{H}^{-1}(\psi_j^l)\} \mathbf{\Lambda}_I^T \mathbf{\Lambda}_i. \quad (294)$$

For the sake of simplicity, let us denote the expression in the brackets as $\Big[\mathbf{I} - \mathbf{H}(\psi^{lh}) \sum_{m=1}^{N} I_m \mathbf{H}^{-1}(\psi_m^l) \Big] = [\;]$. For (I=J), the first member in the above expression can be simplified in the following way:

$$\sum_{i,j,k}^{N} \Delta_k^{ij} 2\delta_I^k \; [\;] \; \mathbf{V}_j \mathbf{\Lambda}_I^T \mathbf{\Lambda}_i = \sum_{i,k}^{N} 2\delta_I^k \; [\;] \; (\Delta_k^{i1} \mathbf{V}_1 + \Delta_k^{i2} \mathbf{V}_2 + ... + \Delta_k^{iN} \mathbf{V}_N) \mathbf{\Lambda}_I^T \mathbf{\Lambda}_i$$

$$= \sum_{i=1}^{N} 2[\;] \; (\delta_I^1 \; \Delta_1^{i1} \mathbf{V}_1 + \delta_I^2 \; \Delta_2^{i1} \mathbf{V}_1 + ... + \delta_I^N \; \Delta_N^{i1} \mathbf{V}_1) \mathbf{\Lambda}_I^T \mathbf{\Lambda}_i +$$

$$\sum_{i=1}^{N} 2[\;] \; (\delta_I^1 \; \Delta_1^{i2} \mathbf{V}_2 + \delta_I^2 \; \Delta_2^{i2} \mathbf{V}_2 + ... + \delta_I^N \; \Delta_N^{i2} \mathbf{V}_2) \mathbf{\Lambda}_I^T \mathbf{\Lambda}_i + ... +$$

$$\sum_{i=1}^{N} 2[\;] \; (\delta_I^1 \; \Delta_1^{iN} \mathbf{V}_N + \delta_I^2 \; \Delta_2^{iN} \mathbf{V}_N + ... + \delta_I^N \; \Delta_N^{iN} \mathbf{V}_N) \mathbf{\Lambda}_I^T \mathbf{\Lambda}_i$$

$$= \sum_{i=1}^{N} 2[\;] \; (\Delta_I^{i1} \mathbf{V}_1 + \Delta_I^{i2} \mathbf{V}_2 + ... + \Delta_I^{iN} \mathbf{V}_N) \mathbf{\Lambda}_I^T \mathbf{\Lambda}_i$$

$$= \sum_{i=1}^{N} 2[\;] \; \Delta_I^{iI} \mathbf{V}_I \mathbf{\Lambda}_I^T \mathbf{\Lambda}_i = \sum_{i=1}^{N} [\;] \; \delta_I^i \mathbf{\Lambda}_I^T \mathbf{\Lambda}_i = \sum_{i=1}^{N} \delta_I^i \; [\;] \; \mathbf{\Lambda}_I^T \mathbf{\Lambda}_i \quad (295)$$

With (295) expression (294) becomes

$$exp\; \hat{\boldsymbol{\psi}}^{lh} = \sum_{i=1}^{N} \delta_I^i \Big[\mathbf{I} - \mathbf{H}(\psi^{lh}) \sum_{m=1}^{N} I_m \mathbf{H}^{-1}(\psi_m^l) \Big] \mathbf{\Lambda}_I^T \mathbf{\Lambda}_i$$

$$+ \sum_{i,j,k}^{N} \Delta_k^{ij} \mathbf{H}(\psi^{lh}) I_k \mathbf{H}^{-1}(\psi_j^l) \mathbf{\Lambda}_I^T \mathbf{\Lambda}_i.$$

Finally, the next equality has to be proven:

$$exp\ \hat{\boldsymbol{\psi}}^{lh} - \mathbf{I} = \mathbf{H}(\psi^{lh})\left[\sum_{i,j,k}^{N} \Delta_k^{ij} I_k \mathbf{H}^{-1}(\psi_j^l) \underbrace{\boldsymbol{\Lambda}_I^T \boldsymbol{\Lambda}_i}_{exp\ \hat{\boldsymbol{\psi}}_i^l} - \sum_{m=1}^{N} I_m \mathbf{H}^{-1}(\psi_m^l)\right]$$

This can be simplified even more

$$\underbrace{\mathbf{H}^{-1}(\psi^{lh})\left(exp\ \hat{\boldsymbol{\psi}}^{lh} - \mathbf{I}\right)}_{(*1)} = \sum_{m=1}^{N} I_m \underbrace{\mathbf{H}^{-1}(\psi_m^l)\left(exp\ \hat{\boldsymbol{\psi}}_m^l - \mathbf{I}\right)}_{(*2)}$$

Terms (*1) and (*2) in the above expression are similar, the first deals with the local interpolated rotations ψ^{lh} and the other with the local nodal rotations ψ^{lh}.

$$(*1) = \left[\mathbf{I} - \frac{1}{2}\hat{\boldsymbol{\psi}}^{lh} - \frac{1}{2}\frac{\psi^{lh}\sin\psi^{lh} + 2\cos\psi^{lh} - 2}{(\psi^{lh})^2(1-\cos\psi^{lh})}(\hat{\boldsymbol{\psi}}^{lh})^2\right]$$
$$\left[\frac{sin\psi^{lh}}{\psi^{lh}}\hat{\boldsymbol{\psi}}^{lh} + \frac{1-\cos\psi^{lh}}{(\psi^{lh})^2}(\hat{\boldsymbol{\psi}}^{lh})^2\right]$$

Multiplying these two brackets and simplifying the terms in it, we can write

$$(*1) = \frac{\sin\psi^{lh}}{\psi^{lh}}\hat{\boldsymbol{\psi}}^{lh} + \frac{1-\cos\psi^{lh}}{(\psi^{lh})^2}(\hat{\boldsymbol{\psi}}^{lh})^2 - \frac{1}{2}\frac{\sin\psi^{lh}}{\psi^{lh}}(\hat{\boldsymbol{\psi}}^{lh})^2 + \frac{1}{2}\frac{1-\cos\psi^{lh}}{(\psi^{lh})^2}(\hat{\boldsymbol{\psi}}^{lh})^3$$

$$-\frac{1}{2}\frac{\psi^{lh}\sin\psi^{lh} + 2(\cos\psi^{lh}-1)}{(\psi^{lh})^2(1-\cos\psi^{l}h)}\frac{\sin\psi^{lh}}{\psi^{lh}}(\hat{\boldsymbol{\psi}}^{lh})^3 - \frac{1}{2}\frac{\psi^{lh}\sin\psi^{lh} + 2(\cos\psi^{lh}-1)}{(\psi^{lh})^4}(\hat{\boldsymbol{\psi}}^{lh})^4$$
$$\frac{\sin\psi^{lh}}{\psi^{lh}}\hat{\boldsymbol{\psi}}^{lh} + \frac{1-\cos\psi^{lh}}{(\psi^{lh})^2}(\hat{\boldsymbol{\psi}}^{lh})^2 - \frac{\sin\psi^{lh}}{2\psi^{lh}}(\hat{\boldsymbol{\psi}}^{lh})^2 - \frac{1-\cos\psi^{lh}}{2(\psi^{lh})^2}(\hat{\boldsymbol{\psi}}^{lh})^3 -$$
$$\frac{\sin\psi^{lh}}{2\psi^{lh}}\frac{\psi^{lh}\sin\psi^{lh} + 2\cos\psi^{lh} - 2}{(\psi^{lh})^2(1-\cos\psi^{lh})}(\hat{\boldsymbol{\psi}}^{lh})^3 - \frac{1-\cos\psi^{lh}}{2(\psi^{lh})^2}\frac{\psi^{lh}\sin\psi^{lh} + 2\cos\psi^{lh} - 2}{(\psi^{lh})^2(1-\cos\psi^{lh})}(\hat{\boldsymbol{\psi}}^{lh})^4$$
$$= \left[\frac{\sin\psi^{lh}}{\psi^{lh}} + \frac{1-\cos\psi^{lh}}{2} + \frac{\sin\psi^{lh}}{2\psi^{lh}}\frac{\psi^{lh}\sin\psi^{lh} + 2\cos\psi^{lh} - 2}{1-\cos\psi^{lh}}\right]\hat{\boldsymbol{\psi}}^{lh} +$$
$$\left[\frac{1-\cos\psi^{lh}}{(\psi^{lh})^2} - \frac{\sin\psi^{lh}}{2\psi^{lh}} + \frac{1-\cos\psi^{lh}}{2(\psi^{lh})^2}\frac{\psi^{lh}\sin\psi^{lh} + 2\cos\psi^{lh} - 2}{1-\cos\psi^{lh}}\right](\hat{\boldsymbol{\psi}}^{lh})^2$$
$$= \left[\frac{\sin\psi^{lh}}{\psi^{lh}} + \frac{1-\cos\psi^{lh}}{2} + \frac{1+\cos\psi^{lh}}{2} - \frac{\sin\psi^{lh}}{\psi^{lh}}\right]\hat{\boldsymbol{\psi}}^{lh} +$$
$$\left[\frac{1-\cos\psi^{lh}}{(\psi^{lh})^2} - \frac{\sin\psi^{lh}}{2\psi^{lh}} + \frac{\sin\psi^{lh}}{2\psi^{lh}} - \frac{1-\cos\psi^{lh}}{(\psi^{lh})^2}\right](\hat{\boldsymbol{\psi}}^{lh})^2 = \hat{\boldsymbol{\psi}}^{lh}$$

In an identical way it can be shown that $(*2) = \hat{\boldsymbol{\psi}}_m^l$, so the following relation can be written

$$\hat{\boldsymbol{\psi}}^{lh} = \sum_{m=1}^{N} I_m \hat{\boldsymbol{\psi}}_m^{\,l}$$

With the above expression we have proven that the interpolation $\tilde{\mathbf{I}}^i$ from [18] enables us to interpolate the nodal rotation matrices in an additive manner.

Appendix D. Derivation of the variation of the function $\mathbf{N}_i$

Function $\mathbf{N}_i$ is given by the expression

$$\mathbf{N}_i = I_i \frac{\psi_i \sin\psi^h}{\psi^h \sin\psi_i} \left[\cos(\psi^h - \psi_i)\mathbf{I} + \sin(\psi^h - \psi_i)\hat{\mathbf{e}}\right] = I_i k\, \mathbf{X} \ ,$$

where

$$k = \frac{\psi_i \sin\psi^h}{\psi^h \sin\psi_i}$$

and

$$\mathbf{X} = \cos(\psi^h - \psi_i)\mathbf{I} + \sin(\psi^h - \psi_i)\hat{\mathbf{e}} \ .$$

Now, the variation of function $\mathbf{N}_i$ is:

$$\delta\mathbf{N}_i = I_i \delta k\, \mathbf{X} + I_i k\, \delta\mathbf{X} \ .$$

- Variation of coefficient k

$$\delta k = k\, \left(\frac{\delta\psi_i}{\psi_i} - \frac{\delta\psi^h}{\psi^h} + \frac{\cos\psi^h}{\sin\psi^h}\delta\psi^h - \frac{\cos\psi_i}{\sin\psi_i}\, \delta\psi_i \right)$$

- Variation of matrix $\mathbf{X}$

$$\delta\mathbf{X} = (\delta\psi^h - \delta\psi_i) \left[\cos(\psi^h - \psi_i)\hat{\mathbf{e}} - \sin(\psi^h - \psi_i)\mathbf{I}\right]$$

The identity matrix in this expression may be written as $\mathbf{I} = \hat{\mathbf{e}}^{-1}\hat{\mathbf{e}} = \hat{\mathbf{e}}^T\hat{\mathbf{e}} = -\hat{\mathbf{e}}^2$ and now the variation of matrix $\mathbf{X}$ can be written as

$$\delta\mathbf{X} = (\delta\psi^h - \delta\psi_i)\ \mathbf{X}\ \hat{\mathbf{e}}$$

Returning these variations into the expression for $\delta\mathbf{N}_i$ gives

$$\delta\mathbf{N}_i = I_i\ k\ \ \mathbf{X} \left(\frac{\delta\psi_i}{\psi_i} - \frac{\delta\psi^h}{\psi^h} + \frac{\cos\psi^h}{\sin\psi^h}\delta\psi^h - \frac{\cos\psi_i}{\sin\psi_i}\, \delta\psi_i \right)$$

$$+I_i\ k\,(\delta\psi^h - \delta\psi_i)\ \mathbf{X}\ \hat{\mathbf{e}}$$

In this expression the basic function $\mathbf{N}_i = I_i\ k\,\mathbf{X}$ can be recognised and the variation further written as

$$\delta\mathbf{N}_i = \mathbf{N}_i\left[\left(\frac{\delta\psi_i}{\psi_i} - \frac{\delta\psi^h}{\psi^h} + \frac{\cos\psi^h}{\sin\psi^h}\delta\psi^h - \frac{\cos\psi_i}{\sin\psi_i}\ \delta\psi_i\right)\mathbf{I} + \left(\delta\psi^h - \delta\psi_i\right)\hat{\mathbf{e}}\right]\ .$$

With $\delta\psi_i = \dfrac{\beta}{2}(\delta\varphi_i - \delta\varphi_r)$, and $\delta\psi^h = \dfrac{\beta}{2}(\delta\varphi^h - \delta\varphi_r)$ the variation of $\delta\mathbf{N}_i$ follows as

$$\delta\mathbf{N}_i = \frac{\beta}{2}\mathbf{N}_i\left\{\left[(\delta\varphi_i - \delta\varphi_r)\,f_i - \left(\delta\varphi^h - \delta\varphi_r\right)\,f^h\right]\mathbf{I} + \left(\delta\varphi^h - \delta\varphi_i\right)\hat{\mathbf{e}}\right\}\ ,$$

with $f_i = \dfrac{1}{\psi_i} - \dfrac{\cos\psi_i}{\sin\psi_i}$ and $f^h = \dfrac{1}{\psi^h} - \dfrac{\cos\psi^h}{\sin\psi^h}$. Finally,

$$\delta\mathbf{N}_i = \frac{\beta}{2}\mathbf{N}_i\sum_{k=1}^{N}\mathbf{M}_{ik}\ \delta\varphi_k\ ,$$

with

$$\mathbf{M}_{ik} = I_k\left(-f^h\mathbf{I} + \hat{\mathbf{e}}\right) + \left(f_i\mathbf{I} - \hat{\mathbf{e}}\right)\ \delta_{ik} - \frac{\delta_{Ik} + \delta_{Jk}}{2}\left(f_i - f^h\right)\mathbf{I}$$

or, for $I = J$,

$$\mathbf{M}_{ik} = I_k(-f^h\mathbf{I} + \hat{\mathbf{e}}) + (f_i\mathbf{I} - \hat{\mathbf{e}})\delta_{ik} - \delta_{Ik}(f_i - f^h)\mathbf{I}\ .$$

Appendix E. Geometric part of the stiffness matrix

- Derivation of the geometric stiffness matrix in a standard way [35]

$$\mathbf{K}^G_{jk} = \int_0^L (\mathbf{D}_2\mathbf{K}_j)^T\mathbf{G}(\mathbf{D}_2\mathbf{K}_k)\ dx_1$$

$$\mathbf{D}_2\mathbf{K}_j = \begin{bmatrix}\dfrac{d}{dx}\mathbf{I}_2 & \mathbf{0}_2\\ \mathbf{0}_2^T & 1\end{bmatrix}\begin{bmatrix}\mathbf{J}_j & \mathbf{j}_j\\ \mathbf{0}_2^T & I_j\end{bmatrix} = \begin{bmatrix}\mathbf{J}'_j & \mathbf{j}'_j\\ \mathbf{0}_2^T & I_j\end{bmatrix}$$

After multiplying these matrices, see also (261), expression for the geometric stiffness matrix can be written in a nice form as follows

$$\mathbf{K}^G_{jk} = \int_0^L \begin{bmatrix}\mathbf{0}_{2x2} & I_k\mathbf{J}_j'^T\hat{\mathbf{e}}\mathbf{\Lambda}\mathbf{N}\\ -I_j\mathbf{N}^T\mathbf{\Lambda}^T\hat{\mathbf{e}}\mathbf{J}'_k & (I_j\mathbf{j}'_k + I_k\mathbf{j}'_j)^T\hat{\mathbf{e}}\mathbf{\Lambda}\mathbf{N} - I_jI_k\mathbf{r}'^T\mathbf{\Lambda}\mathbf{N}\end{bmatrix}dx_1$$

where $\mathbf{N}$ is taken from the vector $\mathbf{S} = \begin{Bmatrix} \mathbf{N} \\ M \end{Bmatrix}$.

- Derivation of the geometric stiffness matrix in our way

As stated in (256), the geometric stiffness matrix consists of two parts, i.e.

$$\mathbf{K}^G_{jk} \begin{Bmatrix} \Delta\mathbf{r}_k \\ \Delta\varphi_k \end{Bmatrix} = \int_0^L \Delta\mathbf{B}^T_{2j}\mathbf{L}\ \mathbf{S}dx_1 + \int_0^L \mathbf{B}^T_j \Delta\mathbf{L}\ \mathbf{S}dx_1$$

$$= \int_0^L \begin{bmatrix} \mathbf{0}_{2x2} & \mathbf{0}_2 \\ I_j\Delta\mathbf{r}'^T\hat{\mathbf{e}} & 0 \end{bmatrix} \begin{Bmatrix} \mathbf{\Lambda N} \\ M \end{Bmatrix} dx_1 + \int_0^L \begin{bmatrix} \mathbf{J}'^T_j & \mathbf{0}_2 \\ \mathbf{j}'^T_j + I_j\mathbf{r}'^T\hat{\mathbf{e}} & I'_j \end{bmatrix} \begin{Bmatrix} \Delta\mathbf{\Lambda N} \\ 0 \end{Bmatrix} dx_1$$

$$= \int_0^L \begin{Bmatrix} \mathbf{0}_2 \\ -I_j\mathbf{N}^T\mathbf{\Lambda}^T\hat{\mathbf{e}} \sum_{k=1}^N (\mathbf{J}_k\Delta\mathbf{r}_k + \mathbf{j}_k\Delta\varphi_k)' \end{Bmatrix} dx_1$$

$$+ \int_0^L \begin{Bmatrix} \mathbf{J}'^T_j\hat{\mathbf{e}}\mathbf{\Lambda N} \sum_{k=1}^N I_k\Delta\varphi_k \\ (\mathbf{j}'^T_j + I_j\mathbf{r}'^T\hat{\mathbf{e}})\hat{\mathbf{e}}\mathbf{\Lambda N} \sum_{k=1}^N I_k\Delta\varphi_k \end{Bmatrix}$$

$$= \sum_{k=1}^N \int_0^L \begin{bmatrix} \mathbf{0}_{2x2} & I_k\mathbf{J}'^T_j\hat{\mathbf{e}}\mathbf{\Lambda N} \\ -I_j\mathbf{N}^T\mathbf{\Lambda}^T\hat{\mathbf{e}}\ \mathbf{J}'_k & (I_j\mathbf{j}'_k + I_k\mathbf{j}'_j)^T\hat{\mathbf{e}}\mathbf{\Lambda N} - I_jI_k\mathbf{r}'^T\mathbf{\Lambda N} \end{bmatrix} dx_1 \begin{Bmatrix} \Delta\mathbf{r}_k \\ \Delta\varphi_k \end{Bmatrix} ,$$

i.e.

$$\mathbf{K}^G_{jk} = \int_0^L \begin{bmatrix} \mathbf{0}_{2x2} & I_k\mathbf{J}'^T_j\hat{\mathbf{e}}\mathbf{\Lambda N} \\ -I_j\mathbf{N}^T\mathbf{\Lambda}^T\hat{\mathbf{e}}\ \mathbf{J}'_k & (I_j\mathbf{j}'_k + I_k\mathbf{j}'_j)^T\hat{\mathbf{e}}\mathbf{\Lambda N} - I_jI_k\mathbf{r}'^T\mathbf{\Lambda N} \end{bmatrix} dx_1 .$$